การวิเคราะห์แบบแรงกระทำด้านข้างแยกโหมดสำหรับโครงสร้างที่มีการเสื่อมถอย

นาย อมรชัย ใจยงค์

MODAL PUSHOVER ANALYSIS FOR DEGRADING STRUCTURES

Mr. Amornchai   Jaiyong

A Dissertation Submitted in Partial Fulfillment of the Requirements
for the Degree of Doctor of Philosophy Program in Civil Engineering
Department of Civil Engineering
Faculty of Engineering
Chulalongkorn University
Academic Year 2010

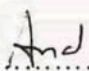| Thesis Title	MODAL PUSHOVER ANALYSIS FOR DEGRADING STRUCTURES
By	Mr. Amornchai Jaiyong
Field of Study	Civil Engineering
Thesis Advisor	Assistant Professor Chatpan Chintanapakdee, Ph.D.

Accepted by the Faculty of Engineering, Chulalongkorn University in Partial Fulfillment of the Requirements for the Doctoral Degree

………………………………Dean of the Faculty of Engineering
(Associate Professor Boonsom Lerdhirunwong, Dr.Ing.)

THESIS COMMITTEE

…………………………………Chairman
(Professor Panitan Lukkunaprasit, Ph.D.)

…………………………….Thesis Advisor
(Assistant Professor Chatpan Chintanapakdee, Ph.D.)

……………………………….Examiner
(Assistant Professor Anat Ruangrassamee, Ph.D.)

…………………………….Examiner
(Withit Pansuk, Ph.D.)

………………………………..External Examiner
(Assistant Professor Arnon Wongkaew, Ph.D.)

อมรชัย ใจยงค์: การวิเคราะห์แบบแรงกระทำด้านข้างแยกโหมดสำหรับโครงสร้างที่มีการเสื่อม
ถอย. (MODAL PUSHOVER ANALYSIS FOR DEGRADING STRUCTURES)
อ. ที่ปรึกษาวิทยานิพนธ์หลัก : ผศ. ดร. ฉัตรพันธ์ จินตนาภักดี, 110 หน้า.

ในปัจจุบันการวิเคราะห์หาผลตอบสนองของอาคารที่ได้รับแรงแผ่นดินไหวที่ถือว่ามีความถูกต้องที่สุดคือ วิธี
ประวัติเวลาไม่เชิงเส้น (Nonlinear Response History Analysis, NL-RHA) แต่เนื่องจากวิธีนี้ยังมีความยุ่งยากและซับซ้อน
ในการคำนวณและต้องใช้เวลาในการคำนวณมาก ดังนั้นวิธีวิเคราะห์แบบสถิตไม่เชิงเส้นโดยคำนึงถึงผลตอบสนองใน
โหมดที่สูงกว่าโหมดพื้นฐานหรือวิธีแรงกระทำด้านข้างแยกโหมด (Modal Pushover Analysis, MPA) ซึ่งมีสมมติฐานว่า
การตอบสนองของโครงสร้างสามารถคำนวณแบบแยกโหมดได้ จึงได้ถูกพัฒนาขึ้นในเวลาต่อมา การประเมินความ
ถูกต้องของวิธีแรงกระทำด้านข้างแยกโหมดในแง่ของการเปรียบเทียบผลตอบสนองที่ได้กับผลการวิเคราะห์ที่ได้จากวิธี
ประวัติเวลาไม่เชิงเส้นได้ถูกนำเสนอโดยเหล่านักวิจัยในอดีต ซึ่งแบบจำลองความเสียหายที่ใช้ในการศึกษามิได้คำนึงถึง
การเสื่อมถอยของสติฟเนสและกำลังต้านทานในชิ้นส่วนอาคารขณะได้รับแรงแผ่นดินไหว ในกรณีของอาคารคอนกรีต
เสริมเหล็ก การเสื่อมถอยของกำลังต้านทานและสติฟเนสของอาคารจะเกิดขึ้นเมื่อชิ้นส่วนอาคารเกิดความเสียหาย ซึ่งผล
ของการเสื่อมถอยนี้ส่งผลให้การตอบสนองของอาคารเช่น การเคลื่อนที่ที่พื้นและการเคลื่อนที่สัมพัทธ์ระหว่างชั้น มีการ
ขยายตัวเพิ่มขึ้น ซึ่งเมื่อนำวิธีแรงกระทำด้านข้างแยก โหมดมาใช้หาผลตอบสนองของอาคารดังกล่าว อาจส่งผลให้
ผลตอบสนองที่ได้มีความคลาดเคลื่อนสูง ดังนั้นในงานวิจัยนี้จึงมุ่งเน้นที่การปรับปรุงและพัฒนาวิธีแรงกระทำด้านข้าง
แยกโหมดให้สามารถใช้ทำนายผลตอบสนองของอาคารที่มีการเสื่อมถอยได้ โดยเริ่มที่ขั้นตอนการหาค่าการเคลื่อนที่
เป้าหมาย (Target Roof Displacement) โดยใช้ระบบขั้นเสรีเดียว (Single Degree of Freedom, SDF) ที่คำนึงถึงผลของ
การเสื่อมถอย จากนั้นจึงทำการประเมินผลตอบสนองที่คำนวณได้จากวิธีที่นำเสนอในรูปของอัตราส่วนของตอบสนอง
ที่วิเคราะห์ได้จากวิธีที่นำเสนอกับผลตอบสนองที่ได้จากวิธีประวัติเวลาไม่เชิงเส้น อาคารที่ใช้ในการศึกษานี้
ประกอบด้วย อาคารคอนกรีตเสริมเหล็กความสูง 8 ชั้น และโครงข้อแข็งที่มีความสูง 3 6 9 12 15 และ 18 ชั้น มากระทำ
ด้วยคลื่นแผ่นดินไหว 20 คลื่น โดยมีระดับความรุนแรงของคลื่นที่แตกต่างกัน จากผลการศึกษาพบว่า (1) การใช้ระบบ
ขั้นเสรีเดียวที่คำนึงถึงผลของการเสื่อมถอยสามารถทำนายค่าการเคลื่อนที่สูงสุดบริเวณยอดอาคารได้ถูกต้องแม่นยำกว่า
การใช้ระบบชั้นเสรีเดียวที่มิได้คำนึงถึงผลของการเสื่อมถอย (2) วิธีที่นำเสนอสามารถประมาณผลตอบสนองของอาคาร
ได้ถูกต้องแม่นยำกว่าวิธีที่ยังมิได้มีการปรับปรุง (3) วิธีที่นำเสนอสามารถประมาณค่าการเคลื่อนที่ที่พื้นได้ใกล้เคียงกับ
ผลตอบสนองที่วิเคราะห์ได้จากวิธีประวัติเวลาไม่เชิงเส้น ในขณะที่การประมาณค่าการเคลื่อนที่สัมพัทธ์ระหว่างชั้นมี
แนวโน้มให้ผลวิเคราะห์สูงกว่าผลตอบสนองของวิธีประวัติเวลาไม่เชิงเส้นในช่วงครึ่งล่างและให้ผลวิเคราะห์ที่ต่ำกว่า
ในช่วงครึ่งบนของอาคาร (4) ความคลาดเคลื่อนของผลตอบสนองที่วิเคราะห์ด้วยวิธีที่นำเสนอมีค่าสูงขึ้นเมื่ออาคารถูก
กระตุ้นด้วยคลื่นแผ่นดินไหวที่มีความรุนแรงมากขึ้นหรือในกรณีที่อาคารถูกออกแบบให้มีกำลังต้านทานต่อแผ่นดินไหว
ลดลง (5) ความคลาดเคลื่อนในการทำนายผลตอบสนองด้วยวิธีที่นำเสนอมีแนวโน้มลดลงเมื่ออาคารมีการออกแบบให้มี
การเสื่อมถอยของสติฟเนสและกำลังในระดับต่ำ

ภาควิชา	วิศวกรรมโยธา	ลายมือชื่อนิสิต
สาขาวิชา	วิศวกรรมโยธา	ลายมือชื่อ อ.ที่ปรึกษาวิทยานิพนธ์หลัก
ปีการศึกษา	2553	

AMORNCHAI JAIYONG: MODAL PUSHOVER ANALYSIS FOR DEGRADING
STRUCTURES. ADVISOR: ASST. PROF. CHATPAN CHINTANAPAKDEE, Ph.D., 110
pp.

While Non-Linear Response History Analysis (NL-RHA) is the most rigorous procedure to
estimate seismic demands for buildings, it is not quite practical for use by regular engineers. Thus, the
static pushover analysis, a simple and approximate method, has been improved, and a Modal Pushover
Analysis (MPA) has recently been proposed with an assumption that structural responses can be
estimated by superposition of modes. Several researchers evaluated MPA procedure by using simple
material model, i.e. bi-linear relation, which did not explicitly account for degradation behavior
representing the moment-rotation relation of plastic hinge. Therefore, conventional MPA procedure may
not be suitable for use with the type of building that takes account degrading behaviour such as
reinforced-concrete (RC) buildings. This study aims to develop MPA procedure for degrading structures
by utilizing the degrading equivalent SDF systems to improve the step for calculating the target roof
displacement of multi-degree-of-freedom (MDF) system. The next step is to evaluate the accuracy of
proposed procedure by comparing the floor displacement and the story drift demands estimated by
proposed procedure to those computed by NL-RHA, which is regarded as the reference value. The bias
is shown by the ratio of floor displacement and story drifts computed by proposed procedure, and
dispersion of the story drift ratios were also examined. The evaluation has been performed on a real RC
8-story building and a wide range of frame buildings with heights varying from 3, 6, 9, 12, 15, to 18
stories, designed by strong-column weak-beam concept, and having different strength levels
corresponding to systems with reduction factors (R) equal to 2, 4, and 6. The structures were subjected to
ground motions: 20 large-magnitude small-distance (LMSR). The following results have been found: (1)
using the degrading equivalent SDF systems can predict the peak roof displacement more accurate than
using non-degrading, or bi-linear, equivalent SDF systems, (2) the proposed procedure provides less bias
of floor displacements and story drift demands than the conventional MPA procedure, (3) the proposed
procedure generally provides floor displacements that are quite similar to NL-RHA's results while story
drift demands tend to overestimate at lower-half, and underestimate at upper-half of building, (4) the
bias and dispersion of both floor displacements and story drift demands tend to increase when the
building is subjected to high intensity ground motion and/or the building components are designed with
low strength level (5) the bias of seismic demands in the mild-degrading structure estimated by proposed
procedure is less than that of the severe-degrading structure.

Department: ....Civil Engineering...........   Student's Signature...
Field of Study: .....Civil Engineering...........   Advisor's Signature..
Academic Year: ...2010..............................

ACKNOWLEDGEMENTS

TABLE OF CONTENTS

LIST OF TABLES

LIST OF FIGURES

CHAPTER I

INTRODUCTION

1.1 Background

The Seismic response of building deforms beyond the limitation of linearly elastic behavior when subjected to earthquake excitation can be directly determined from dynamic analysis procedure or a Non-Linear Response History Analysis (NL-RHA). However, NL-RHA requires a great number of computational efforts; therefore, the method is not pratical for engineers. Although NL-RHA is widely regarded as the most rigorous procedure, several researchers attempt to develop a Nonlinear Static analysis Procedure (NSP), a pushover analysis that is practical to engineers to utilize with the result being an approximation. In the application of pushover analysis, the seismic demand of buildings can be estimated by nonlinear static analysis of the structure subjected to a single invariant force pattern until the roof displacement reachs to the target roof displacement determined from the deformation of an equivalent SDF system. The assumtion of NSP is that the structural response is dominated by the fundamental mode and that the mode shape remains unchanged after the structure yields. Therefore, the response of buildings that typically dominated by the first mode, such as low-and medium-rise buildings, can be predicted well by pushover analyis (Chintanapakdee and Chopra, 2003a).

NSP can be classified into two major groups based on the type of lateral load patterns applied to the structural model during the analysis: (1) invariant single load vectors such as the load pattern proposed by Federal Emergency Management Agency (FEMA-273, FEMA-356); (2) invariant multi-mode vectors, i.e. Modal Pushover Analysis (MPA), Modified Modal Pushover Analysis (MMPA) developed by Chopra and Goel (2002).

For FEMA lateral load patterns, the invariant force pattern which expect to provide peak response of the building close to NL-RHA responses were shown in Figure 1.1. However, as the structure becomes higher, the participation of higher modes may increase. These higher mode effects may contribute to the structure's response significantly. In this case, the single invariant force distribution proposed by

FEMA-356 cannot represent the potential range of loading experienced in dynamic response.
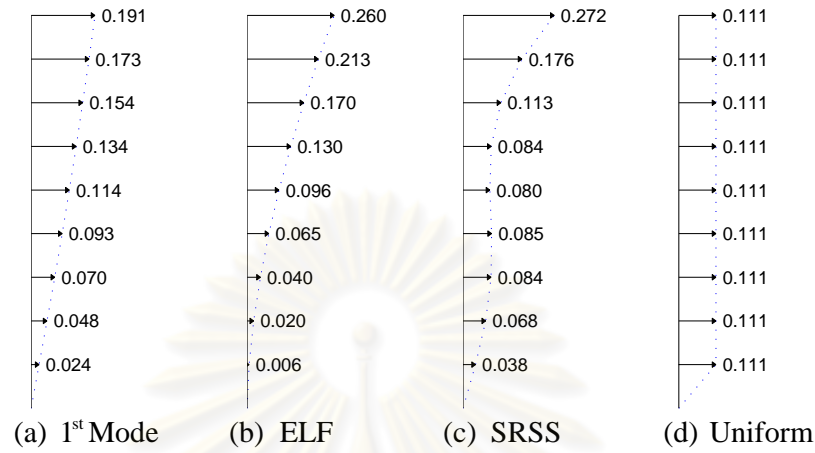
Figure 1.1: FEMA-356 force distributions for a 9-story generic frame: (a) first "mode"; (b) ELF; (c) RSA; (d) uniform (Chintanapakdee, 2003b).

However, as the structure becomes higher, the participation of higher modes may increase. The limitation of these patterns is the invariant force distributions do not account for the contribution of higher modes, which are significant in long period structures, i.e. high-rise building. Therefore, several new analysis procedures have been developed to overcome the limitations of conventional pushover analysis that is "MPA" procedure. The modal lateral load pattern that includes the contribution of several "modes" of vibration shown in Figure 1.2.
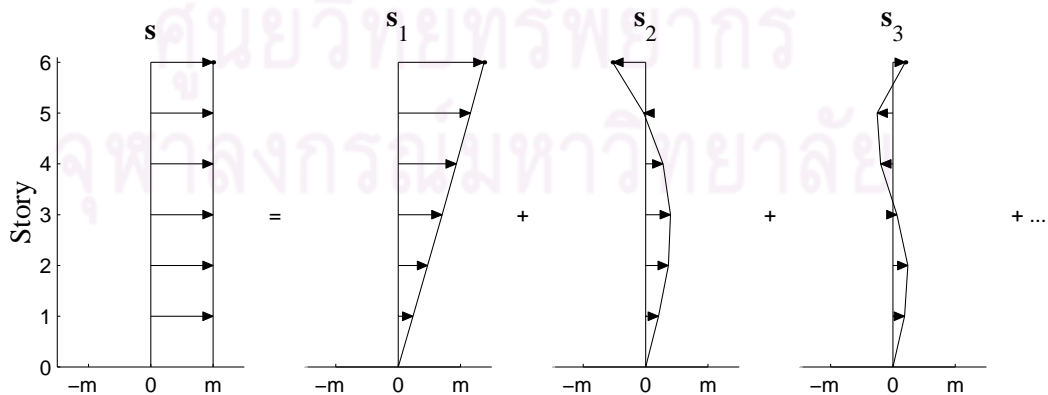
Figure 1.2 Modal expansion of the effective earthquake force for a 6-story frame (m=story mass) (Chintanapakdee and Chopra, 2003b).

1.2 Literature Review

In last decade. The accuracy of seismic demands of building estimated by NSP has been evaluated from several researchers. These results are summarized in this section.

1.2.1   Pushover Analysis (PA)

Krawinkler and Seneviratna (1998) evaluated the accuracy of seismic demand of the frame and wall structures height 2 to 40 stories when applied the triangular and SRSS load patterns. The analysis result concluded that the triangular and SRSS load patterns obtained in FEMA-273 provide good estimation of the target roof displacement especially in low-rise building (2 to 5 stories). However, the accuracy tends to deteriorate when the building become higher because higher modes contribution was significant in long period building.

Kim and D'Amore (1999) investigated the accuracy of NSP, which employs the capacity spectrum method, delineated in Applied Technology Council (ATC-40) by comparing with the response determined from NL-RHA. A six-story steel office building was selected for a case study; and it subjected to near-fault ground motions. The case study demonstrated that the predictions of the distribution of damage in the structure between NSP and NL-RHA were not agreement. In addition, the distribution of damage pattern from NSP significantly differed from those of NL-RHA.

1.2.2   Modal Pushover Analysis (MPA)

Chintanapakdee and Chopra (2003a) evaluated the seismic demands of steel moment-resisting by modeling the inelastic material property such as moment-rotation relation of plastic hinge based on simple material model. The evaluation demonstrates that MPA procedure is more accurate than FEMA force distribution in terms of providing the seismic demand.

Goel and Chopra (2004) evaluated the seismic demands of 9-story and 20-story steel moment resisting frames designed based on engineering guidelines of Structural Engineering Association of California (SEAOC), the Applied Technology Council (ATC), and the Consortium of University for Research in Earthquake Engineering (CUREE). As a whole, this particular engineering guidelines are known

as SAC-building. SAC-building is compared with the results from Non-Linear Response History Analysis (NL-RHA). These buildings were subjected to a set of 20 ground motions recorded in Los Angeles, CA, Seattle, WA, and Boston, MA. This evaluation also demonstrates that the MPA procedure provides the seismic demand more accurate than FEMA force distributions.

The 13-story RC building with steel braced frame was evaluated by Yu et al. (2004). The FEMA force distribution and the MPA procedure were adopted to estimate the seismic demands, and then compared with the results determined from NL-RHA. The methods comparison to NL-RHA confirms the MPA procedure is more accurate than the FEMA force distributions for estimating the story-drift demand, plastic hinge rotation, and floor displacement of building.

However, Chopra et al. (2004) modified the MPA procedure to be the Modified Modal Pushover Analysis (MMPA) procedure by assuming that the response of higher modes to be linearly elastic. MMPA procedure is an alternative procedure to estimate seismic demands because it tend to provides overestimatation of seismic demands for a variety frame building and ground motion ensembles. In some cases, MMPA procedure may improve the accuracy of MPA results, and increases their conservatism as well. Furthermore, MMPA generally provides the seismic demand, i.e. story drift much closer to the demands from NL-RHA when compare with using FEMA-356 lateral load pattern (Kalkan and Kunnath, 2006); but it is unable to reasonably predict plastic rotation demands in the upper stories because the inelastic contribution of higher modes was ignored.

Although MPA and its modified version, MMPA, provide satisfied estimatation of seiscmic demands for steel moment resisting frame (SMRF), the methods' conclusion may not support RC structures because the degradation in RC member affects seismic demands of reinforced-concrete (RC) structures when they are damaged due to ground motion or cyclic load. The cyclic behavior of RC structure is described in section 1.2.1.

1.2.3   Cyclic Behavior of RC Members

According to experimental test of cyclic behavior of RC members (Sezen 2000, Pujol 2002, Lowes et al. 2003), when RC members are subjected to cyclic load, the characteristic of degradation can be observed from the force-deformation relationship. For example, experimental test of non-ductile column tested by Sezen (2000) is shown in Figure 1.3, and the characteristic of degradation can be perceived as follow:
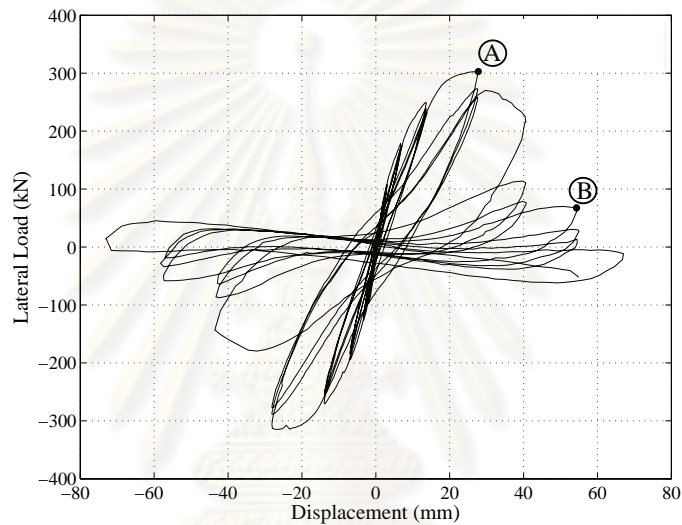
Figure 1.3 Force-deformation relationship of non-ductile column tested by Sezen (2000)

1.2.3.1 The strength degradation

When the inelastic deformation is increased and/or repeated at previous maximum amplitude, the resistance of yield force tends to decrease due to concrete crushing, rebar buckling, and longtitudinal steel yielding. The reduction of resisting force is called "strength degradation." In figure 1.3, the strength degradation can be observed when resisting force at "Loop-A," R_{max} =304 kN, deteriorate to "Loop-B," R_{max} = 78 kN.

1.2.3.2 The stiffness degradation

This experimental result indicates that the stiffness was altered, both unloading and reloading, due to the flexural cracking of concrete and the tensile yielding of the longitudinal reinforcement. The reduction of stiffness is called "stiffness degradation." The unloading stiffness degradation and reloading stiffness degradation can be observed in variant slope of force-deformation in unloading path and reloading path respectively.

1.2.4 Cyclic Behavior of RC Structures

Degradation of RC structures has been studied by several researchers (Otani 1981, Shimazaki and Sozen 1985, Qi and Moehle 1991, Rahnama and Krawinkler 1993, Pujol 2002, Lowes *et al*. 2003) to understand the behavior and its effects on the performance of RC structures during strong earthquakes. The degradation characteristics in a reinforced-concrete structural member are primarily controlled by the ratio of axial load and corresponding axial capacity, amount of transverse and longitudinal reinforcement, and deformation ductility encountered (Haselton and Deierlein 2007). Many extensive researches have been conducted to understand the hysteretic behaviour of RC structural components such as flexural and shear behaviour of RC columns and RC beam-column joints by experiment on physical models of RC member. The rate of degradation is controlled by damage index, which had been proposed to predict the degradation behaviour based on dissipated energy, number of cycles, and deformation ductility (Park and Ang 1985, Wang and Shah 1987)

1.2.5 Effect of Degradation on SDF System

Several researchers have studied the influence of degradation on response of SDF systems (Gupta and Krawinkler 1998, Aschheim and Black 1999, Song and Pincheira 2000, Miranda and Ruiz-Garcia 2002, Pekoz and Pincheira 2004, Chenouda and Ayoub 2008), and generally learned that deformations of short-period degrading system are significantly larger than those of non-degrading system (i.e., bi-linear system). Moreover, the effect of strength degradation is more important than stiffness degradation.

1.2.6   Effect of Degradation on MDF System

Some researchers studied the influence of degradation on response of MDF systems, and majority of these researchers emphasized on the influence of stiffness degradation only (Chopra and Kan 1973, Anderson and Townsend 1977, Naeim *et al.* 2000), and they learned that the reduction of stiffness on structural members can increase the maximum lateral displacement and relative floor displacement (story drift) at the upper story; and ductility requirements of short-period building are significantly larger than those of long-period building.

1.2.7   Cyclic Pushover Analysis (CPA)

The seismic performance to resist the earthquake load and dissipate seismic capacity of building can be investigated by reversal load pattern proposed as a cyclic pushover analysis (CPA). Some researchers adopt this procedure to evaluate the hysteretic behavior and estimate the seismic demand of structure.

For example, Intarakamheng and Ruangrassamee (2003) used CPA procedure and NSP procedure to estimate the floor displacement, inter-story drift, and damage mechanism of a five-story reinforced concrete building by assuming that the building was subjected to the 1940 El Centro, the 1985 Mexico SCT, and the 1995 Baiyoke ground motion record. The result indicated that both CPA and NSP procedures provide the maximum responses closed to that of NL-RHA procedure. The bias of CPA procedure is about 5-26 % whereas NSA procedure provides bias by about 3-30%. However, the sequence of yielding locations estimated by CPA is differeces from that of NSP procedure due to the difference in force distribution. In addition, the strength degradation can be observed from CPA procedure as well.

Next, Jia et al. (2008) adopts CPA procedure to evaluate the hysteretic behavior and energy dissipation capacity of a Buckling-Restrained Braced Steel Frame (BRBSF) whereas its seismic demands were estimated by MPA procedure. They found that MPA procedure provides adequate predictions of peak roof displacement whereas CPA procedure is a good method to evaluate the hysteretic behavior of a structure.

1.3 Problem Statement and Objectives

It is well aware that the effect of degradation can lead to larger displacement of structures. The basic Modal Pushover Analysis (MPA) for estimating global seismic demands, such as peak (target) roof displacement, floor displacement, and story-drift demand, are based on using response of non-degrading equivalent SDF system. This method may not be suitable for application to degrade RC buildings that are taken into effect of degradation. Therefore, this research aims to develop and evaluate the modal pushover analysis to estimate the seismic demands of degrading MDF structure with the following objectives:

1. To propose a method to determine the parameters of equivalent degrading SDF system by cyclic pushover analysis.
2. To evaluate the accuracy of target roof displacements of RC frames predicted by using equivalent degrading SDF system.
3. To develop the modal pushover analysis for RC frame.
4. To determine the accuracy of seismic demand of RC frame by using proposed method.

1.4 Research Scopes and Limitations

The limitations of research are stated as follows:

1. The structural system is only considered for one-bay frame of six different heights: 3, 6, 9, 12, 15, and 18 stories, and five different ductility design based on SDF system:1, 1.5, 2, 4, and 6.
2. Research assumes no shear failure, and only flexural behavior is considered.
3. The plastic hinge forms only at beam ends, and the base of the first-story is based on the strong-column weak-beam philosophy; consequently, column-hinges at another story is not reflected on.
4. Reseach considers only the response of building when subjected to a set of LMSR ensemble.

1.5 Outlines

After an introduction in Chapter 1, the proposed procedure to estimate peak roof displacement and seismic demands on RC frame by using response of equivalent degrading SDF system is determined by Non-Linear Response History Analysis (NL-RHA) presented in Chapter 2. Chapter 3 describes modeling of the structure including the degrading behaviour, the ensemble of 20 ground motions used in the study, and response statistics. The accuracy of the the target roof displacement estimated by using response of equivalent degrading SDF system and non-degrading SDF system and comparison are presented in Chapter 4. In Chapter 5, the estimated seismic demands of RC frame determined by proposed procedure is compared to 'reference' values obtained from NL-RHA. Last of all, research is concluded in Chapter 6.

CHAPTER II

THEORETICAL BACKGROUND

The seismic demand of building beyond elastic range is determined by two major structural analysis procedures: 1) Non-Linear Response time History Analysis (NL-RHA) – a response regarded as "reference" values for evaluating the propose procedure. 2) Non-linear static analysis consists of Modal Pushover Analysis procedure (MPA), Modified Modal Pushover Analysis (MMPA) procedures, and the proposed procedures developed from MPA procedure are described in this chapter.

2.1 Response History Analysis (RHA)

The equations of motion for multistory building due to earthquake ground acceleration ($\ddot{u}_g(t)$) are as follow:

For elastic system:

$$\mathbf{m}\ddot{\mathbf{u}} + \mathbf{c}\dot{\mathbf{u}} + \mathbf{k}\mathbf{u} = -\mathbf{m}\boldsymbol{\iota}\ddot{u}_g(t) \tag{2.1a}$$

For inelastic system:

$$\mathbf{m}\ddot{\mathbf{u}} + \mathbf{c}\dot{\mathbf{u}} + \mathbf{f}_s(\mathbf{u}, \text{sign } \dot{\mathbf{u}}) = -\mathbf{m}\boldsymbol{\iota}\ddot{u}_g(t) \tag{2.1b}$$

where $\mathbf{m}$, $\mathbf{c}$, $\mathbf{k}$, $\mathbf{f}_s$, and $\boldsymbol{\iota}$ are mass, classical damping, stiffness, lateral forces at the N floor levels depending on the history of the displacements, and the influence vector equal to unity respectively. The solution determined from Eq. (2.1a) and Eq. (2.1b) is known as floor displacements relative to the ground. The solution regarded as "exact" values can be solved directly from these equations.

The right side of Eq. (2.1a) and (2.1b) can be interpreted as effective earthquake forces:

$$\mathbf{p}_{\text{eff}}(t) = -\mathbf{m}\boldsymbol{\iota}\ddot{u}_g(t) \tag{2.2}$$

the spatial distribution of forces can be defined by vector $\mathbf{s} = \mathbf{m}\boldsymbol{\iota}$; and this force can be expanded into its modal components $\mathbf{s}_n$:

$$\mathbf{s} = \sum_{n=1}^{N}\mathbf{s}_n = \sum_{n=1}^{N}\Gamma_n\mathbf{m}\boldsymbol{\phi}_n \tag{2.3}$$

Where ϕ_n is the nth elastic mode shape of vibration of the multistory building, and

$$\Gamma_n = \frac{L_n}{M_n} \qquad L_n = \phi_n^T \mathbf{m} \boldsymbol{\iota} \qquad M_n = \phi_n^T \mathbf{m} \phi_n \qquad (2.4)$$

Substituting Eq.(2.3) into Eq.(2.2), the effective earthquake forces can be expressed as

$$\mathbf{p}_{\text{eff}}(t) = \sum_{n=1}^{N} \mathbf{p}_{\text{eff},n}(t) = \sum_{n=1}^{N} -\mathbf{s}_n \ddot{u}_g(t) \qquad (2.5)$$

For linear system, when the building subjected to modal effective earthquke force, $\mathbf{p}_{\text{eff},n}(t)$, The displacement, $u(t)$, can be expressed as the modal floor displacement, $u_n(t)$, which relate with ϕ_n:

$$\mathbf{u}_n(t) = \phi_n q_n(t) \qquad (2.6)$$

where $q_n(t)$ is the modal coordinate of nth-mode

The total displacement, $u(t)$, due to effective earthquake force, $\mathbf{p}_{\text{eff}}(t)$, can be expressed as the superposition of modal coordinates:

$$\mathbf{u}(t) = \sum_{r=1}^{n} \phi_r q_r(t) \qquad (2.7)$$

Substituting Eq. (2.7) into Eq. (2.1a), and pre-multiplying both sides with ϕ_n^T, then use orthogonality properties of modes, $\phi_n^T \mathbf{m} \phi_r \equiv 0$, $\phi_n^T \mathbf{c} \phi_r \equiv 0$, and $\phi_n^T \mathbf{k} \phi_r \equiv 0$ where $r \neq n$;

$$\ddot{q}_n + 2\zeta_n \omega_n \dot{q}_n + \omega_n^2 q_n = -\Gamma_n \ddot{u}_g(t), \ n = 1,2,\ldots,N \qquad (2.8)$$

Eq. (2.8) can be interpreted as the governing equation of motion of single-degree-of-freedom (SDF) system for elastic system.

In case of inelastic system, the floor displacement of building due to $\mathbf{p}_{\text{eff},n}(t)$ can not be expressed as Eq. (2.6) because the coupling of modal coordinates due to

yielding of the structure. The "modes" other than the nth-"mode" also contribute to the system response:

$$\mathbf{u}_n(t) = \sum_{r=1}^{N} \phi_r q_r(t) \tag{2.9}$$

Consider Eq. (2.1b) subjected to $\mathbf{p}_{\text{eff},n}(t)$:

$$\mathbf{m\ddot{u}} + \mathbf{c\dot{u}} + \mathbf{f}_s(\mathbf{u}, \text{sign } \dot{\mathbf{u}}) = \mathbf{p}_{\text{eff},n}(t) \tag{2.10}$$

Substitute Eq. (2.9) into Eq. (2.10), and pre-multiply with ϕ_n^T, then use orthogonality properties of modes, $\phi_n^T \mathbf{m} \phi_r \equiv 0$, $\phi_n^T \mathbf{c} \phi_r \equiv 0$ gives

$$\ddot{q}_n + 2\zeta_n \omega_n \dot{q}_n + \frac{F_{sn}(\mathbf{q}, \text{sign } \dot{\mathbf{q}})}{M_n} = -\Gamma_n \ddot{u}_g(t) \tag{2.11}$$

where

$$F_{sn}(\mathbf{q}, \text{sign } \dot{\mathbf{q}}) = \phi_n^T \mathbf{f}_s(\mathbf{u}, \text{sign } \dot{\mathbf{u}}) \tag{2.12}$$

In Eq. (2.11), Although using the orthogonality properties can expand the degree of freedom in inertia and damping forces to be modal inertia and modal damping forces respectively, the modal coordinate remains couple in part of resisting forces, $\mathbf{f}_s$, because of yielding in structure.Typically, for inelastic system, Eq. (2.1b) is solved direclty in stead of Eq (2.11)

2.2 Modal Pushover Analysis (MPA)

Although the superposition cannot be utilized in non-linear problem because of the coupling of modes due to yielding of structure remain obtained in part of resisting force, $\phi_n^T \mathbf{k} \phi_r \neq 0$ where $r \neq n$, the effect of coupling between modes may be neglected when the contributions of "mode" other than the nth-mode are relatively small (Chopra and Goel, 2002). With this assumption, the displacements of inelastic system in term of modal coordinate can be approximated as

$$\mathbf{u}(t) \approx \sum_{n=1}^{n} \phi_n q_n(t) \tag{2.13}$$

Substituting Eq. (2.13) into Eq. (2.10), and pre-multiplying by ϕ_n^T, then by using the orthogonality property of modes the equation yields

$$\ddot{q}_n + 2\zeta_n\omega_n\dot{q}_n + \frac{F_{sn}(q_n,\text{sign }\dot{q}_n)}{M_n} = -\Gamma_n\ddot{u}_g(t) \tag{2.14}$$

The resisting force in Eq. (2.14) depend on the modal coordinate at nth-"modes", q_n.

As a result, Eq. (2.14) can be written to the governing equation of motion of SDF system by using the follwing relation:

$$q_n(t) = \Gamma_n D_n(t) \tag{2.15}$$

With this relation, the solution of Eq. (2.14) can be expressed by Eq.(2.15) where $D_n(t)$ is governed by

$$\ddot{D}_n + 2\zeta_n\omega_n\dot{D}_n + \frac{F_{sn}}{L_n} = -\ddot{u}_g(t) \tag{2.16}$$

and

$$F_{sn} = F_{sn}(D_n,\text{sign }\dot{D}_n) = \phi_n^T\mathbf{f}_s(D_n,\text{sign }\dot{D}_n) \tag{2.17}$$

Eq. (2.16) can be construed as the governing equation of motion for the nth-"mode" inelastic SDF system. In MPA procedure, the peak roof displacement of MDF system can be estimated from the peak response of SDF system , D_n, which is directly determined from Eq. (2.16). The target roof displacement of MDF system, u_{rno} can be converted from the nth-"mode" peak displacement of SDF system by using the following relation:

$$u_{rno} = \Gamma_n\phi_{rn}D_n \tag{2.18}$$

The force-deformation relation $F_{sn}/L_n - D_n$ for inelastic modal SDF systems in Eq.(2.16) is determined from the nth-"mode" pushover curve for the lateral force distribution s_n^* as following:

$$\mathbf{s}_n^* = \mathbf{m}\phi_n \tag{2.19}$$

the peak modal response, r_{no}, such as story drift, bending moment, shear force in structural members can be determined by defining the modal force in Eq.(2.19) pushing over the building height until the roof displacement reaches the target roof displacement obtained in Eq.(2.18). The peak value, r_o of the total response, can be determined by using the Square-Root-of-Sum-of-Squares (SRSS), which is valid for structures with well-separated natural frequencies.

$$r_o \approx \left(\sum_{n=1}^{N} r_{no}^2 \right)^{1/2} \tag{2.20}$$

Step-by-step MPA Procedure

Step-by-step of conventional MPA procedure, which is regularly used to estimate the seismic demand of building, is summarized as follow:

1. Compute the natural frequencies, ω_n, and modes shape vector, ϕ_n, for linearly-elastic vibration of the building.
2. For the nth-"mode", develop the base-shear versus roof-displacement $(V_{bn} - u_{rn})$ pushover curve by using the modal force distribution in Eq. (2.19).
3. Idealize the pushover curve to be the bi-linear curve with post-yield stiffness ratio α_n, yield base shear V_{bny}, yield roof-displacement (u_{rny}) (Figure 2.1) that satisfies the two criterias [by any optimization algorithm]: (a) the first linear segment shall intersect the actual curve at 60% of the idealized yield force and (b) the strain energy (area under the curve) associated with the peak response has to be the same as the area under the actual curve (Chintanapakee and Chopra, 2003b)
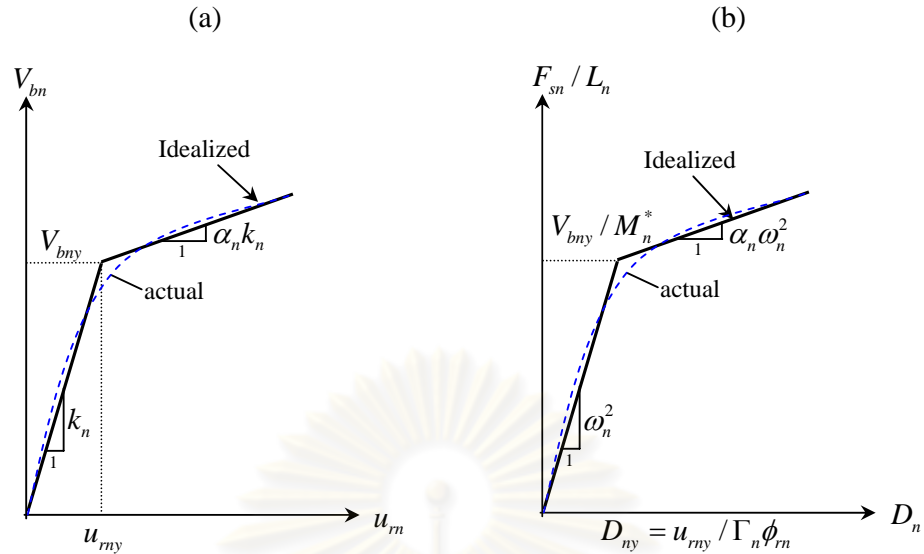
Figure 2.1 (a) Pushover curve and (b) Idealized force-deforamtion relationship of SDF system.

4. Compute the resisting yield force (V_{bny}), yield displacement (u_{rny}) and post-yield stiffness ratio (α_n) of MDF system from bi-linear curve in step 3. Next, convert the idealized pushover curve to the force-deformation ($F_{sn}/L_n - D_n$) relation of the nth-"mode" by using $F_{sny}/L_n = V_{bny}/M_n^*$, and $D_{ny} = u_{rny}/\Gamma_n\phi_{rn}$ where ϕ_{rn} is the value of mode shape at roof level.

5. Determine the peak deformation of SDF system, D_n, of nth-"mode" due to ground exitation by using NL-RHA procedure.

6. Calculate the peak roof displacement, u_{rno}, of nth-"mode" from Eq. (2.18).

7. Apply monotonic modal force, $\mathbf{s}_n^*$, for nth-"mode" push along the building height until the roof displacement reaches to the peak roof displacement, u_{rno}, in step 6. The peak response of nth-"mode" will be recorded as, r_{no}.

8. Repeat Step 2 to 7 for as many "modes" as required for sufficient accuracy.

9. Determine the total response by combining the peak demands of each mode using the SRSS modal combination rule in Eq. (2.20)

2.3 Modified Modal Pushover Analysis (MMPA)

Modified modal pushover analysis (MMPA) procedure was developed by Chopra *et al.* (2004) to reduce the computation effort of MPA procedure in estimating seismic demands. The additional assumption of MMPA is that responses of higher modes were assumed to be linearly elastic.

Summarized below are the steps of MMPA for estimating the peak inelastic response of building subjected to ground excitation.

1. Compute the natural frequencies, ω_n, and modes shape vector, ϕ_n, for linearly-elastic vibration of the building.
2. For the fundamental mode (1$^{\text{st}}$ "mode"), calculate the peak response of first mode, r_{1o}, as described in step 2 to 7 in MPA procedure.
3. Develop the base-shear versus roof-displacement $\left(V_{bn} - u_{rn}\right)$ pushover curve by modeling the structural system as linearly elastic.
4. Idealize the pushover curve in step 3 to be the force-deformation relationship of elastic-SDF system
5. Determine the peak deformation of elastic-SDF system, D_n, of nth-"mode" from RHA procedure.
6. Calculate the peak roof displacement, u_{rno}, of nth-"mode" from Eq. (2.18)
7. Apply monotonic modal force, $\mathbf{s}_n^*$, for nth-"mode" push over the building height until the roof displacement reaches the peak roof displacement, u_{rno}, in step 6. The peak response of nth-"mode" is recorded as, r_{no}.
8. Repeat Step 2 to 7 for as many "modes" as required for sufficient accuracy.
9. Determine the total response by combining the peak demands of each mode using the SRSS modal combination rule in Eq. (2.20)

2.4 Proposed Extension of MPA Procedure for Degrading Structures

In order to estimate seismic demands of building components due to an earthquake ground motion in application of the MPA procedure, the peak (target) roof displacement needs to be estimated to quantify the global seismic demand. Most of

the methods for this estimation are based on using response of an equivalent single-degree-of-freedom (SDF) system that does not explicitly account for degradation behaviour; hence, they may not be suitable procedure for reinforced-concrete (RC) buildings. This proposed procedure suggests that the equivalent SDF system should include the effects of degradation, and its degrading properties can be determined from cyclic pushover analysis. Therefore, the cyclic lateral load for developing the cyclic pushover curve is included.

2.4.1 Cyclic modal pushover analysis (CMPA)

The main objective for using the cyclic load to develop the cyclic pushover curve is to investigate the characteristic of degradation on cyclic behavior of the global system (whole structure). The cyclic load with an invariant vertical distribution, s_n^*, of lateral forces is applied to the buildings whereas the target roof displacement is imposed by the displacement history protocol as shown in Figure 2.2, and the description of this protocol is shown in Table 2.1.
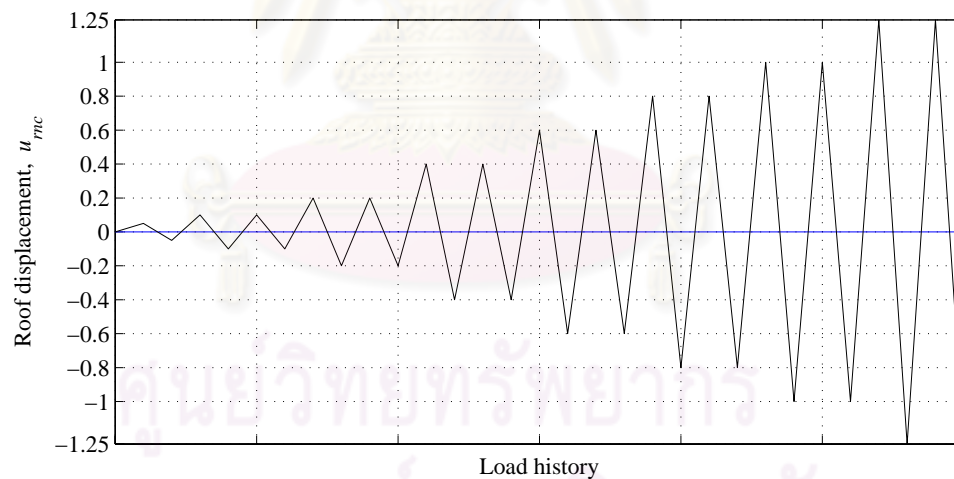
Figure 2.2 Displacement history of roof displacement according to the modified-ISO protocol.

Table 2.1: Displacement history of the modified-ISO protocol

No. of cycles	1	2	2	2	2	2	2	2
Displacement	$0.05\,u_{rnc}$	$0.1\,u_{rnc}$	$0.2\,u_{rnc}$	$0.4\,u_{rnc}$	$0.6\,u_{rnc}$	$0.8\,u_{rnc}$	u_{rnc}	$1.25\,u_{rnc}$

This displacement history protocol is modified from the ISO displacement protocol that has been used in Krawinkler (2009).
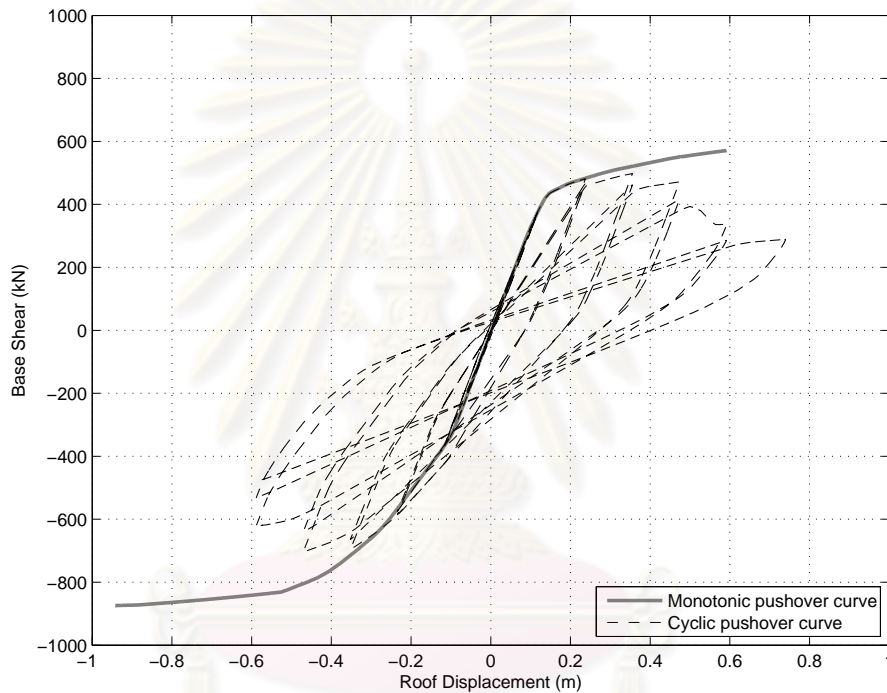
Figure 2.3 1st mode-monotonic and cyclic pushover curve of a real RC 8-story building due to the invariant lateral force, $\mathbf{s}_1^*$

Figure 2.3 shows the skeleton of cyclic pushover curve including stiffness and strength degradation. The monotonic pushover curve can be interpreted as the envelop curve of roof displacement-base shear relationship whereas the cyclic pushover curve presents the rate of stiffness and strength deterioration. Therefore, the force-deformation relation of an equivalent-degrading SDF system should be able to represent the degradation behavior of the degrading-MDF system. The properties of the degrading equivalent SDF system can be determined from non-linear static pushover analysis of the MDF-system model of the building in 2 states: (1) monotonic

pushover analysis to obtain the envelop curve, and (2) cyclic pushover analysis to obtain the degradation parameters.

Step-by-step of Proposed Procedure

State 1: Monotonic pushover analysis

1. Compute the natural frequencies, ω_n, and mode shape vectors, ϕ_n, for linearly elastic vibration modes of the building.

2. For the nth-'mode', develop the base-shear versus roof-displacement $(V_{bn} - u_{rn})$ pushover curve by using the modal force distribution in Eq. (2.19).

3. Idealize the pushover curve as a tri-linear curve obtaining yield base-shear (V_{bny}), yield roof-displacement (u_{rny}), the post–yield stiffness ratio (α), capping base-shear (V_{bnc}), capping roof-displacement (u_{rnc}), and post-capping (α_{cap}) as shown in Figure 2.4a. that satisfies the three criterias: (a) the first linear segment shall intersect the actual curve at 60% of the idealized yield force and (b) the strain energy (area under the curve) associated with the peak response has to be the same as the area under the actual curve, and (c) capping base-shear (V_{bnc}) in idealized curve to be the same as the peak base-shear obtained in pushover curve.

4. Convert the idealized pushover curve, which is the envelop curve, to the force-deformation $(F_{sn}/L_n - D_n)$ relation of the nth-'mode' inelastic-degrading SDF system (Figure 2.4b) by $F_{sny}/L_n = V_{bny}/M_n^*$, and $D_{ny} = u_{rny}/\Gamma_n\phi_{rn}$ where ϕ_{rn} is the value of mode shape at roof level.

(a) Idealized Pushover Curve
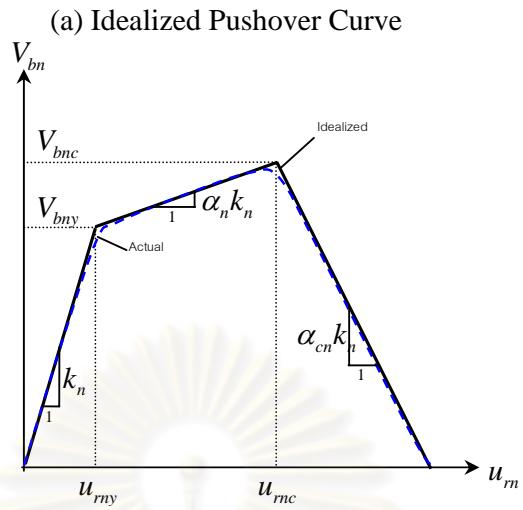
(b) $F_{sn}/L_n - D_n$ Relationship
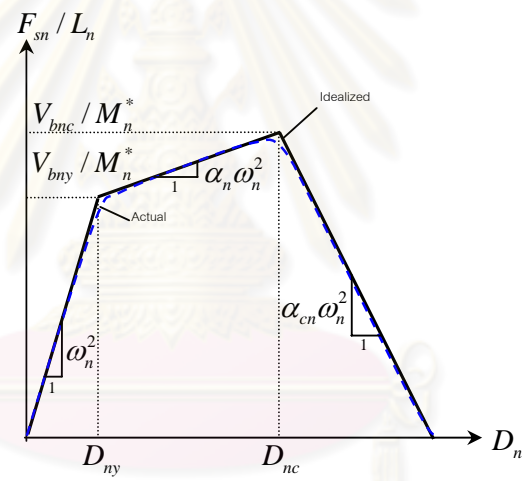
Figure 2.4 Properties of the nth-"mode" inelastic degrading SDF system from the monotonic pushover curve.

State 2: Cyclic pushover analysis

After developing the envelop curve by monotonic pushover analysis, cyclic pushover analysis is the second stage for calculating the degradation parameters and estimating target roof displacement of degrading-MDF system.

Summarized below are steps of cyclic pushover analysis for determining the peak response, D_n, of inelastic-degrading SDF system.

5. For the nth-'mode', develop the cyclic pushover curve $\left(V_{bn} - u_{rn}\right)$ by using the force distribution in Eq. (2.19) followed by the load history protocol in Table 2.1.

6. At the same mode, determine the degrading parameter of an equivalent degrading SDF system by trial and error those values of degrading parameters until the cyclic force-deformation $\left(F_{sn}/L_n - D_n\right)$ relation of that mode is consistent with the cyclic pushover curve $\left(V_{bn} - u_{rn}\right)$ in step 5.

7. Compute the peak deformation, D_n, of the nth-'mode' inelastic system with the degradation parameter determined from step 6 by using NL-RHA.

8. Calculate the peak roof displacement u_{rno} associated with the nth-'mode' inelastic degrading SDF system form Eq. (2.18).

9. Extract other desired responses, r_{no}, from the pushover database when roof displacement equals to u_{rno}.

10. Repeat Steps 2-9 for as many 'modes' as required for sufficient accuracy.

11. Determined the total response by using Eq. (2.20).

CHAPTER III

EXAMPLE STRUCTURES, GROUND MOTIONS, AND RESPONSE STATISTICS

3.1 Introduction

The building systems that include the effect of degradation are selected from two sets: (1) a real 8-story RC frame building which was not designed for earthquake resistance; and (2) Generic frames that was designed based on the strong-column weak-beam concept. The details for these buildings are described in this section.

3.2 Example Structures

3.2.1   Real 8-story RC building.

The real 8-story RC building is used for classrooms and offices in Chulalongkorn University, Bangkok. The total height is 27.9 m, the total length is 66 m and the total width is 17 m as shown in Figure 3.1.

Figure 3.1 Photograph of the real 8-story building

The cross section of the left-most column has dimensions of 0.40 x 0.40 m throughout the height, whereas the dimensions of the middle and right-most columns (Figure 3.2) are 0.40 x 0.60 m. The slab between the middle and right columns is 12 cm thick, whereas the rest is 10 cm thick. The reinforcement in all beams and columns are shown in Figure 3.2.
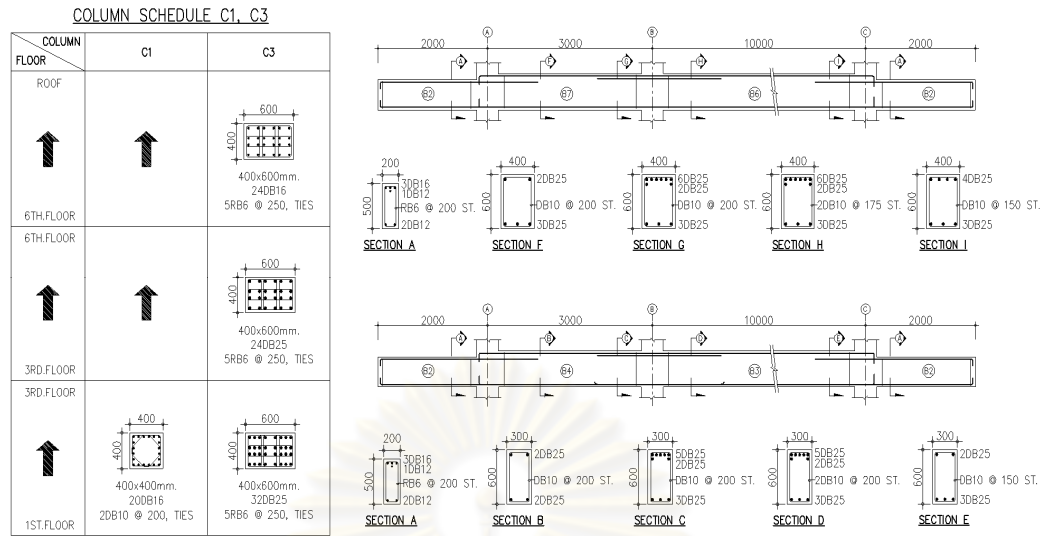
Figure 3.2 Cross section of all beams and columns. All dimensions are in millimetres. "DB" denotes deformed bar, whereas the following number indicates the diameter of rebar in mm.

The lateral force resisting system consists of RC moment-resisting frames which are rather regular vertically and horizontally. Therefore, the analysis of this building considers the response of a typical 2-dimensional frame along the shorter dimension of the building floor plan with the tributary width of 4 meters. The concrete compressive strength is 23.5 MPa and the nominal yield strength of longitudinal steel is 392 MPa. There is no infill-masonry in the typical frame where the space between the columns is used for classroom and corridor. This building is assumed to have Rayleigh damping with 5% damping ratio in the first and second modes. The total weight of this frame is 303 tons. The modal natural periods of vibration are shown in Table 3.1.

Table 3.1 Modal natural periods of the real 8-story building.

Mode	1	2	3	4	5
Period (sec)	1.511	0.460	0.265	0.178	0.134

The nonlinear plastic-hinge elements were included at both ends of the beams and columns to simulate plastic deformation when bending moment exceeds the yield moment of the cross section as shown in Figure 3.3.
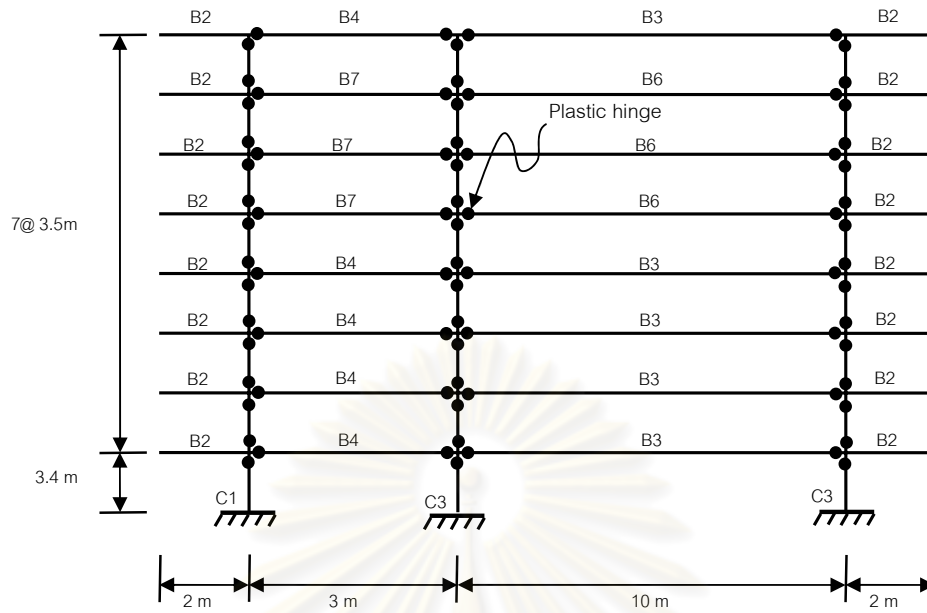
Figure 3.3 Plastic-hinge model of a real RC 8-story building.

3.2.2 Generic frames

The second set of structures consists of one-bay generic frames, which are 3-, 6-, 9-, 12-, 15-, and 18-story tall (Figure 3.4).

3-story   6-story   9-story 12-story 15-story 18-story

Figure 3.4 Generic one-bay 3, 6, 9, 12, 15, and 18-story frames used in this study.

These frames are used to extend the accuracy evaluation of the proposed procedure to more cases of structural periods and strength levels. They are similar to the 'regular' generic frames used by Chintanapakdee and Chopra (2003) with the exception that the strength level of the frames in this study is defined in term of yield-strength reduction factor (R) equals to 2, 4, and 6. Each building corresponds to the fundamental vibration period, T_1, equals to

$$T_1 = 0.028 H^{0.8} \tag{3.1}$$

where H is the height of the frame measured in feet.

The stiffness distribution of these frames is designed to achieve equal drifts in all stories under the lateral forces specified in the International Building Code (IBC2000)

$$F_i = V_b \frac{w_i h_i^k}{\sum\limits_{j=1}^{N} w_j h_j^k} \tag{3.2}$$

where
$$k = \begin{cases} 1 & T_1 \le 0.5\,\text{sec} \\ (T_1 + 1.5)/2 & 0.5 < T_1 < 2.5\,\text{sec} \\ 2 & T_1 \ge 2.5\,\text{sec} \end{cases} \tag{3.3}$$

F_i, w_i, h_i, and V_b are lateral forces, story weight, the elevation at ith-floor, and total base shear respectively.

In each story, the second moment of cross sectional area of the beam and its supporting columns are assumed to be the same. Each frame has the story height of 3.66 m and the beam span of 7.32 m. The weight of each floor is 90806 kg (200 kips). These frames were designed according to the strong-column weak-beam concept, so plastic hinges would occur only at the beam ends and the base of the first story columns (Figure 3.5).
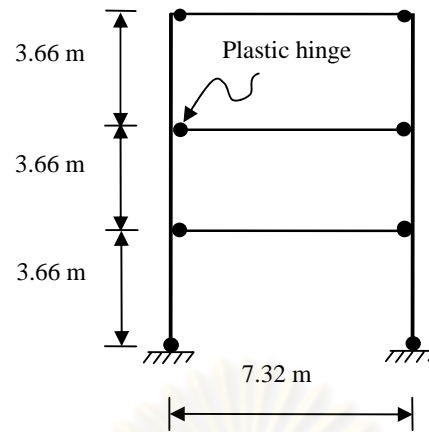
Figure 3.5 Beam-hinge model of the 3-story one-bay generic frame.

The modal vibration period, T_n, of the first-five modes for these frames is shown in Table 3.2.

Table 3.2 First-five modal natural periods of generic frames

Mode	Modal vibration period, T_n					
	Number of stories					
	3	6	9	12	15	18
1	0.492	0.857	1.186	1.492	1.784	2.064
2	0.164	0.323	0.458	0.580	0.693	0.799
3	0.074	0.178	0.268	0.348	0.422	0.491
4	-	0.109	0.177	0.238	0.294	0.346
5	-	0.073	0.125	0.174	0.219	0.261

3.3 Modeling of Degrading Structures

The nonlinear material model including the effect of stiffness and strength degradations is described in this section. In this study, the nonlinear behavior of structure is appeared when the bending moment of building component due to earthquake force exceed the yielding moment.

3.3.1 Plastic hinge model

The moment-rotation relation of the plastic hinge was selected to denote the inelastic behavior of the structural members. Typical moment-rotation hysteretic rule

of the plastic hinge in degrading systems used in this study can be shown schematically in Figure 3.6.
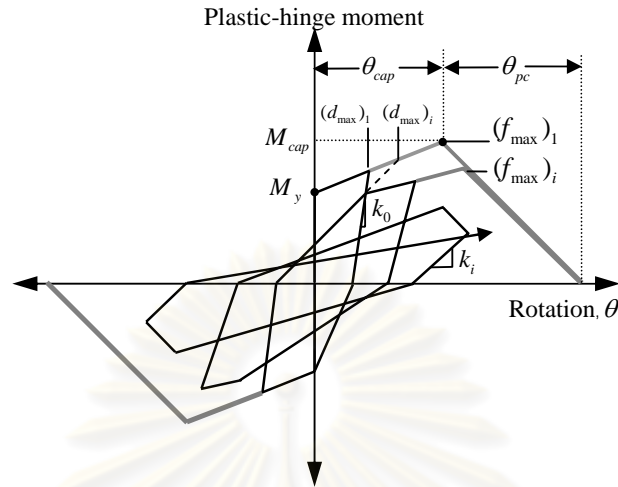
Figure 3.6 Moment-rotation relationship of the plastic hinge in the degrading system.

The envelope curve which delineates the upper bound of the moment-rotation relation, is defined by a tri-linear curve governed by four parameters: yielding moment (M_y), maximum moment capacity (M_{cap}), plastic rotation capacity (θ_{cap}) and post-capping rotation capacity (θ_{pc}). Determination of these paremeters and their degrading parameters that define the hysteresis behavior of plastic hinge are described in the next section.

3.3.2 Types of degradation behaviors

In this study, the moment-rotation relation of the plastic hinge model includes three damage rules: (1) unloading stiffness degradation, (2) reloading stiffness degradation and (3) strength degradation. From the hysteretic rule, the degree of degradation in each damage rule is controlled by a damage index according to the following equations:

$$k_i = k_0 \cdot \left(1 - \delta k_i\right) \tag{3.4}$$

$$\left(d_{\max}\right)_i = \left(d_{\max}\right)_0 \cdot \left(1 + \delta d_i\right) \tag{3.5}$$

$$\left(f_{\max}\right)_i = \left(f_{\max}\right)_0 \cdot \left(1 - \delta f_i\right) \tag{3.6}$$

where k_0, $(d_{max})_0$, and $(f_{max})_0$ are initial unloading stiffness, maximum historic deformation, initial envelope maximum strength respectively; k_i, $(d_{max})_i$, and $(f_{max})_i$ are unloading stiffness, deformation defining the end of the reloading cycle, current envelope maximum strength respectively at time t_i; δk_i, δd_i, and δf_i are damage indices of unloading stiffness, reloading stiffness, and strength degradation respectively as proposed by Park and Ang (1985). Each damage index depends on four parameters ($\gamma K1, \gamma K2$, $\gamma K3$, and $\gamma K4$ for δk_i; $\gamma D1$, $\gamma D2$, $\gamma D3$, and $\gamma D4$ for δd_i; and $\gamma F1$, $\gamma F2$, $\gamma F3$, and $\gamma F4$ for δf_i), peak ductility $\left(\tilde{d}_{max} = d_{max,i}/d_{cap}\right)$ and accumulated dissipated energy (E_i) as the following equations:

$$\delta k_i = \left(\gamma K1 \cdot \left(\tilde{d}_{max}\right)^{\gamma K3} + \gamma K2 \cdot \left(\frac{E_i}{E_{monotonic}}\right)^{\gamma K4} \right) \tag{3.7}$$

$$\delta d_i = \left(\gamma D1 \cdot \left(\tilde{d}_{max}\right)^{\gamma D3} + \gamma D2 \cdot \left(\frac{E_i}{E_{monotonic}}\right)^{\gamma D4} \right) \tag{3.8}$$

$$\delta f_i = \left(\gamma F1 \cdot \left(\tilde{d}_{max}\right)^{\gamma F3} + \gamma F2 \cdot \left(\frac{E_i}{E_{monotonic}}\right)^{\gamma F4} \right) \tag{3.9}$$

where maximum energy dissipation capacity is defined by energy dissipated under monotonic loading multiplied by an additional parameter (γE):

$$E_{monotonic} = \gamma E \left(\int_{\substack{monotonic\ load\ history}} dE \right) \tag{3.10}$$

This hysteretic rule is available as a material model called "Pinching4" (Lowes *et al.* 2003) in Open System for Earthquake Engineering Simulation (OpenSees) software, which is used as the main structural analysis program for this research.

3.3.3 *Real 8-story RC building.*

For real 8-story RC building, the shear capacity of cross section was assumed to be larger than moment capacity. Therefore, the failure mode of RC members was

occured only in flexure mode. The example for calculating the bending and shear capacity of RC column was shown in Appendix C.

The moment-rotation relation parameters governing the envelop curve for the real 8-story RC building can be determined from Panagiotakos and Fardis (2001) for yeiding moment (M_y), and from predictive equation developed by Haselton and Deierlein (2007) for other parameters.

Currently, there is no method to calculate the value of degradation parameters: $\gamma K1, \gamma K2$, $\gamma K3$, $\gamma K4$, $\gamma D1$, $\gamma D2$, $\gamma D3$, $\gamma D4$, $\gamma F1$, $\gamma F2$, $\gamma F3$, $\gamma F4$, and γE, appropriate for a real structure, so those values used in this study were obtained by calibrating the above hysteretic rule with test results from a physical model of a non-ductile RC column tested by Sezen (2000). The force-displacement relation of the column specimen subject to cyclic loading is plotted as a solid line in Figure 3.7.
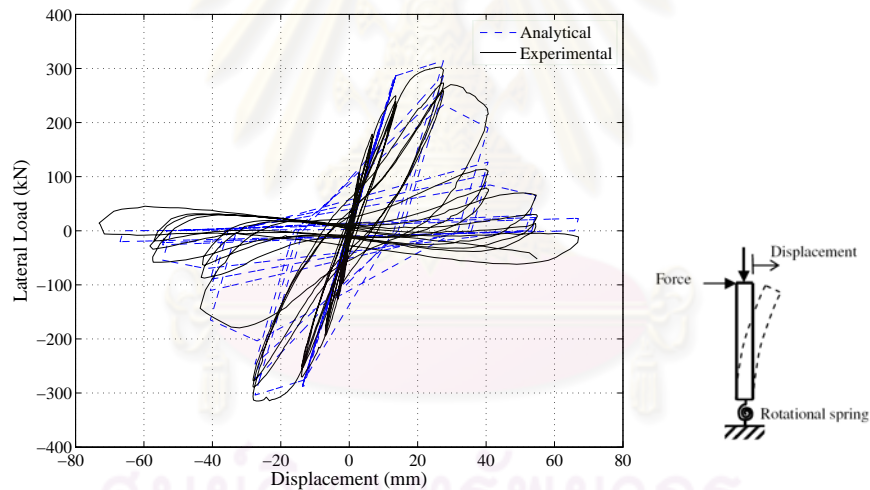
Figure 3.7 Comparison of force-displacement relation from laboratory test of a physical model (Sezen 2000) and numerical model considering stiffness and strength degradation of the plastic hinge.

The analytical model of the column specimen was modelled as cantilever column with a degrading plastic hinge at the base. The degrading parameters were determined by trial and error until the force and displacement relationship in analytical model became consistent with the experimental results. The calibrated degradation parameters of a plastic hinge are shown in Table 3.2; and they will be used for all plastic hinges in this study.

Table 3.3 Stiffness and strength degradation parameters of the plastic hinge model obtained from the calibration against experimental results of Sezen (2000)

Degrading Parameters for a plastic hinge		
Unloading Stiffness Degradation	$\gamma K1$	0.00
	$\gamma K2$	1.00
	$\gamma K3$	0.00
	$\gamma K4$	1.00
Reloading Stiffness Degradation	$\gamma D1$	0.50
	$\gamma D2$	0.00
	$\gamma D3$	1.00
	$\gamma D4$	0.00
Strength Degradation	$\gamma F1$	0.00
	$\gamma F2$	1.00
	$\gamma F3$	0.00
	$\gamma F4$	1.10
Energy Dissipation	γE	4.50

3.3.4 Generic frames

In case of generic frames, the capping moment (M_{cap}), plastic rotation capacity (θ_{cap}) and post-capping rotation capacity (θ_{pc}) were calibrated from the experimental results as shown in Table 3.4, while the degradation parameters were also used in a real 8-story RC building.

Table 3.4 Moment-rotation relation parameters of the generic frame.

$M - \theta$ parameters	M_{cap}	θ_{cap}	θ_{pc}
Values	$1.13\,M_y$	0.0115	0.0555

3.4 Ground Motions

A set of 20 Large-Magnitude-Small-distance (LMSR) records used in this study were selected from California earthquake records of magnitude ranging from 6.6 to 6.9 recorded at distances of 13 to 30 km on firm soil (Chintanapakdee and

Chopra 2003b). The ground acceleration time histories of the LMSR ensemble (Listed in Table 3.5) are shown in Figure 3.8.
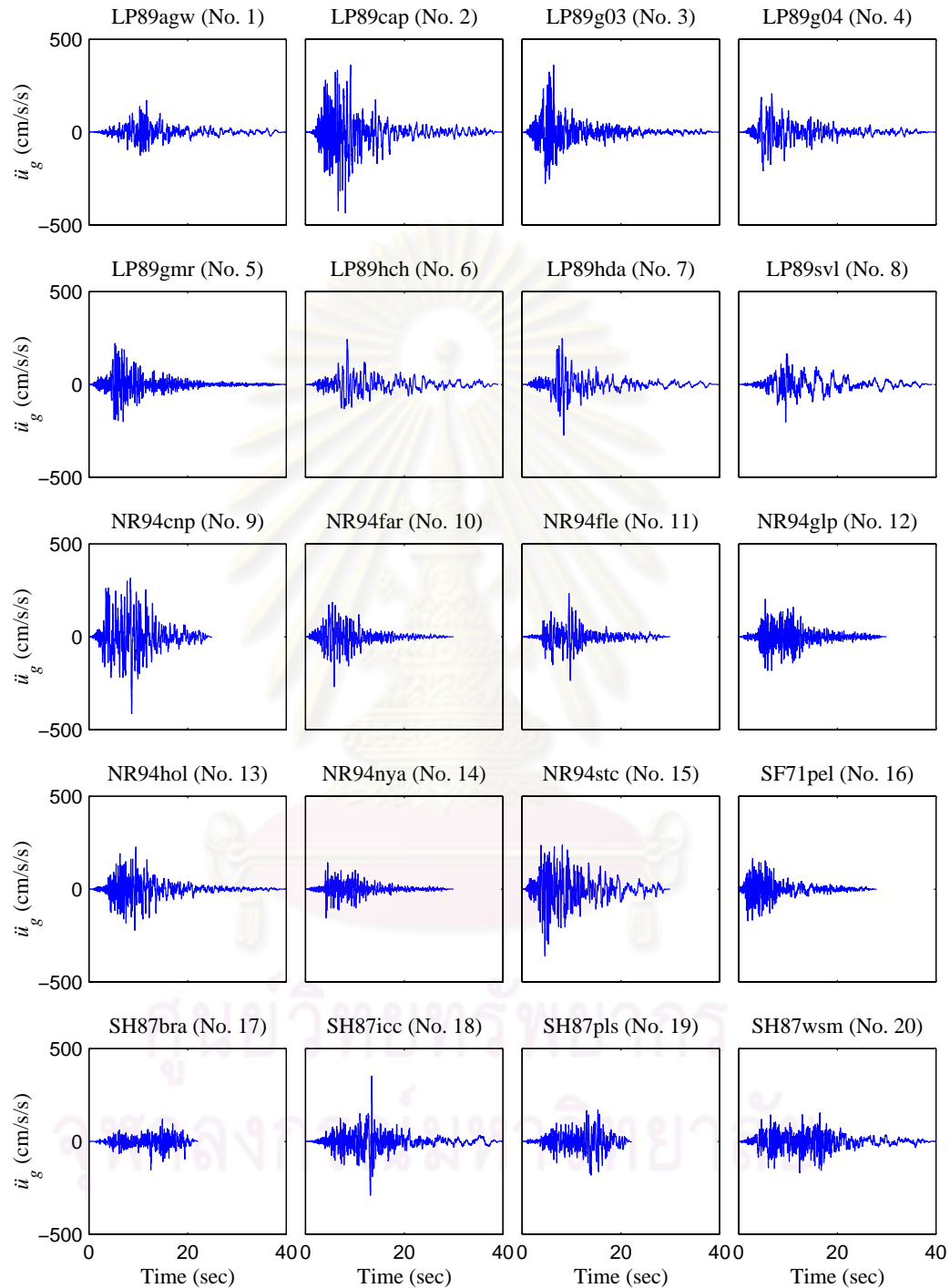
Figure 3.8 LMSR ensemble of 20 ground motions: ground accelerations.
(Chintanapakdee and Chopra, 2003).

Table 3.5 Lists of ground motion records in LMSR ensemble

No.	Earthquake Name	Recording station	Magnitude	Distance to fault rupture (km)	PGA (cm/s^2)
1	1989 Loma Prieta	Agnews State Hospital	6.9	28.2	169
2	1989 Loma Prieta	Capitola	6.9	14.5	435
3	1989 Loma Prieta	Gilroy Array #3	6.9	14.4	360
4	1989 Loma Prieta	Gilroy Array #4	6.9	16.1	208
5	1989 Loma Prieta	Gilroy Array #7	6.9	24.2	221
6	1989 Loma Prieta	Hollister City Hall	6.9	28.2	242
7	1989 Loma Prieta	Hollister Diff Array	6.9	25.8	274
8	1989 Loma Prieta	Sunnyvale–Colton Ave.	6.9	28.8	203
9	1994 Northridge	Canoga Park–Topanga Canyon	6.7	15.8	412
10	1994 Northridge	LA-N Faring Rd	6.7	23.9	268
11	1994 Northridge	LA-Fletcher Dr	6.7	29.5	236
12	1994 Northridge	Flendale–Las Palmas	6.7	25.4	202
13	1994 Northridge	LA–Hollywood Stor FF	6.7	25.5	227
14	1994 Northridge	La Crescenta–New York	6.7	22.3	156
15	1994 Northridge	Northridge–Saticoy St	6.7	13.3	361
16	1971 San Fernando	LA–Hollywood Stor Lot	6.6	21.2	171
17	1987 Supersitition Hills	Brawley	6.7	18.2	153
18	1987 Supersitition Hills	El Centro Imp. Co. Center	6.7	13.9	351
19	1987 Supersitition Hills	Plaster City	6.7	21.0	182
20	1987 Supersitition Hills	Westmorland Fire Station	6.7	13.3	169

when analyzing the example 8-story RC building, these ground motions are scaled to three different intensity levels such that the spectral acceleration at the fundamental period of the building, $A(T_1)$, equal to 0.208g, 0.50g, and 0.70g to investigate the deterioration of the method as the structure experiences more yielding and damage. The value of $A(T_1) = 0.208g$ corresponds to the elastic design spectrum for Chiang Mai province in the northern part of Thailand, which has the highest seismic risk. Figure 3.7 shows the median spectrum of the scaled ground motions.
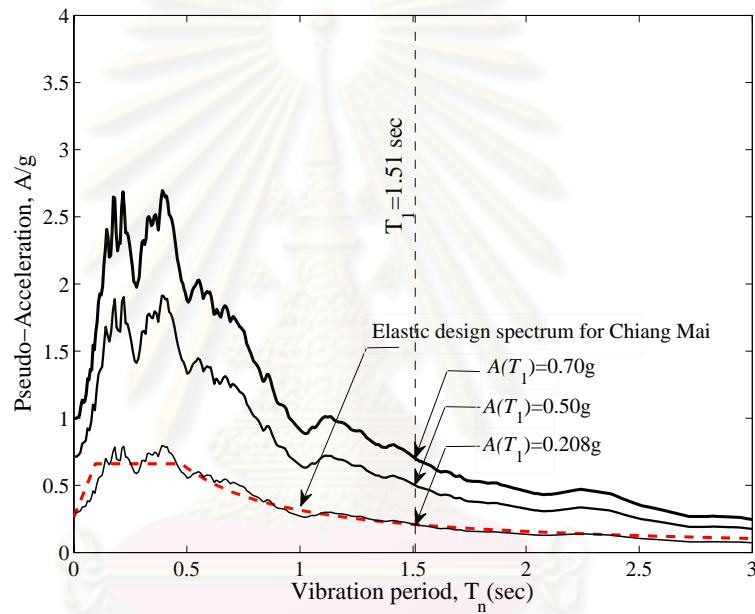
Figure 3.9 Median of the scaled ground motion such that $A(T_1)$=0.208g, 0.50g, and 0.70g.

For analysis of the generic frames, each record was scaled such that $A(T_1)$ equate to the median value of the elastic spectral acceleration of un-scaled ground motions because this value was used as the reference elastic demand in the strength design of the generic frames. Figure 3.8 shows the pseudo-acceleration spectra of the scaled ground motions used in the analysis of the 3-, 6-, 9-, 12-, 15-, and 18-story generic frames.
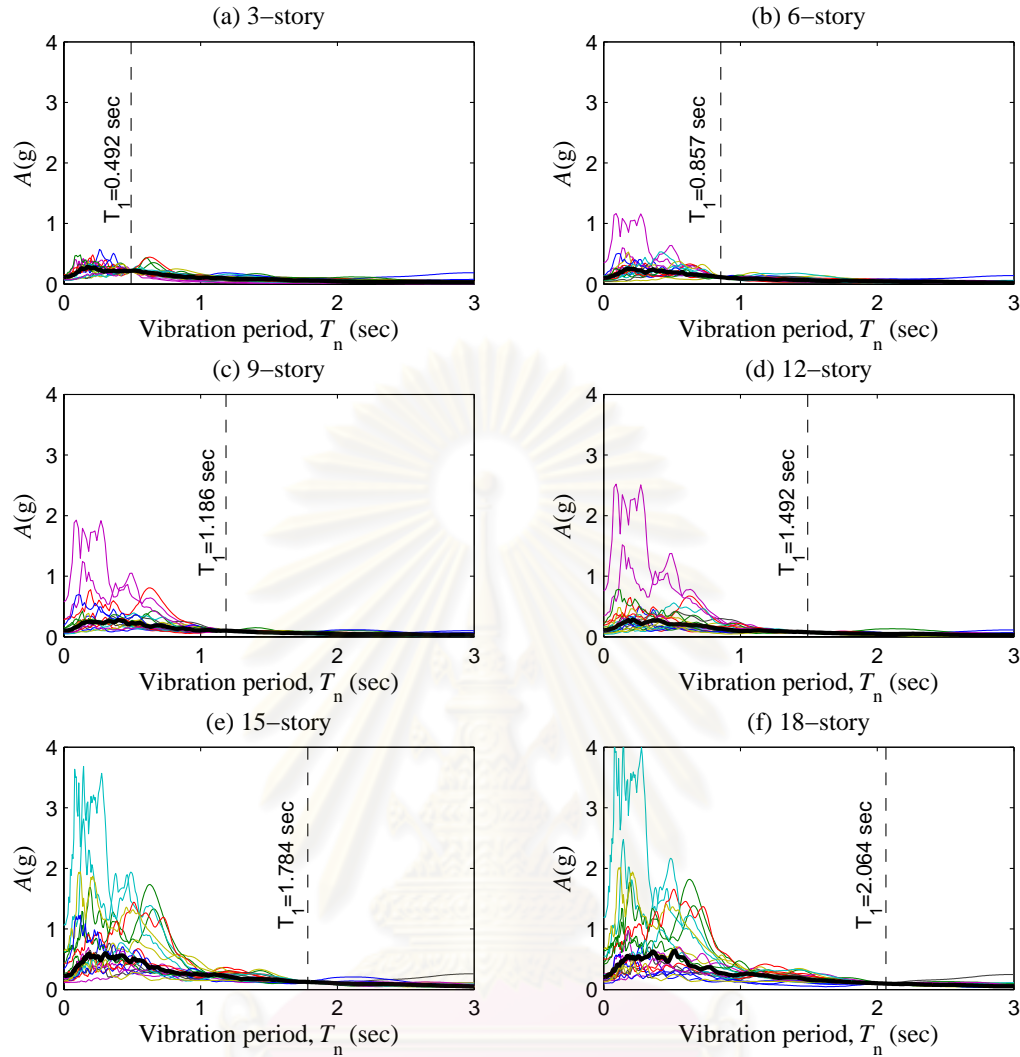
Figure 3.10 Pseudo-acceleration spectra of individual records and their median value used in the analysis of the 3-, 6-, 9-, 12-, 15-, and 18-story generic frame; damping ratio, $\zeta = 5\%$.

3.5 Response Statistics

The seismic demands of each structural system to each set of a 20 ground motions were determined by the two procedures: 1) the nonlinear static analysis asscoiated with the MPA procedure and the proposed procedure. 2) the nonlinear reponse time history analsysis (NL-RHA) which its solution regarded as "reference" values. The seismic demands estimated by the MPA, and the propose procedure will be compared with the NL-RHA solution in term of the ratio: $r^*_{MPA} = r_{MPA} \div r_{NL-RHA}$,

$r^{*}_{Proposed} = r_{Proposed} \div r_{NL-RHA}$ where r_{MPA}, $r_{Proposed}$, and r_{NL-RHA} are denoted as the response estimated from the MPA, proposed procedure, and NL-RHA respectively. The data was evaluated in term of the median of the response ratio. If the ratio is close to unity, the proposed procedure provides good estimate seismic demand. In this study, Assuming that the distribution of the data is lognormal, the median of 20 response values is calculated as the geometric mean and the dispersion is calculated as the standard deviation of the logarithm of the data:

$$\hat{x} = \exp\left[\frac{\sum_{i=1}^{n} \ln x_i}{n}\right] \tag{3.11}$$

$$\delta = \left[\frac{\sum_{i=1}^{n}(\ln x_i - \ln \hat{x})^2}{n-1}\right]^{1/2} \tag{3.12}$$

3.5.1 Number of "modes" considered in the proposed procedure.

In this study, the sufficient numbers of "modes" will be considered to two sets of the example structures: 1) 3-"modes" for a real RC 8-story building, and 2) 2 for 3-story building, 3 for 6-story building, 4 for 9-, and 12-story buildings, and 5 for 15- and 18-story buildings.

CHAPTER IV

TARGET ROOF DISPLACEMENT OF DEGRADING STRUCTURES

4.1 Estimating Target Roof Displacement by Using Response of Degrading Equivalent SDF System.

According to the proposed procedure, the peak (target) roof displacement of a degrading-MDF system is relevant to the deformation of an equivalent degrading-SDF system. The stiffness and strength degradation parameters, controlling the force-deformation relation of an equivalent degrading-SDF system, can be calculated from the cyclic pushover curve as explained in Chapter 2.

Chapter four investigates the basic premise that the roof displacement of the degrading structure can be determined from the deformation of an equivalent degrading-SDF system by only considering the fundamental period. The target roof displacement of a real 8-story building and the generic frames estimated from the proposed procedure are compared to the "reference" value determined rigorously by NL-RHA. The statistics described in chapter 3 is adopted to evaluate the accuracy of this procedure.

4.1.1 Using Monotonic Pushover Analysis Develops the envelop curve

Only the fundamental mode is considered in this Chapter; thus, the vertical force distribution proportional to the effective modal force in the fundamental mode ($\mathbf{s}_n^* = \mathbf{m}\phi_n$; $n = 1$) is used in all pushover analyses in this Chapter.

Refer to the proposed procedure described in section 2.4, the envelope curve of global system (degrading MDF system) can be developed by the monotonic pushover analysis. In figure 4.1, the envelop curve of the example 8-story building is shown as a dashed line. This curve is idealized to a tri-linear system (solid line) in order to determined yield base-shear (V_{b1y}), yield roof-displacement (u_{r1y}), the post – yield stiffness ratio (α), capping base-shear (V_{b1c}), capping roof-displacement (u_{r1c}), and post-capping (α_{cap}).
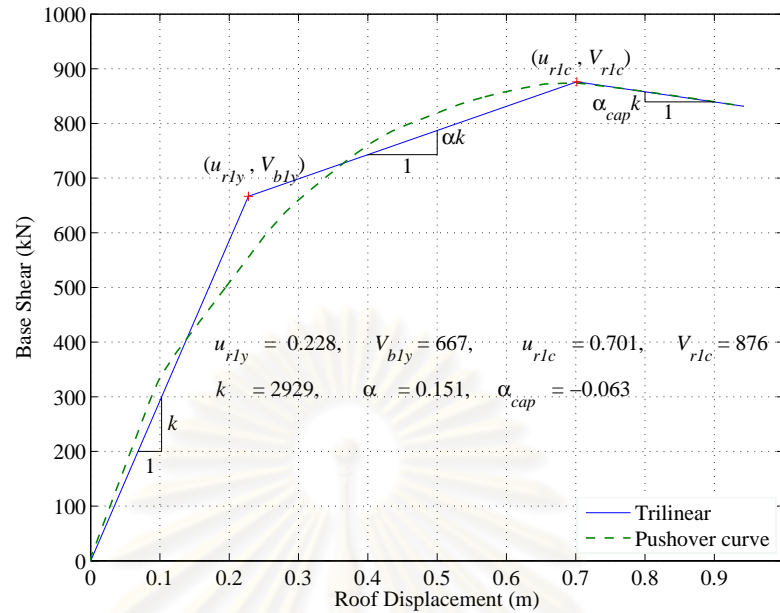
Figure 4.1 Monotonic pushover curve of the real RC 8-story building idealized as a tri-linear force-displacement relationship.

The envelop curve of global system $(V_b - u_r)$ is converted to force and deformation relation of equivalent SDF system ($F_s / L_1 - D_1$) by

$$F_y / L_1 = V_{by} / M_1^* \qquad \text{and} \qquad D_y = u_{ry} / \Gamma_1 \phi_{r1} \qquad (4.1)$$

$$F_{cap} / L_1 = V_{cap} / M_1^* \qquad \text{and} \qquad D_{cap} = u_{cap} / \Gamma_1 \phi_{r1} \qquad (4.2)$$

where M_1^* is the effective modal mass (Chopra and Goel 2002).

4.1.2 Using Cyclic Pushover Analysis determines degradation parameters

The next step is to determine the degrading parameter of an equivalent-degrading SDF system. The cyclic pushover curve is developed by applying the cyclic modal force, $\mathbf{s}_n^*$, along the buidling height, and control the roof displacement by modified-ISO displacement history protocol. The cyclic pushover curve of the example 8-story building is shown in Figure 4.2.
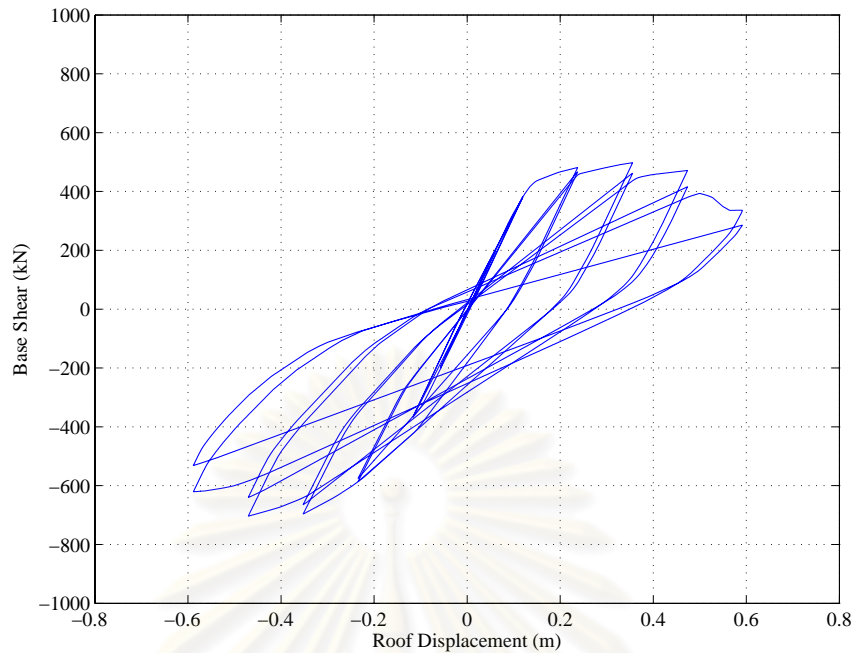
Figure 4.2 Cyclic pushover curve of a real RC 8-story building due to $\mathbf{s}_1^* = \mathbf{m}\phi_1$

The degrading parameters of an equivalent degrading SDF system are determined by trial and error until the force and displacement relationship of SDF system become consistent with the cyclic pushover curve of MDF system as shown in Figure 4.3.

Figure 4.3 Comparisons of cyclic pushover curves and hysteresis loop of equivalent SDF system using modified-ISO load history protocol.

The degrading parameters of an equivalent SDF system for the real RC 8-story building are shown in Table 4.1.

Table 4.1 Stiffness and strength degradation parameters for the real RC 8-story building determined from cyclic pushover curve.
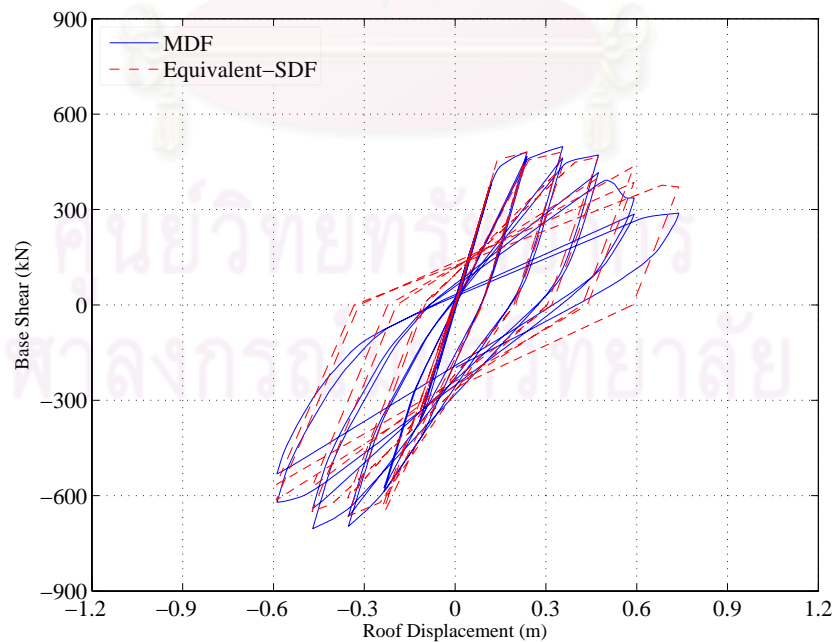
Degrading parameters		Modified-ISO
γK	$\gamma K1$	1.22
	$\gamma K2$	0.30
	$\gamma K3$	0.82
	$\gamma K4$	0.90
γD	$\gamma D1$	0.00
	$\gamma D2$	1.78
	$\gamma D3$	1.21
	$\gamma D4$	1.02
γF	$\gamma F1$	0.42
	$\gamma F2$	0.72
	$\gamma F3$	1.08
	$\gamma F4$	0.65
γE		2.84

Then, contain the parameters D_{1y}, F_{1y}, $D_{1,cap}$, $F_{1,cap}$, α, and α_{cap} that control the envelop curve; and the degradation parameter controlling hysteresis loop into the analytical model and Determined the maximum deformation of an equivalent degrading-SDF system, D_1, by using NL-RHA. The result of this example building and the accuracy of this procedure will be discussed in section 4.3.

4.2 Sensitivity of Degradation Parameters

To capture the degradation behaviour of the structure, the cyclic loads with an invariant vertical distribution of lateral forces were applied to the buildings, while the roof displacement was being monitored and controlled. The roof displacement history (protocol) can be chosen in many possible ways, so this study refers to three load history protocols that have been used in the literature (Krawinkler 2009): (1) ATC-24,

(2) ISO, and (3) SPD protocols as shown in Tables 4.2 to 4.4, and Figures 4.3a to 4.3c, respectively.

Table 4.2 ATC-24 displacement history

No.of cycles	3	3	3	3	3	3	3
Displacement	$0.5\,u_{rny}$	$0.8\,u_{rny}$	u_{rny}	$2\,u_{rny}$	$3\,u_{rny}$	$4\,u_{rny}$	$5\,u_{rny}$

Table 4.3 ISO displacement history

No.of cycles	1	2	3	3	3	3	3	3
Displacement	$0.05\,u_{rnc}$	$0.1\,u_{rnc}$	$0.2\,u_{rnc}$	$0.4\,u_{rnc}$	$0.6\,u_{rnc}$	$0.8\,u_{rnc}$	u_{rnc}	$1.25\,u_{rnc}$

Table 4.4 SPD displacement history

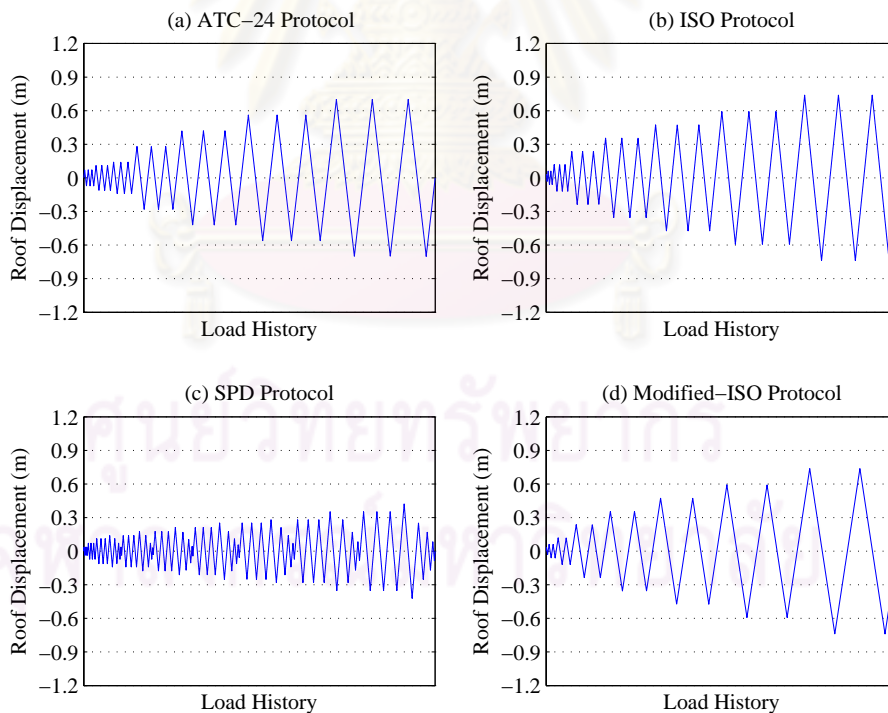| No.of cycles	3	3	3	1	1	1	1	3	…
Displacement	$0.25\,u_{rny}$	$0.5\,u_{rny}$	$0.8\,u_{rny}$	u_{rny}	$0.8\,u_{rny}$	$0.5\,u_{rny}$	$0.25\,u_{rny}$	u_{rny}	…

Figure 4.4 Displacement history of roof displacement according to the (a) ATC-24, (b) ISO, (c) SPD, and (d) modified-ISO protocol.

The cyclic pushover curves obtained from using these protocols are shown as solid lines in Figures 4.4a to 4.4c, respectively.
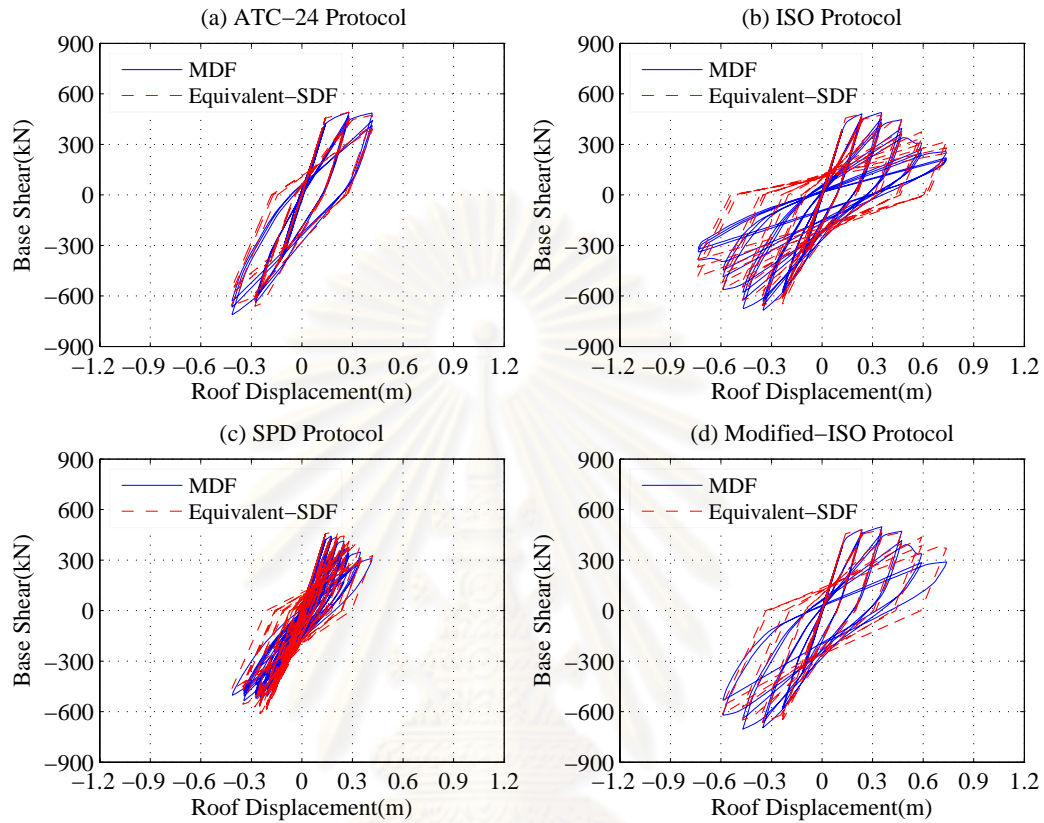

Figure 4.5 Comparisons of cyclic pushover curves and hysteresis loop of equivalent SDF system using various displacement history protocols.

The degradation parameters as appeared in Equations (3.7) to (3.9) can be obtained by optimization minimizing the sum of squares of differences between the force-deformation relationships obtained from cyclic pushover curve and the equivalent SDF system (Figure 4.5). The values of those parameters obtained from using different protocols are compared in Table 4.5.

Table 4.5 Stiffness and strength degradation parameters for the real RC 8-story
building

Degradation Parameters		8-story building			
		ATC-24	ISO	SPD	Modified-ISO
γK	$\gamma K1$	1.21	1.22	1.22	1.22
	$\gamma K2$	0.30	0.30	0.30	0.30
	$\gamma K3$	0.82	0.82	0.82	0.82
	$\gamma K4$	0.90	0.90	0.90	0.90
γD	$\gamma D1$	0.00	0.00	0.00	0.00
	$\gamma D2$	1.75	1.78	1.78	1.78
	$\gamma D3$	1.23	1.21	1.21	1.21
	$\gamma D4$	1.02	1.02	1.02	1.02
γF	$\gamma F1$	0.42	0.42	0.42	0.42
	$\gamma F2$	0.72	0.72	0.72	0.72
	$\gamma F3$	1.08	1.08	1.08	1.08
	$\gamma F4$	0.65	0.65	0.65	0.65
γE		2.83	2.84	2.70	2.84

As the results in Table 4.5, the degradation parameters is very similar though using different protocols. Therefore, these parameters are not sensitive to the load history protocol. Figure 4.5b shows that ISO protocol can capture the post-capping behaviour in relatively fewer cycles, so this protocol is more preferable. We could also simplify it, namely modified-ISO protocol, by reducing the number of cycles being repeated at a certain displacement to further reduce the computation effort (Figure 4.4d). The results for this proposed protocol are shown along with the other protocols in Table 4.5 and Figure 4.5d.

4.3 Accuracy of Target Roof Displacement of Degrading Structures

After the properties of the degrading equivalent SDF system are obtained, the peak deformation (D_1) can be determined by solving the governing equation of motions of the equivalent SDF system (Equation 2.16). In this study, the nonlinear response history analysis (NL-RHA) of SDF system is adopted to determine D_1 and the peak (target) roof displacement is estimated according to Equation (2.18).

The accuracy of the proposed procedure to estimate peak roof displacement of degrading RC building will be examined next by applying the method to the real RC 8-story building subjected to a set of 20 ground motions and compare the results to the 'reference' value determined by NL-RHA of MDF-system model of the building. Subsequently, the proposed procedure will also be applied to generic one-bay 3-, 6-, 9-, and 12-story frames with three different strength levels to investigate the accuracy in more cases.

4.3.1 Real 8-story RC building

Figure 4.6 plots the peak roof displacements of the 8-story building estimated by NL-RHA of equivalent SDF systems ($u_{r,SDF}$) versus the value determined by NL-RHA of the MDF-system model ($u_{r,MDF}$). The median and dispersion of the ratios $\left(u_r^*\right)_{SDF}$ are also noted.
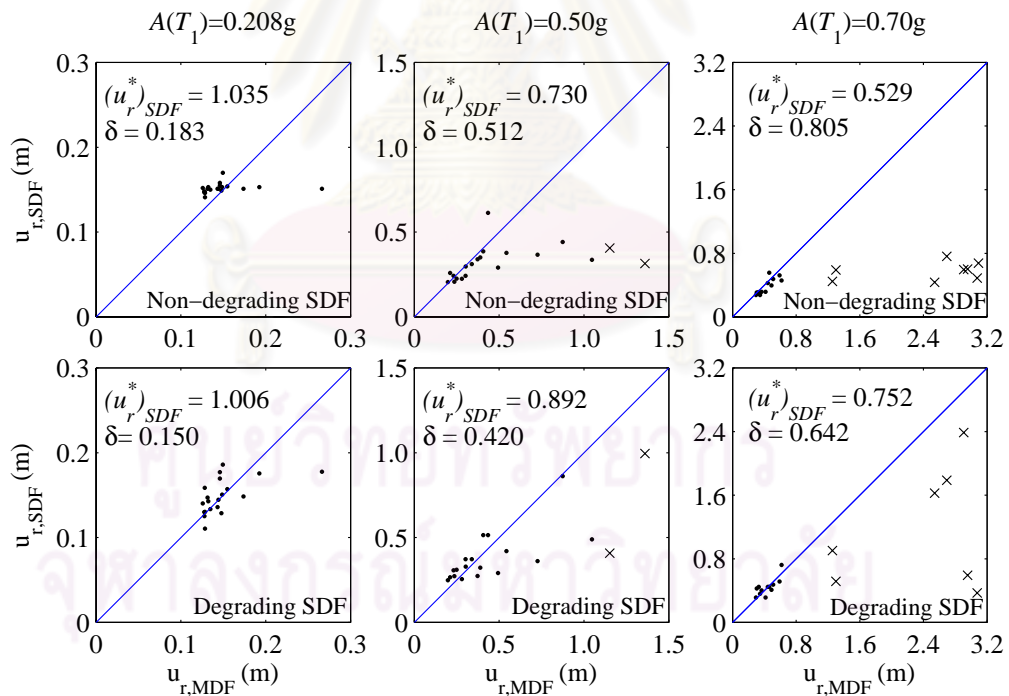

Figure 4.6 Plots of peak roof displacement estimates using equivalent SDF systems versus the 'reference' values from NL-RHA of MDF-system model of the 8-story building ('x' data point denotes collapse indicated by numerical instability).

There are 20 data point corresponding to the responses due to the 20 ground motions. Data points located near the diagonal line indicates accurate estimation. The upper row of plots shows the estimates from using a non-degrading (bilinear) equivalent SDF system, whereas the lower row shows the estimates from using a degrading equivalent SDF system. The NL-RHA of MDF system also considers P-Δ effects and the building collapses in some cases when the ground motions are strong. Those collapse cases are marked by 'x' data point. In such cases, the peak displacements shown are the last values before numerical instability occurs and the statistics of peak roof displacements are based on these values. It can be observed that the accuracy deteriorates as the ground motions become stronger, or as inelastic deformations become larger. The use of degrading equivalent SDF system as shown in the bottom row of Figure 4.6 can provide significantly more accurate estimation of peak roof displacement.

To demonstrate this superiority, Figure 4.7 shows the response history of roof displacement of the 8-story building when subjected to the Agnews State Hospital ground motion record from 1989 Loma Prieta earthquake determined by three methods: (1) NL-RHA of MDF system, (2) NLRHA of degrading equivalent SDF system, and (3) NLRHA of non-degrading (bilinear) equivalent SDF system.
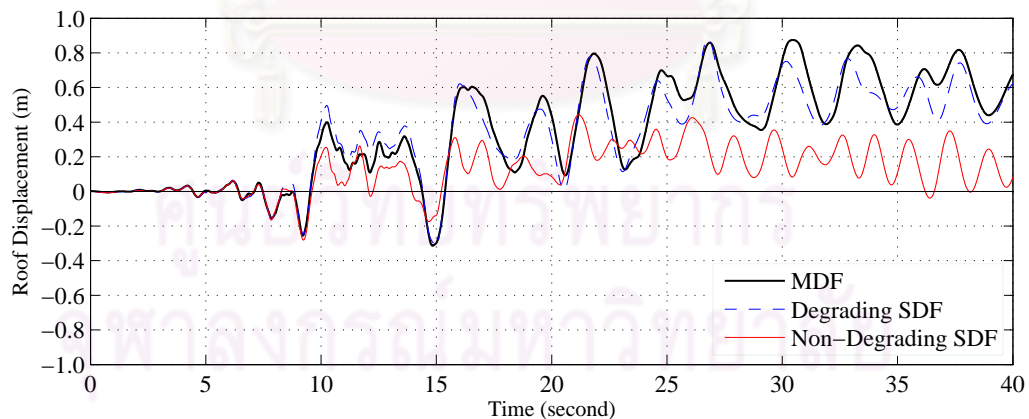

Figure 4.7 Roof displacement response history of the 8-story building from NL-RHA of (a) MDF-system model, (b) degrading equivalent SDF system, and (c) non-degrading (bilinear) equivalent SDOF system when subjected to Agnews State Hospital ground motion from 1989 Loma Prieta earthquake (scaled to $A(T_1)$=0.5g).

It is clear that result from using degrading equivalent SDF system can follow the result of NL-RHA of MDF system surprisingly well, whereas the result from using non-degrading equivalent SDF system can not. However, we can not always achieve such excellent accuracy; the estimation could be inaccurate in some cases as shown in Figure 11. If the median displacement ratio shows that the bias is small, but dispersion is large, then there can be inaccurate estimation in for individual ground motions.

When the base-shear force is plotted versus roof displacement as a hysteresis loop for each of those three methods in Figure 4.8, we can observe that the result from using degrading equivalent SDF system are quite similar to the result of NL-RHA of MDF system, whereas using non-degrading equivalent SDF system resulted in a different shape. Therefore, using a degrading equivalent SDF system should be more appropriate than non-degrading SDF system in the estimation of target roof displacements of degrading RC buildings.
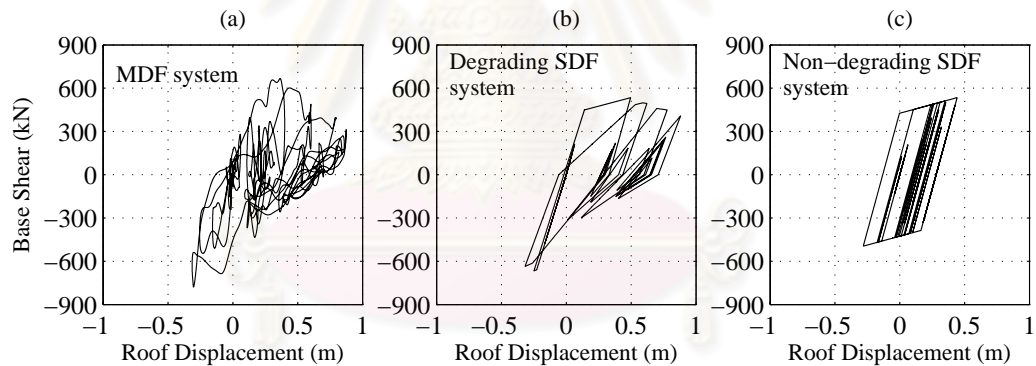

Figure 4.8 Base-shear force versus roof displacement hysteresis loop of the 8-story building calculated by NL-RHA of (a) MDF-system model, (b) degrading equivalent SDF system, and (c) non-degrading equivalent SDF system subjected to Agnews State Hospital ground motion from 1989 Loma Prieta earthquake (scaled to $A(T_1) = 0.5\text{g}$).

4.3.2 Generic frames

The proposed procedure is applied to the 3-, 6-, 9-, and 12-story generic frames with three strength levels to expand the accuracy evaluation to more cases of structural period and strengths. Figure 4.9 plots $u_{r,SDF}$ versus $u_{r,MDF}$ similar to Figure

4.5, but these results are for the generic frames with $R = 6$ when subjected to the LMSR set of 20 ground motions. As observed earlier, the use of degrading equivalent SDF systems led to more accurate estimation of peak roof displacement than non-degrading systems.
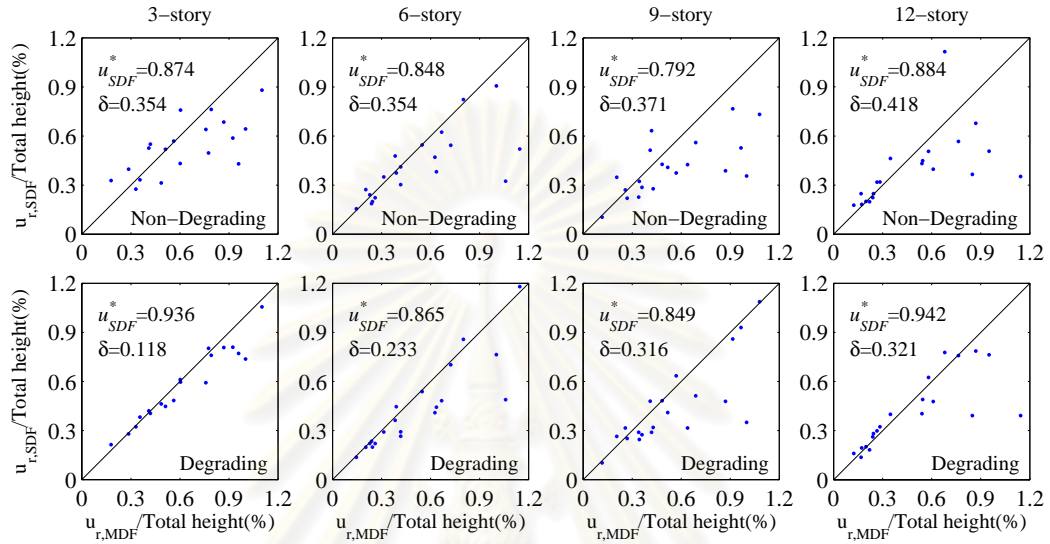

Figure 4.9 Plots of peak roof displacement estimate using equivalent SDF systems versus the 'reference' value from NL-RHA of MDF-system model of the 3-, 6-, 9-, 12-story generic frames with $R = 6$.

The accuracy deteriorates as the frame height increases because of more contributions of higher modes, similar trend as noted by Chopra *et al.* (2003). The bias and dispersion in the case of generic frames are smaller than the real 8-story building partly because degradation in generic frames is less severe than the real 8-story building as the columns of generic frames are assumed to be stronger than beams and plastic hinges do not occur in columns except at the base of the first story.

To summarize the bias and dispersion of the proposed procedure, the histograms of roof displacement ratios $\left(u_r^*\right)_{SDF}$ are plotted for all generic frames considered in Figure 4.10.
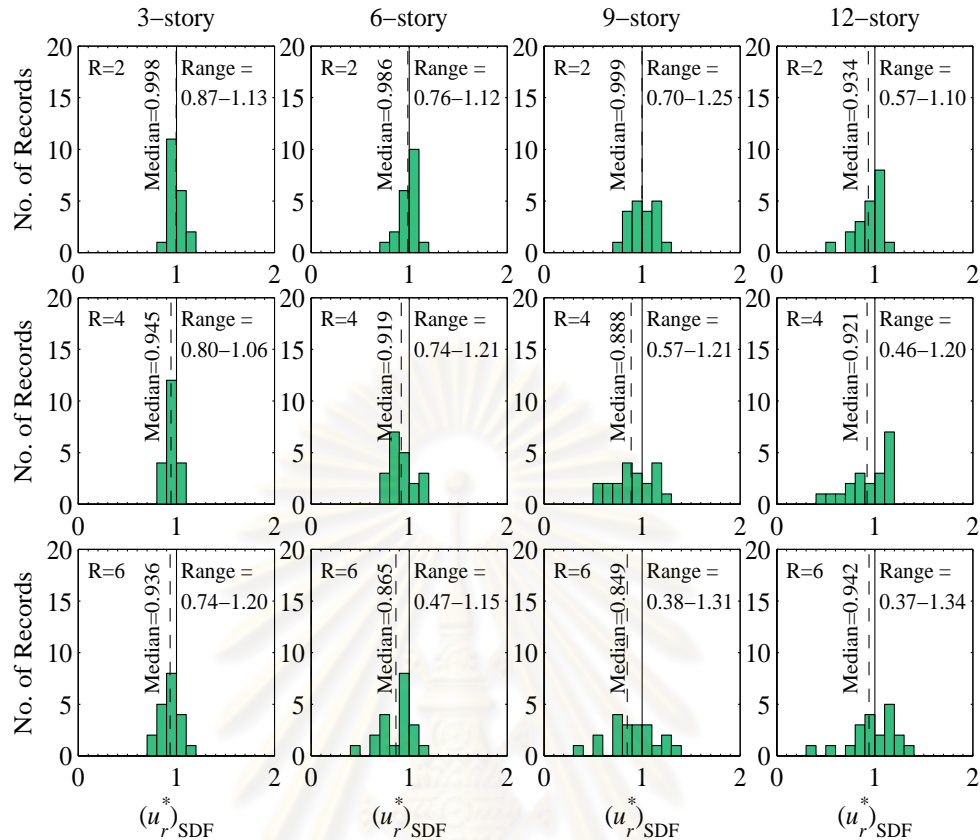
Figure 4.10 Histograms of roof displacement ratios $(u_r^*)_{SDF}$ for 3-, 6-, 9-, and 12-story building designed with $R = 2$, 4 and 6 subjected to the LMSR set of 20 ground motions.

The accuracy tends to deteriorate as the frame height increases or the strength becomes weaker. However, the bias in estimating the peak (target) roof displacement for all cases of generic frames considered is less than 15% and tends to be under-estimation. For the tallest and weakest generic frame considered (12-story with $R = 6$), the bias, indicated by median of roof displacement ratios $(u_r^*)_{SDF}$, is less than 5 percents, but the dispersion is large. This means that the error in estimating the target roof displacement due to an individual ground motion could be large.

CHAPTER V

EVALUATION OF MPA PROCEDURE FOR DEGRADING STRUCTURES

As results in previous Chapter, using an equivalent degrading SDF system can predict the target roof displacement of degrading structures more accurately than using non-degrading, or bilinear equivalent SDF systems. The target roof displacement estimated from degrading SDF system are implemented to determined another seismic demands, i.e. floor displacement, and story drift demand. In this Chapter, The accuracy of the proposed procedure is evaluated by compare with the "reference" values determined from NL-RHA.

5.1 Modal Pushover Analysis for Degrading Structures

For the degrading structures, whose cyclic behavior has an effects on the seismic demands, the suitable modal lateral forces, and monotonic or cyclic, utilized to extract have not been proposed.

In this section, the seismic response of degrading structures is determined by a set of 3-MPA procedure: 1) Modal Pushover Analysis (MPA), 2) Modified-Modal Pushover Analysis (MMPA), and 3) Cyclic Modal Pushover Analysis (CMPA). In this comparative evaluation of analysis procedures, the target roof dispalcement of each building is determined by using an equivalent-degrading SDF system as proposed previously.

Figure 5.1 and Figure 5.2 show the median values of floor displacement and bias of 3-, 6-, 9-, and 12-story building designed for the strength reduction factor $R = 2$, 4, and 6 determined by NL-RHA, MPA, MMPA and CMPA denoted as u_{NL-RHA}, u_{MPA}, u_{MMPA}, and u_{CMPA}. By comparing u_{MPA}, u_{MMPA} and u_{CMPA} to u_{NL-RHA}, the comparisons demonstrate that modal pushover analysis procedures provide similar values of floor displacement, and the values are underestimation in short period frames when compared to reference value. For longer period frames and larger strength reduction factor, these procedures tend to overestimate floor displacement. Particularly, the bias of CMPA procedure is larger than others by 20% for 12-story building.
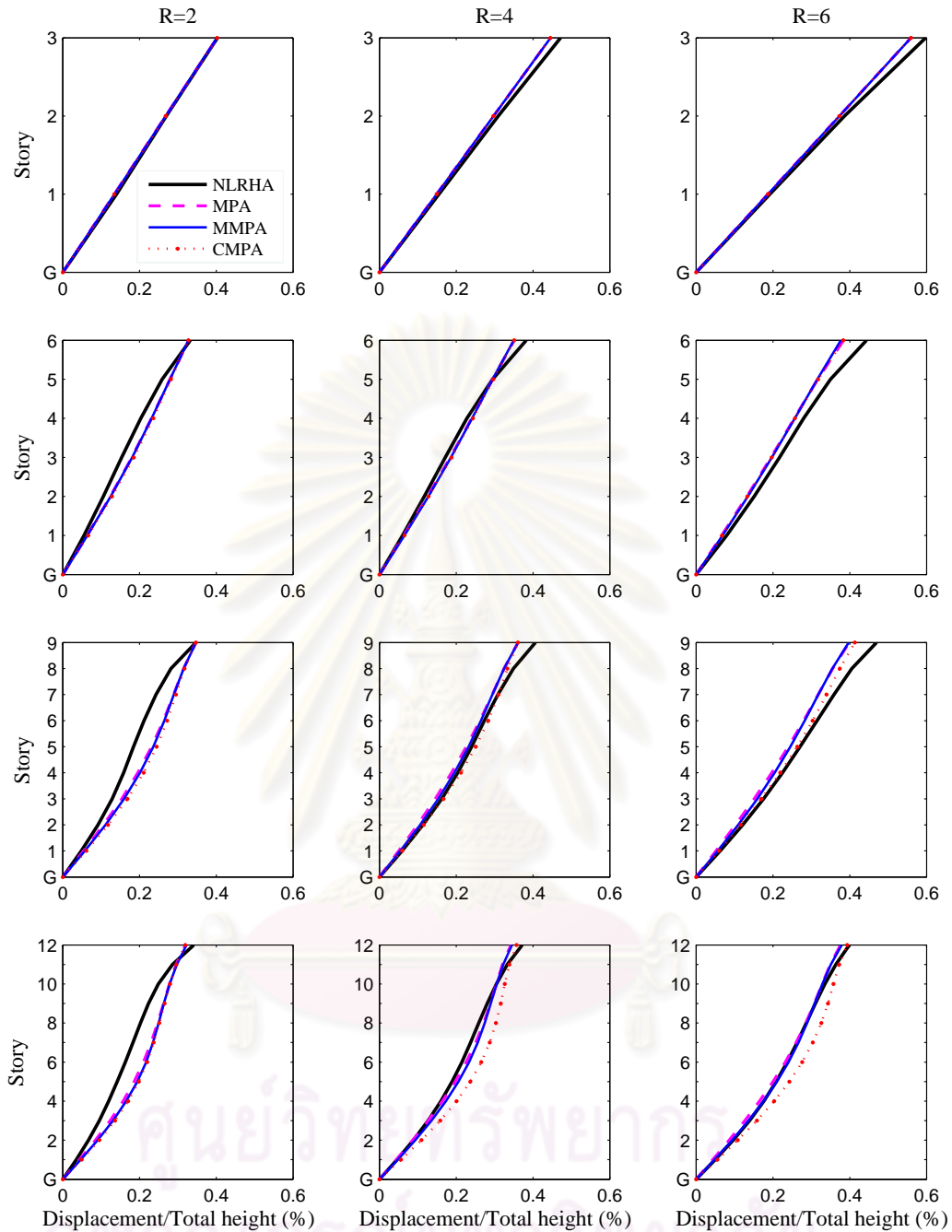
Figure 5.1 Median floor displacement of 3, 6, 9, and 12 story building determined by

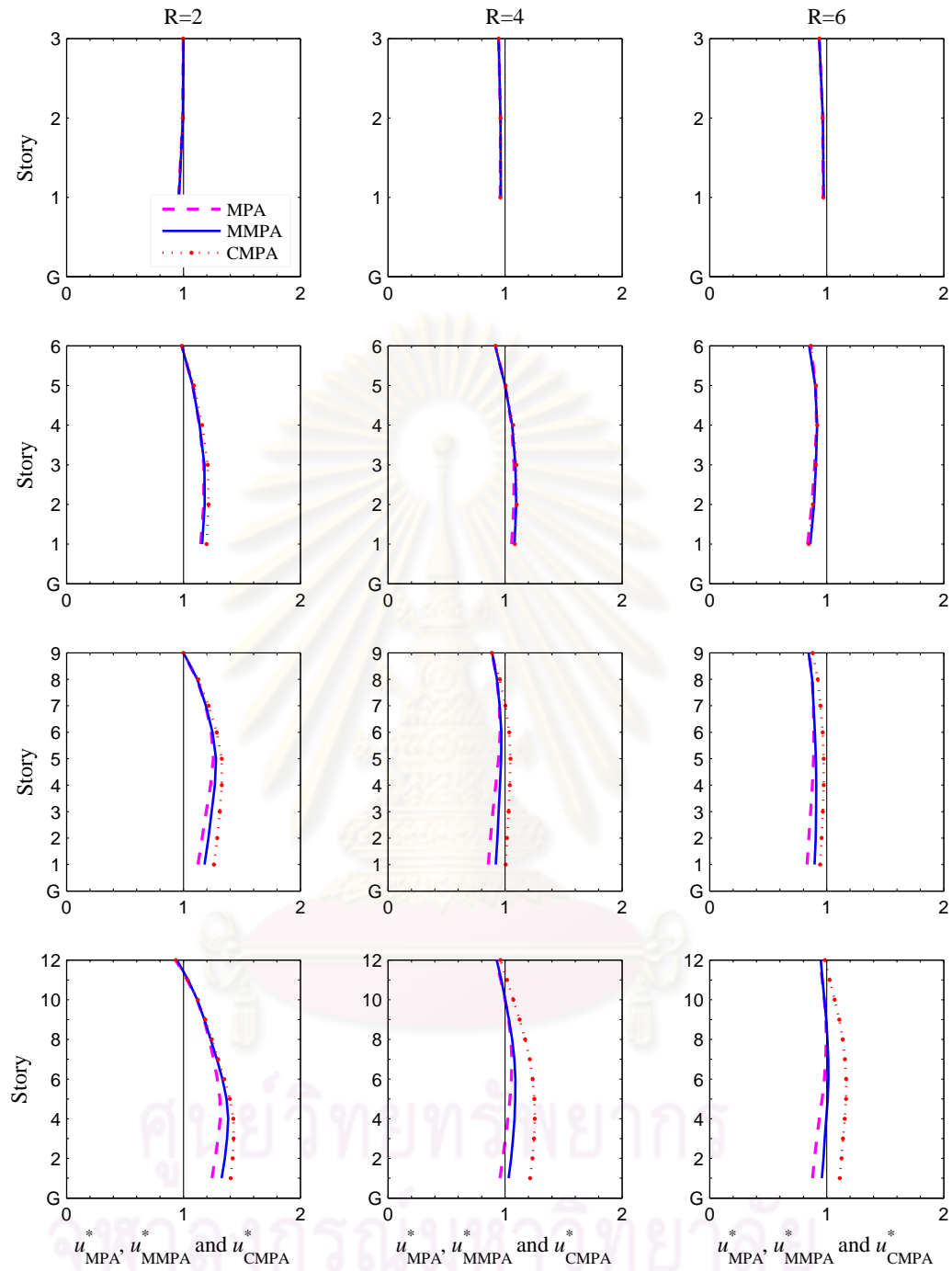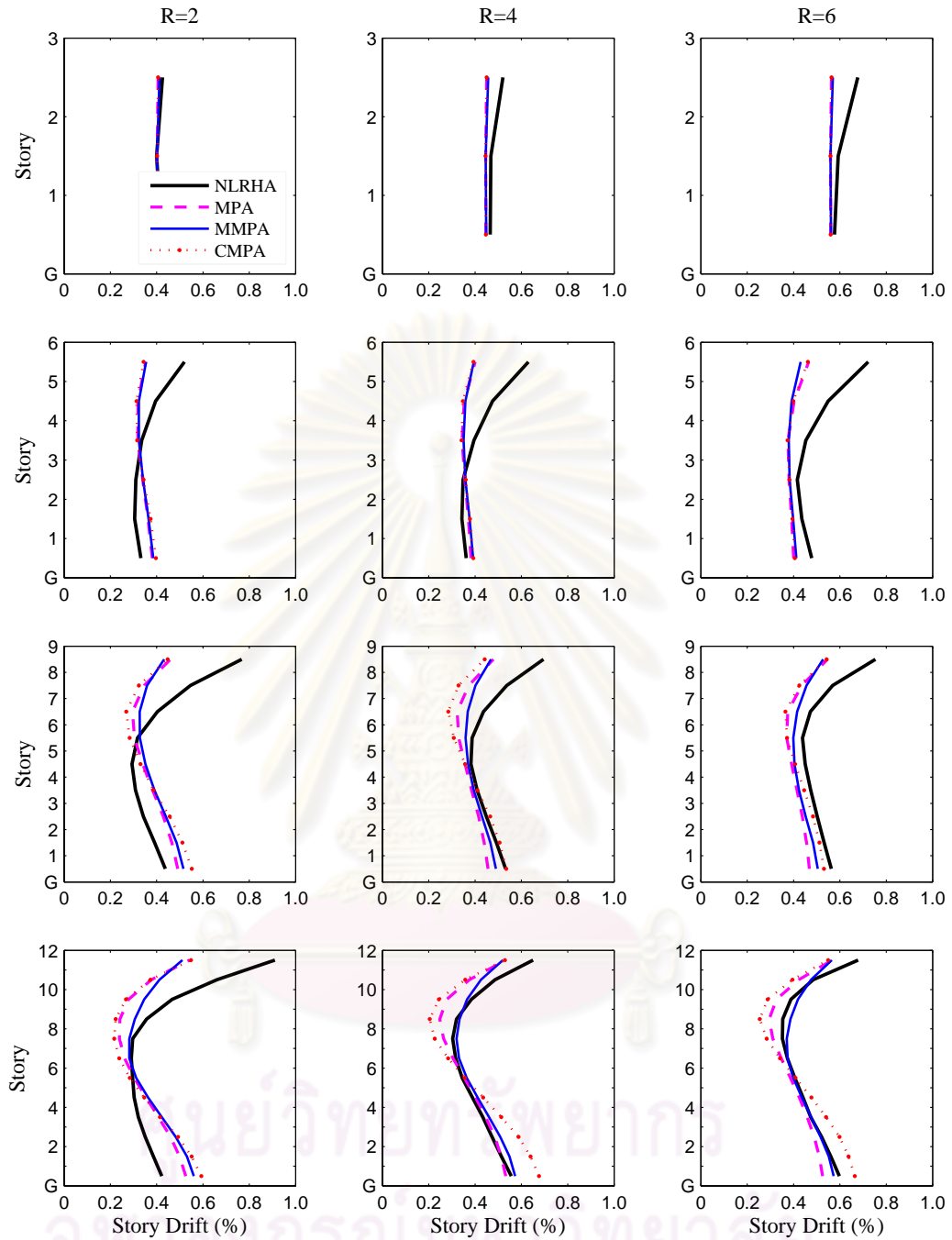NLRHA, MPA, MMPA, and CMPA, each strength designed for R =2, 4, and 6.

Figure 5.2 Median floor-displacement ratios u^*_{MPA}, u^*_{MMPA}, and u^*_{CMPA} for 3, 6, 9, and 12-story buildings, each designed for R=2, 4, and 6.

Figure 5.3 and Figure 5.4 show the median values of story-drift demand and bias of 3-, 6-, 9-, and 12-story building designed for the strength reduction factor $R = 2$, 4, and 6 determined by NL-RHA, MPA, MMPA and CMPA. Most of modal pushover analsysis procedure provide overestimation story drift demand in the lower half whereas underestimate in upper half about 20% for 3-story and 40% for 6-,9-, and 12-story building. The tendency of bias provided by these procedures is quite similar in 3- and 6-story building whereas these tend to different for longer period buildings (12-story building), In this case, bias of MMPA is smaller than others about 20%.

Figure 5.5 and Figure 5.6 show dispersion of floor displacement and story-drift demands estimated by MPA, MMPA, and CMPA. In short period building (3-, and 6-story building), the dispersions of these procedures are quite similar values through the building height whereas those tend to different value for longer period building. Surprisingly, dispersion of MMPA is smaller than others when the buildings are designed with low strength level (R=6).

The overall of the results indicates that the MMPA procedure can estimate the seismic demand with less bias and dispersion than others. Therefore, MMPA procedure is selected for estimating the seismic demand of degrading structure in this study. In addition, MMPA is also reduce the computational effort of MPA procedure in estimating seismic demands of degrading structures in step for developing the cyclic pushover curve in order to calculate the degradation parameters.

Figure 5.3 Median story-drift demand of 3, 6, 9, and 12 story building determined by NLRHA, MPA, MMPA, and CMPA, each strength designed for *R* =2, 4, and 6.
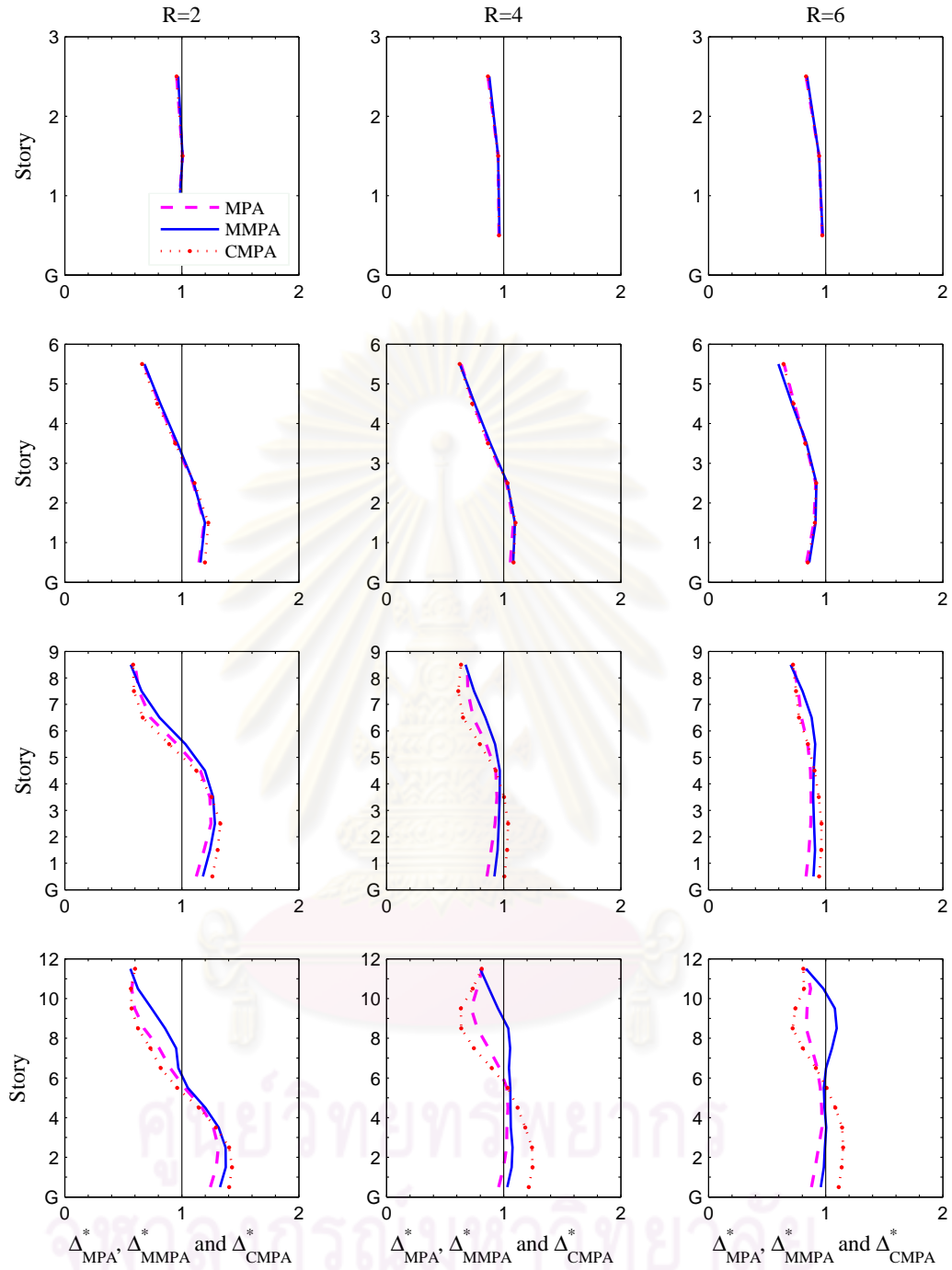
Figure 5.4 Median story-drift ratios Δ^*_{MPA}, Δ^*_{MMPA} and Δ^*_{CMPA} for 3, 6, 9, and 12-story buildings, each designed for R=2, 4, and 6.
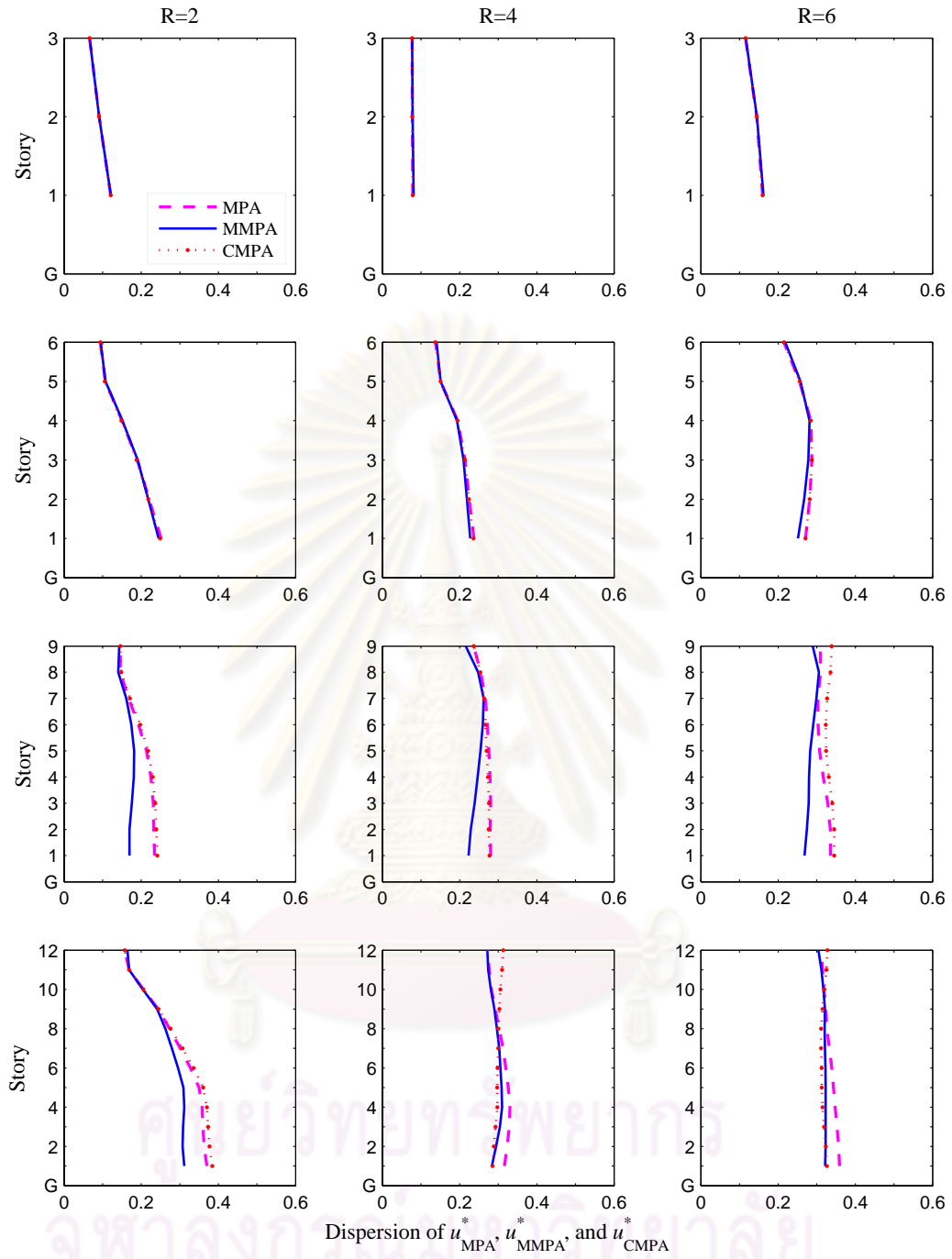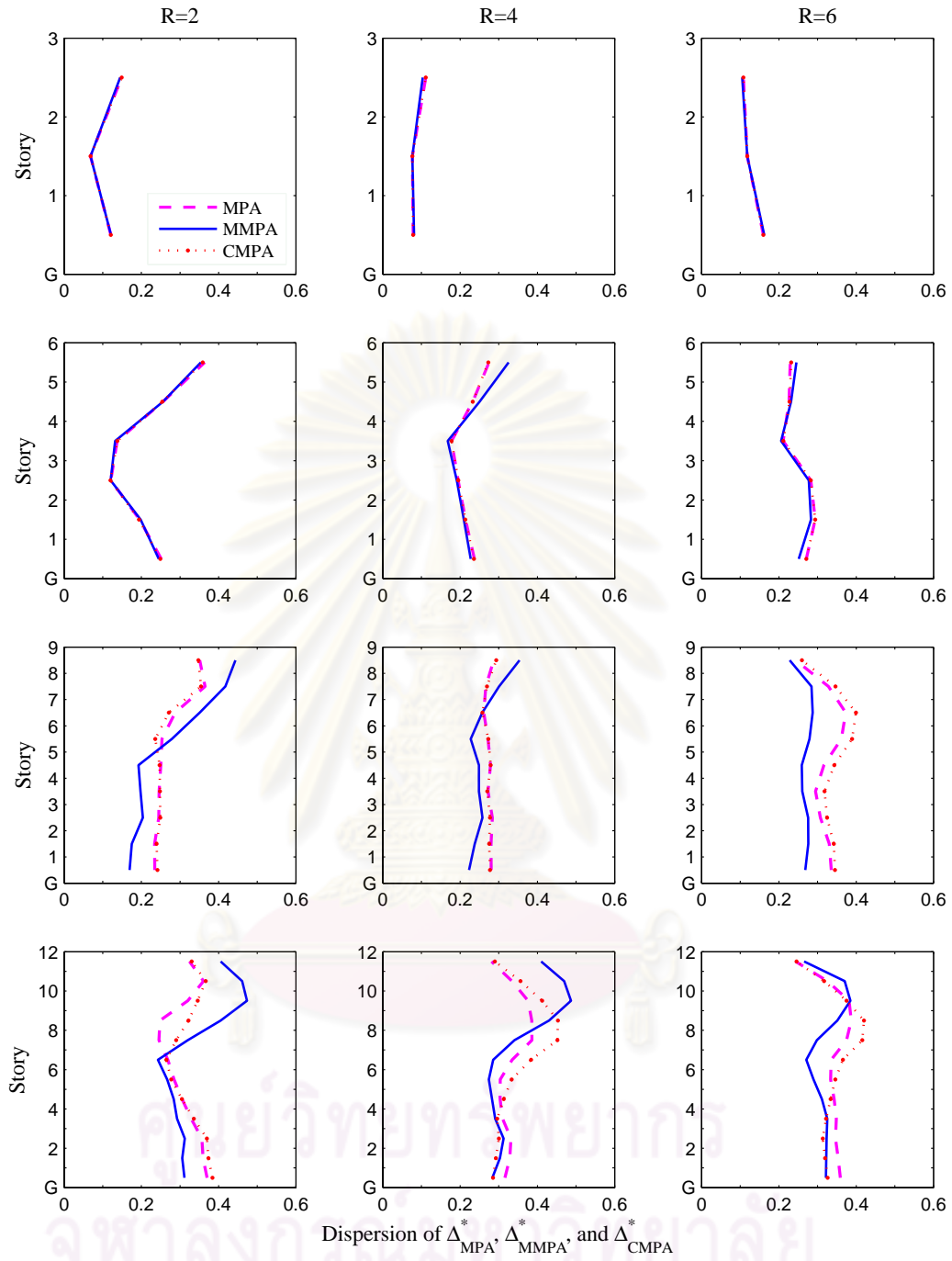
Figure 5.5 Dispersion of floor-displacement ratios u^*_{MPA}, u^*_{MMPA} and u^*_{CMPA} for 3, 6, 9, and 12-story buildings, each designed for R=2, 4, and 6.

Figure 5.6 Dispersion of story-drift ratios Δ^*_{MPA}, Δ^*_{MMPA} and Δ^*_{CMPA} for 3, 6, 9, and 12-story buildings, each designed for R=2, 4, and 6.

5.2 Real 8-Story RC Building

Figure 5.7 and Figure 5.8 show median floor displacement and its bias of a real 8-story RC building subjected to three scaled ground motions. The results indicate that the proposed procedure provide overestimation of floor displacement when the building subjected to ground motion with low intensity level , $A(T_1) = 0.208g$ (behavior of most RC members remain elastic). When the RC members are damaged due to severe ground motion ($A(T_1) = 0.70g$), the use of proposed procedure tends to underestimate floor displacement through the building height.
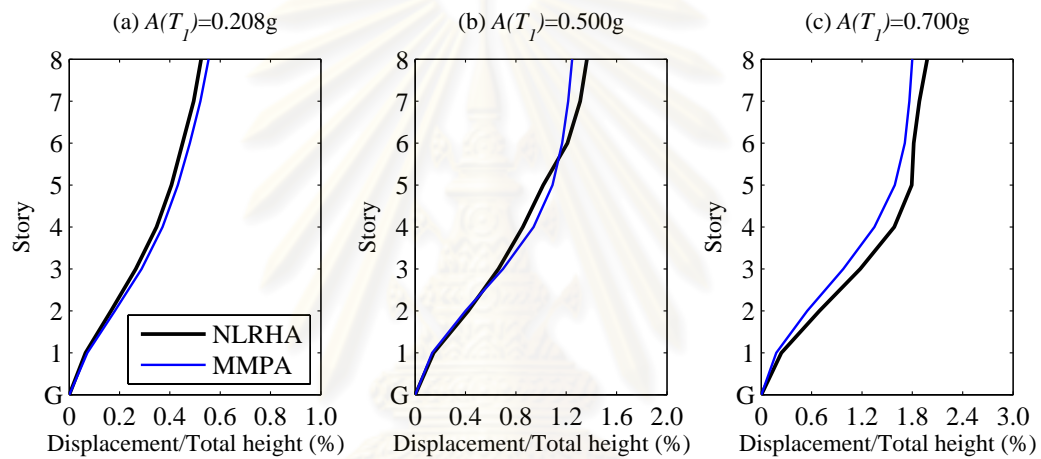
Figure 5.7 Median floor displacement of a real RC. 8 story building determined by NLRHA, MMPA
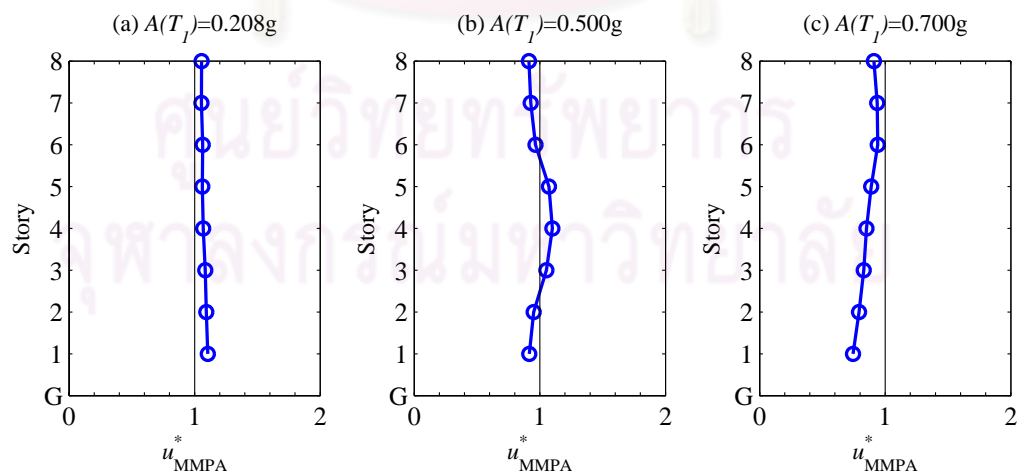
Figure 5.8 Median floor displacement ratios of a real RC. 8 story building determined by NLRHA, MMPA

The story drift demands estimated by the proposed procedure are shown in Figure 5.9 and the bias of story drift demands, which shown as the story drift ratios, is shown in Figure 5.10. these results demonstrate that the proposed procedure tend to provide underestimation of story drift demand though the building is subjected to low intensity level of ground motion. In case of severe ground motion, the proposed procedure provides underestimation of story drift demand by about 60% of NL-RHA.
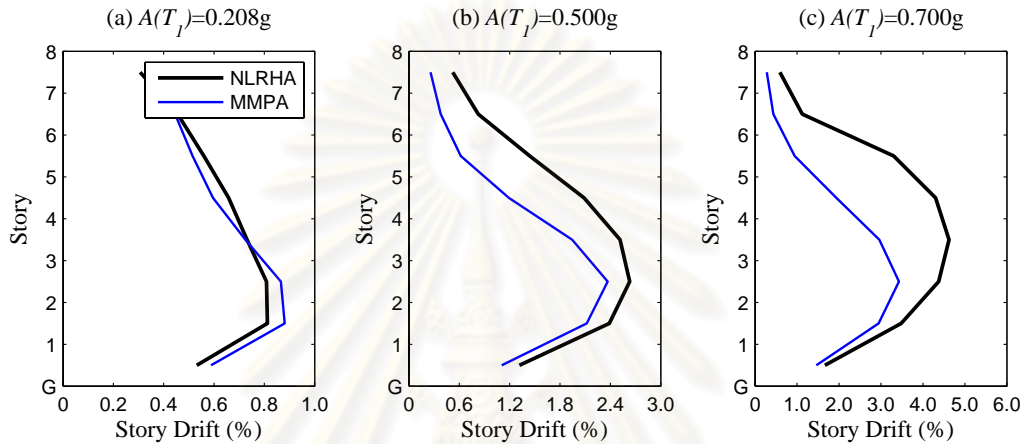

Figure 5.9 Median story drift demands of a real RC. 8 story building determined by NLRHA, MMPA
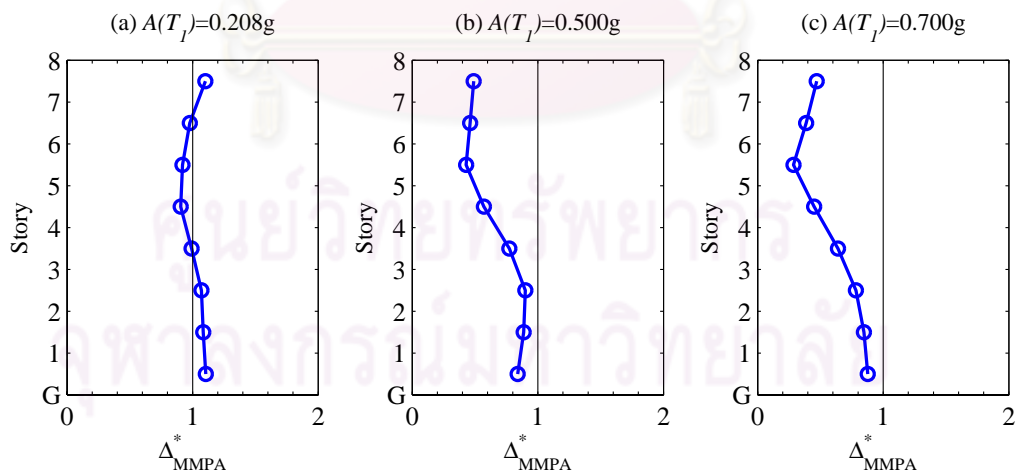
Figure 5.10 Median story-drift ratios of a real RC. 8 story building determined by NLRHA, MMPA

Next, the seismic demands of a real RC building determined by proposed procedure are compared to the conventional MPA procedure. In conventional MPA procedure, the target roof displacement determined from the peak response of an equivalent non-degrading SDF system. The seismic demand of building which extracted from the target roof displacement calculated from non-degrading SDF system is denoted as "BI-MMPA" whereas detemination of those responses from degrading SDF system is denoted as "PH-MMPA".

Figure 5.11 shows the comparison of median floor displacement of a real 8-story RC building determined by PH-MMPA and BI-MMPA. This building is also subjected to three scaled ground motions with different intensity levels 0.208g, 0.50g, and 0.70g. These results indicate that floor displacement of PH-MMPA is quite similar to Bi-MMPA in case of the building excited with low intensity level $A(T_1) = 0.208g$. The proposed procedure (PH-MMPA) predicts floor displacement more accurately than BI-MMPA when the building subjected to severe ground motion.
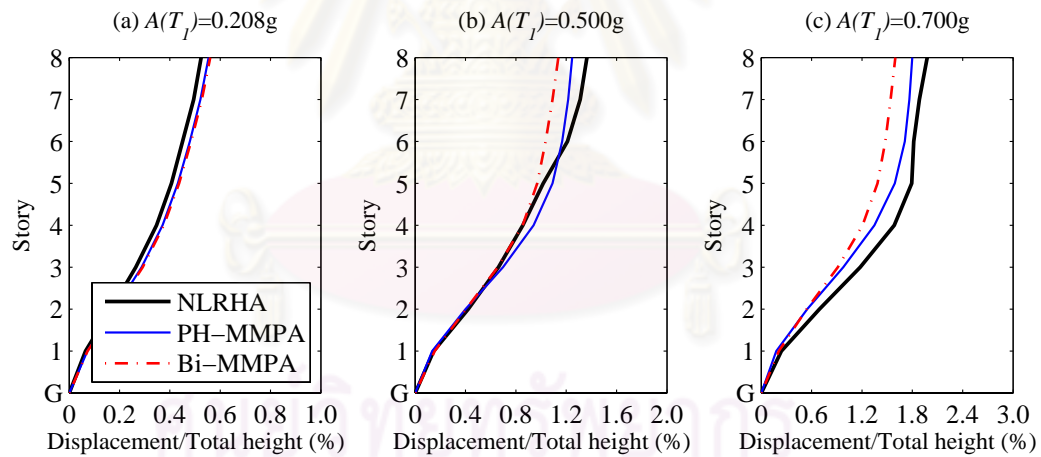
Figure 5.11 Median floor displacement of a real RC. 8 story building determined by NLRHA, PH-MMPA, and BI-MMPA.

Figure 5.12 shows the comparison of median story drift deamand of a real 8-story RC building determined by the proposed procedure (PH-MMPA) and the conventional MPA (BI-MMPA). The results demonstrate that the proposed procedure provides less bias story drift demand in lower half of building whereas provides large bias in upper half of building.

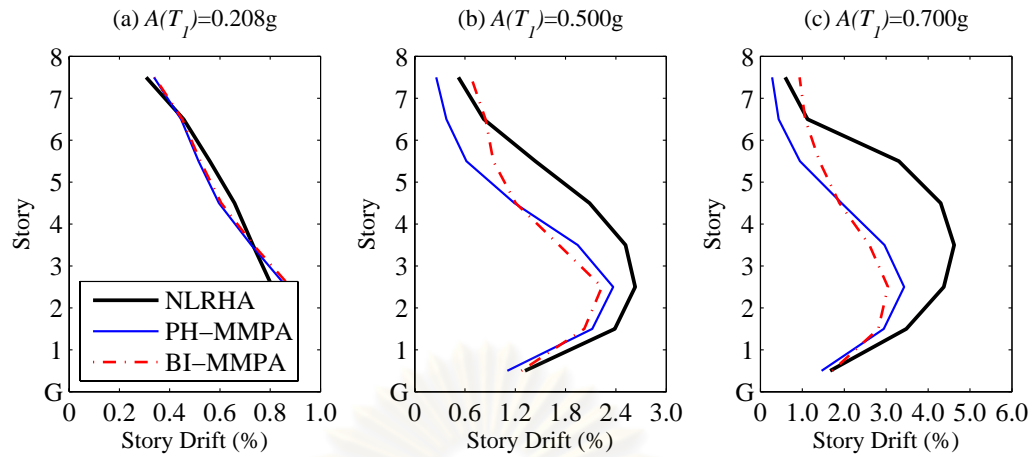(a) $A(T_1)$=0.208g (b) $A(T_1)$=0.500g (c) $A(T_1)$=0.700g

Figure 5.12 Median story-drift demand of a real RC. 8 story building determined by
NLRHA, PH-MMPA, and BI-MMPA.

Figure 5.13 shows the bias of median floor displacements of a real-8 story RC
building. In case of estimated floor displacemt, the proposed procedure provide more
accurately than the conventional MPA procedure. The maximum bias of the proposed
procedure less than 10% for low intensity level, and reach to 25% when the building
subjected to severe ground motion whereas the maximum bias of the conventional
procedure equal to 25% and 40 % for low- and high intensity level, respectively.
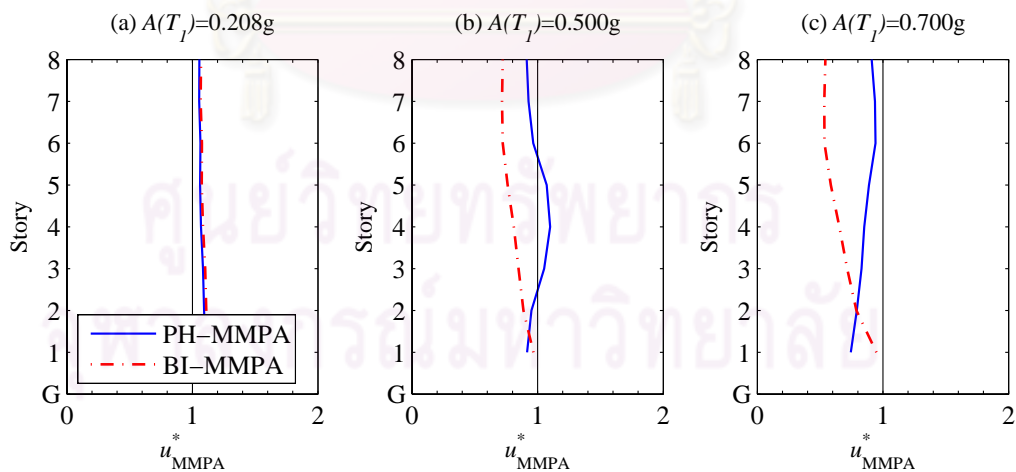
Figure 5.13 Comparison of median floor-displacement ratios, u^*_{MMPA} for a real RC. 8-
story building determined by PH-MMPA and BI-MMPA.
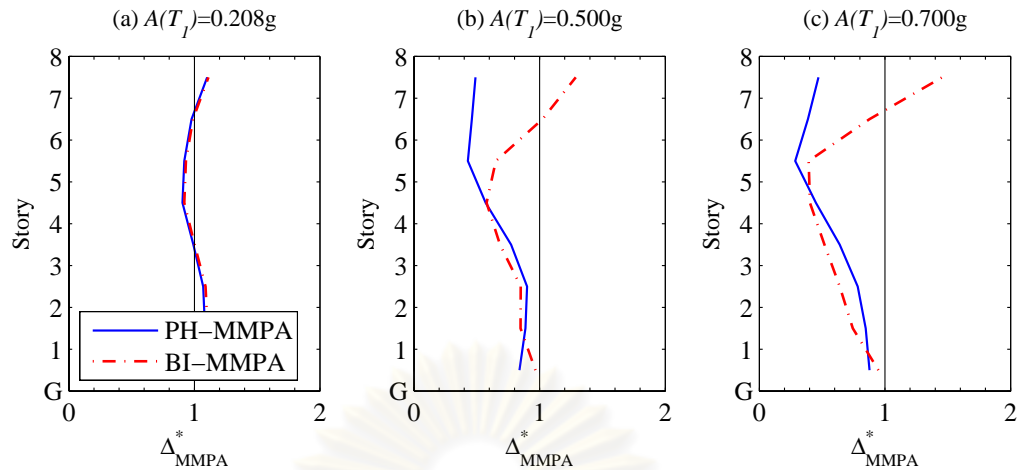
Figure 5.14 Comparison of median story-drift ratios, Δ^*_{MMPA} for a real RC. 8-story

building determined by PH-MMPA and BI-MMPA.

The bias of story drift demands estimated by both procedures are plotted in Figure 5.14. The bias of proposed procedure is less than those of the conventional procedure. In contrast, the proposed procedure provide lagre bias at the upper half of building.

As the results, investigation of bias on seismic demands of a real-8 story RC building estimated by the proposed procedure leads to conclude that using the proposed procedure can estimate the seismic demand more accurately than the conventional MPA procedure, especially the building is excited by ground motion with high intensity level.

5.3 Generic Frames

The one-bay generic frames 3-, 6-, 9-, 12-, 15-, and 18-story tall are used to extend the accuracy evaluation of the proposed procedure to more cases of structural periods and strength levels defined in term of yield-strength reduction factor (R)Iequal to 2, 4, and 6.

Figure 5.15 and Figure 5.16 show the median floor-displacement and the median floor-displacement ratios (bias). These results show that the proposed procedure provides good estimate for the frame with R=4, and 6. For this case, the bias of floor displacement estimated by the proposed procedure is not more than 20%. while R=2, the proposed procedure provides overestimation of floor displacement by about 40% in 12-story building

Next, Figure 5.17 and Figure 5.18 show the median story-drift and the median story-drift ratios. For fixed designed strength level, The proposed procedure tends to provide overestimate story-drift demand at the upper half and underestimate at the lower half of building when designed strength reduction factor $R = 2$ whereas the bias tends to underestimate through the building height when designed strength level is decrease. Except for 3-story, the bias tends to decrease when the frame heigth is increase because the effect of degradation are more significant in shorter period structures. For fixed the frame height, the bias tends to increase when the designed strength level decrease because inelastic behavior becomes more sinificant. In worse case, the proposed procedure provides underestimation of story-drift demand by less than 40%.

Figure 5.19 and Figure 5.20 show the dispersion of floor displacement rations and of story drift ratios of 3-story to 18-story building, each designed with R=2, 4, and 6. the dispersion of both demands tend to increase when the height of building is increase because inelastic behavior becomes more sinificant by more than 30% though the height of building is only 6-story building.
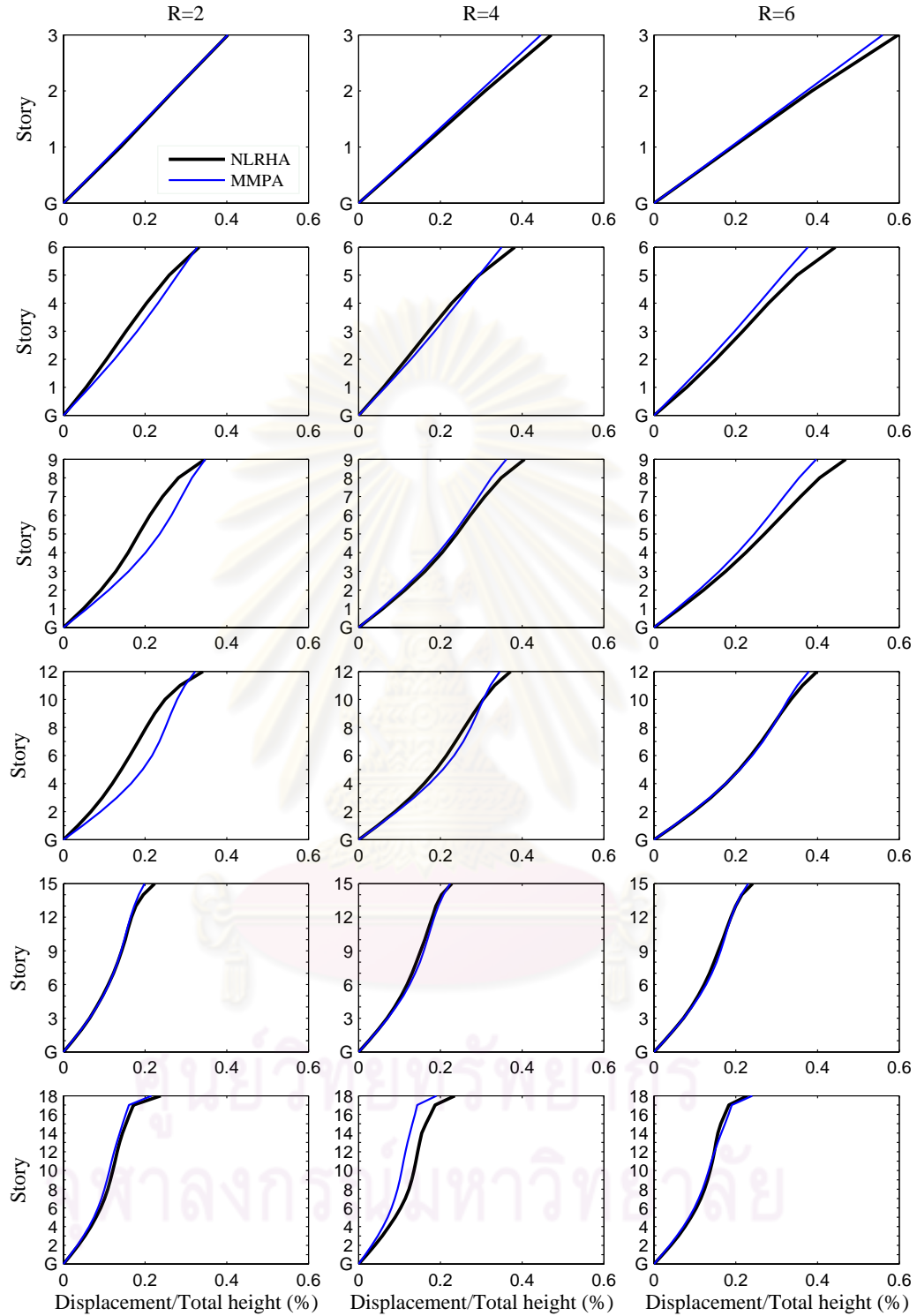
Figure 5.15 Median floor displacement of 3, 6, 9, 12, 15, and 18 story building
determined by NLRHA and MMPA, each strength designed for *R* =2, 4, and 6.
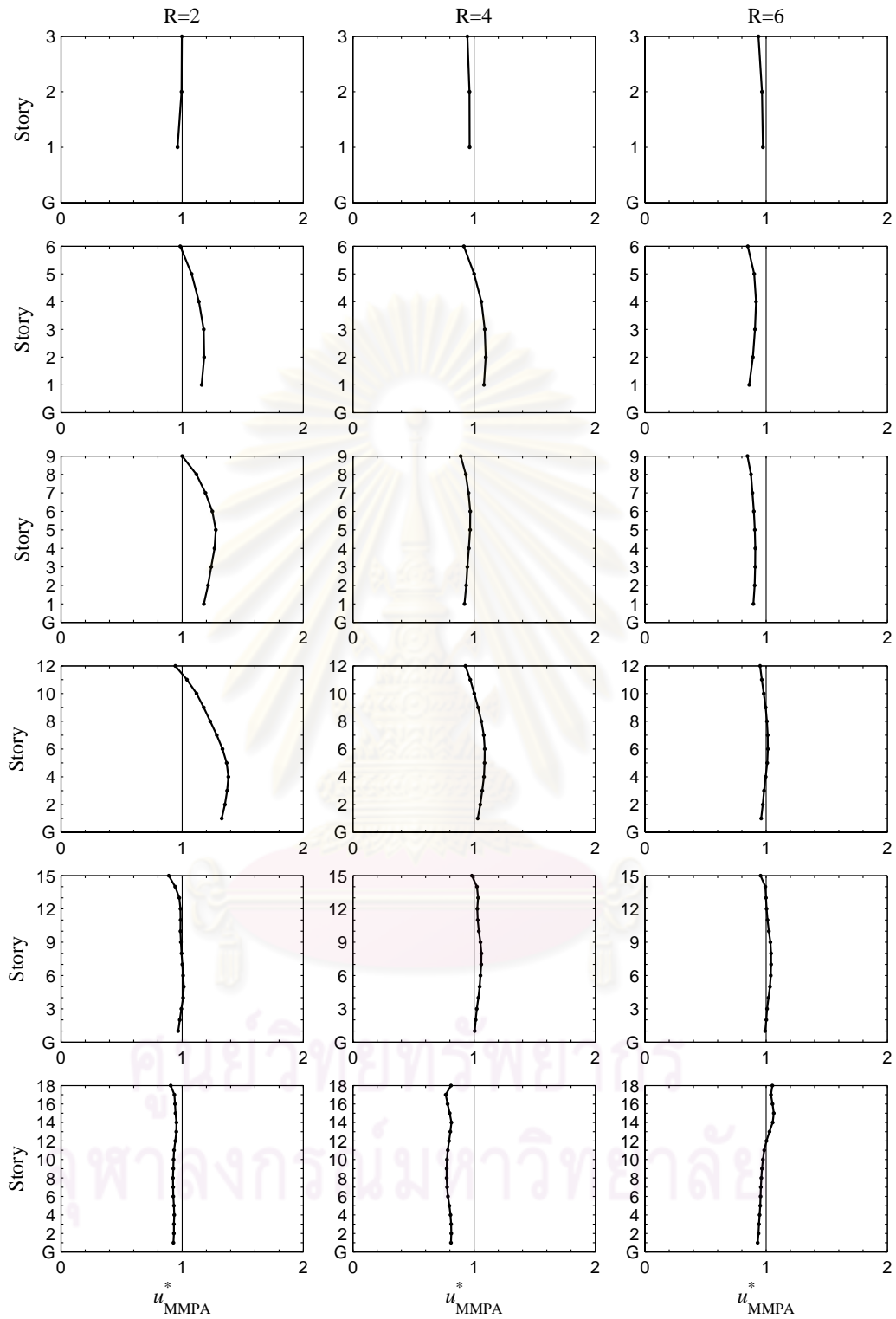
Figure 5.16 Median floor-displacement ratios, u^*_{MMPA} for 3, 6, 9, 12, 15, and 18-story buildings, each designed for R=2, 4, and 6.
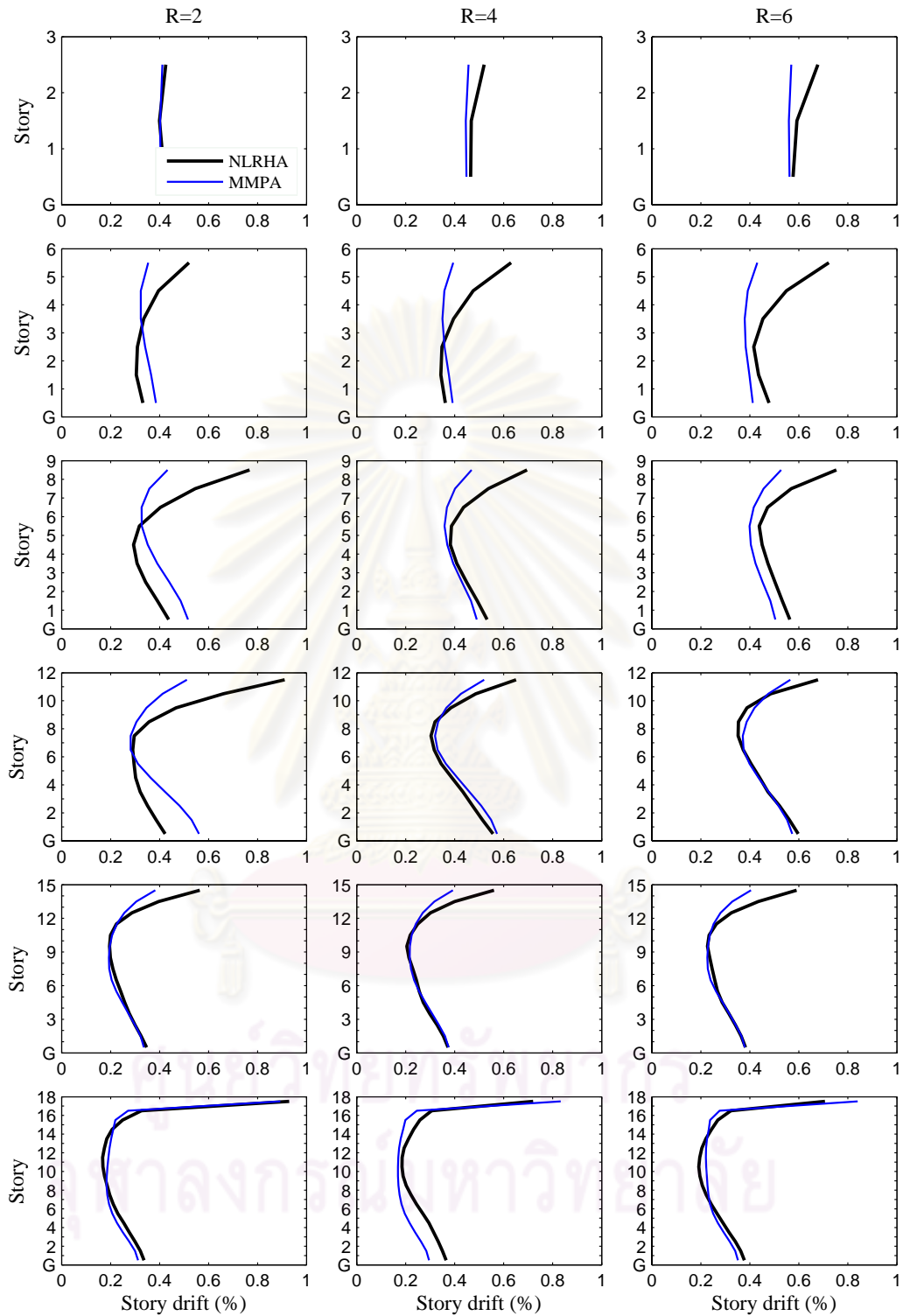
Figure 5.17 Median story drift demand of 3, 6, 9, 12, 15, and 18 story building determined by NLRHA and MMPA, each strength designed for R =2, 4, and 6.
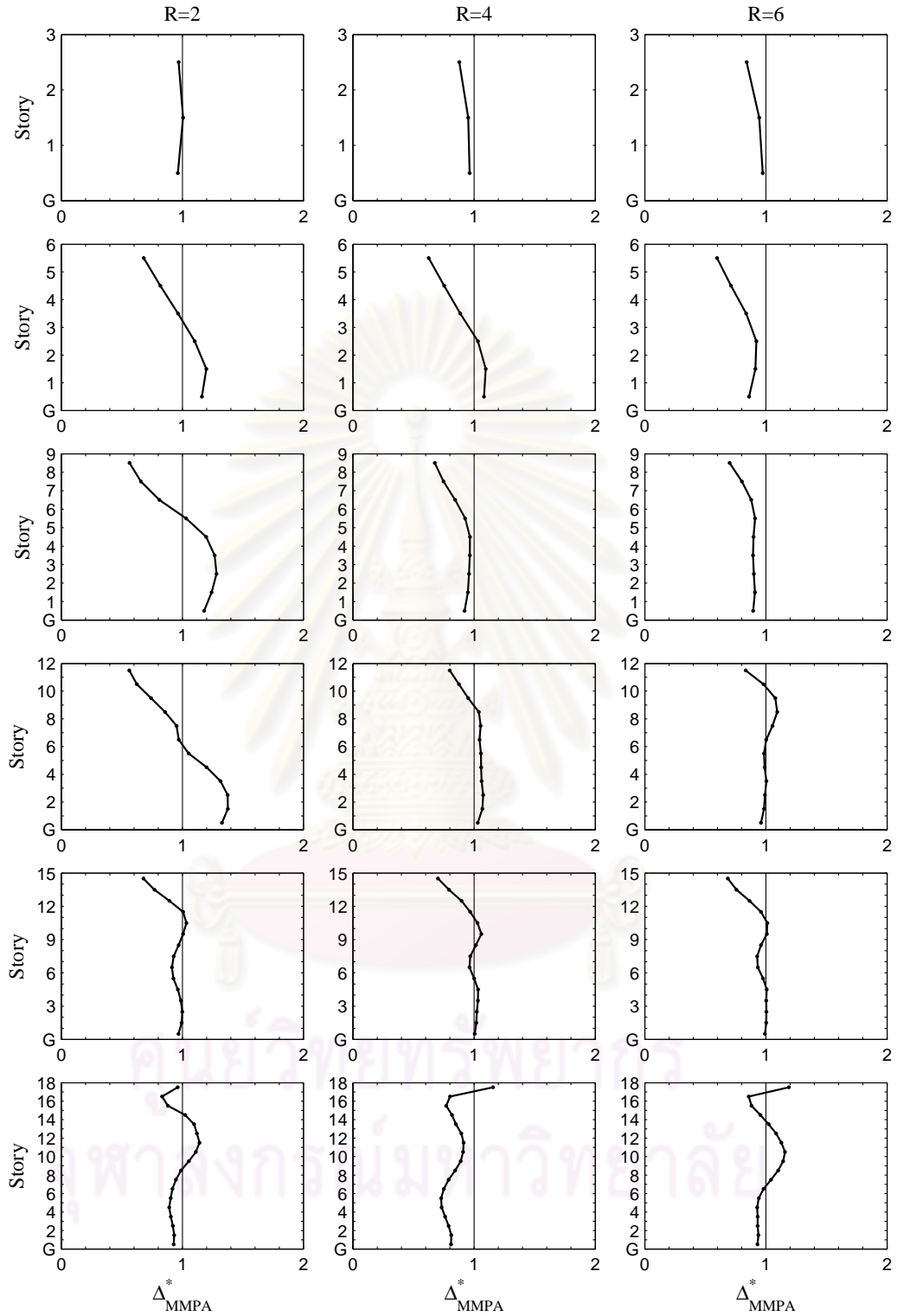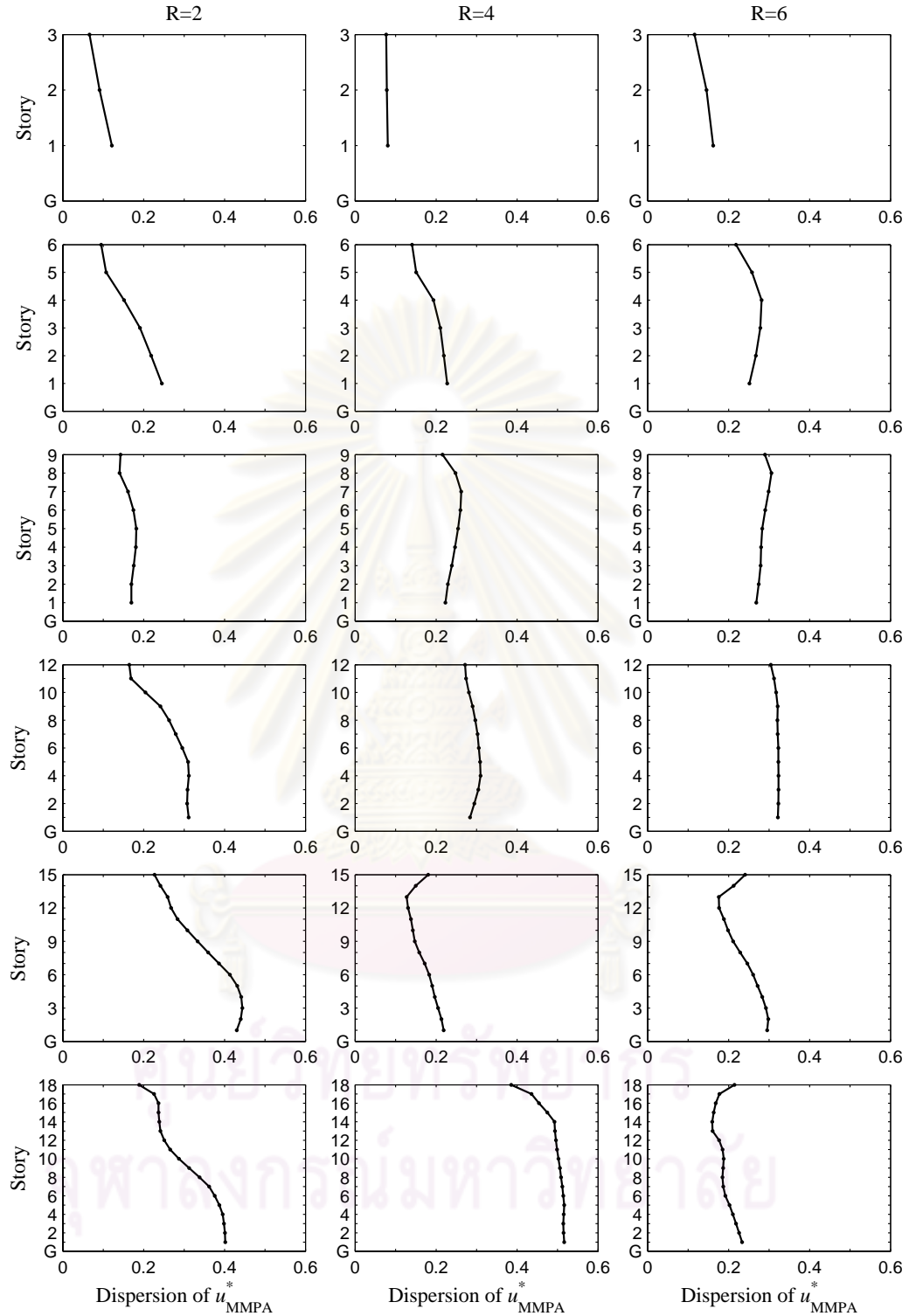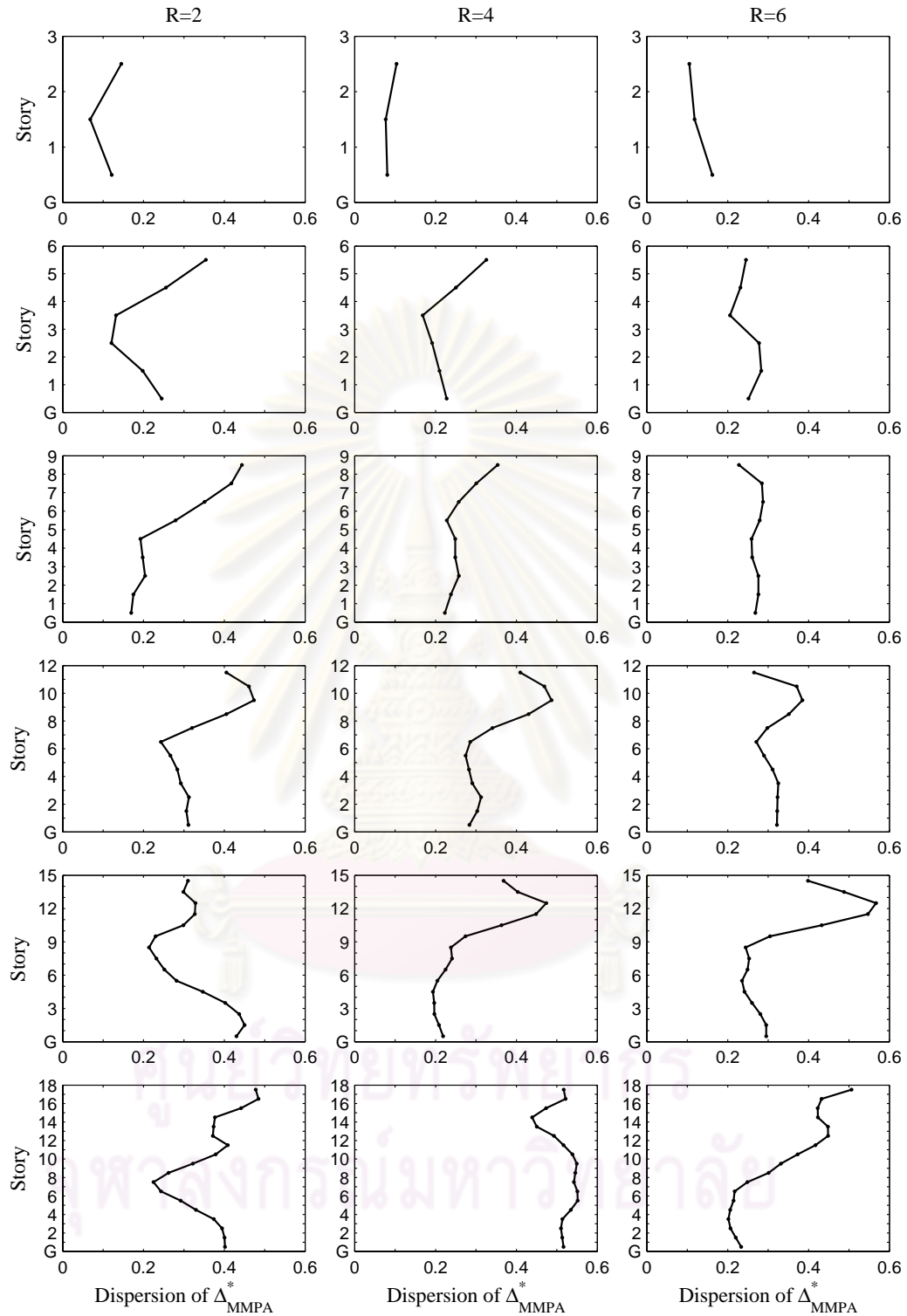
Figure 5.18 Median story-drift ratios Δ^*_{MMPA} for 3, 6, 9, 12, 15, and 18-story

buildings, each designed for R=2, 4, and 6.

Figure 5.19 Dispersion of floor-displacement ratios u^*_{MMPA} for 3, 6, 9, 12, 15 and 18-story buildings, each designed for R=2, 4, and 6.

Figure 5.20 Dispersion of story-drift ratios Δ^*_{MMPA} for 3, 6, 9, 12, 15 and 18-story

buildings, each designed for R=2, 4, and 6.

5.4 Approximation of Incremental Dynamic Analysis for Degrading Structure by using The Proposed Procedure

In 2002, Vamvatsikos and Cornell proposed the method to estimate the structural performance under seismic loads. This method offers thorough seismic demand and capacity prediction capability by using a series of nonlinear dynamic analysis (NL-RHA) under a multiply scaled ground motion records. More details of this procedure can be found in Vamvatsikos and Cornell (2002). This may spend a lot of time to develop the IDA curve if a large number of ground motion record is considered. In order to reduce the time spent for developing the IDA curve, the proposed procedure is tried to apply for estimating the maximum interstory drift demands of the real 8-story building subjected to several intensity level of a set of 20 LMSR ensemble. These approximated demands are compared with the IDA curve determined by NL-RHA.

Figure 5.21 shows the maxmimum interstory drift of the real RC 8-building subjected to the multiple scaled intensity level estimated by the proposed procedure and compared with the exact responses. These results show that the maximum interstory drift demands estimated by the proposed procedure are quite similar to the exact responses when the ground motions are scaled to intensity level $A(T_1)$ less than 0.4g. For the intensity level more than 0.4g, the numerical instability are occurred due to collapse of structures. It can conclude that using the proposed procedure can extimate the IDA curve in case of the building does not collapse.

The limitation of the proposed procedure for estimating the IDA curve is to it can not indicate the real inelastic limit state when the building collapse (numerical instability) in the pushover analysis.

(a) Incremental dynamic analysis
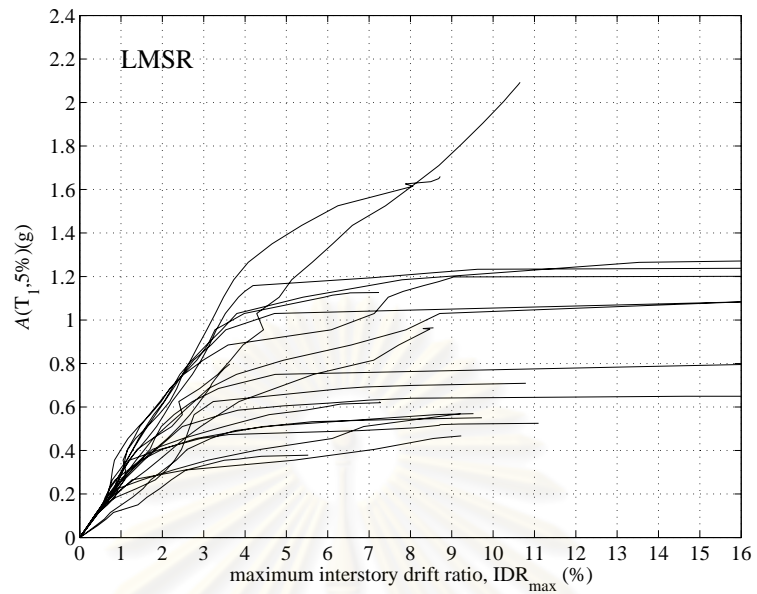
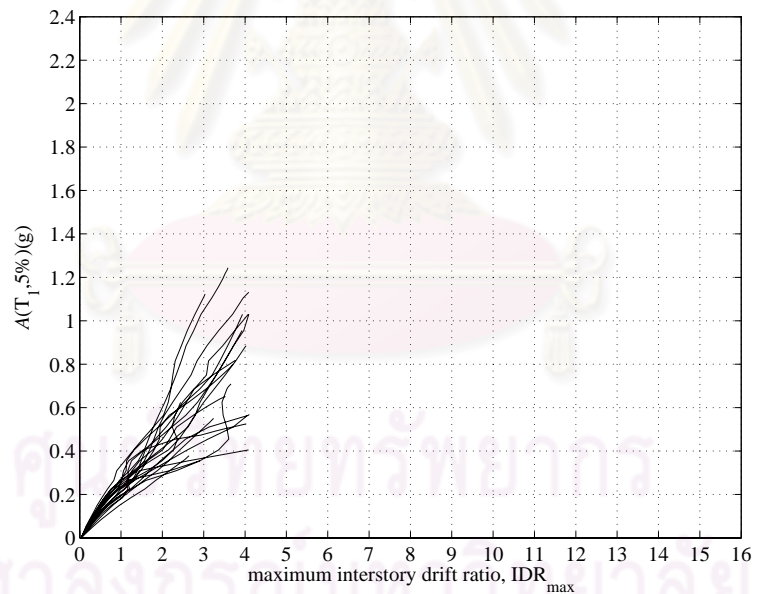(b) Incremental nonlinear static analysis

Figure 5.21 The maximum interstory drift ratio of the real RC 8-story building subjected to the scaled 20 LMSR ensemble determined by (a) the incremental dynamic analysis, and (b) the incremental nonlinear static analysis.

5.5 Comparative Evaluation of Bias in MPA when Apply to Severe vs Mild degrading Frames

To explore the trend of bias of the proposed procedure that affect the rate of degradation. The reinforced-concrete bridge column tested by Singhasut and Ruangrassamee (2009) was adopted to calibrate the moment rotation ralationship of the plastic hinge model. The description of this column consist of

(1) Dimension of cross section = 0.40x0.40 m.,

(2) The longitudinal reinforcement ratios = 0.0123,

(3) The axial force ratio = 0.057

(4) The transverse reinforcement ratios = 0.00424

The experimental and analytical results of ductile column are shown in Figure 5.24.
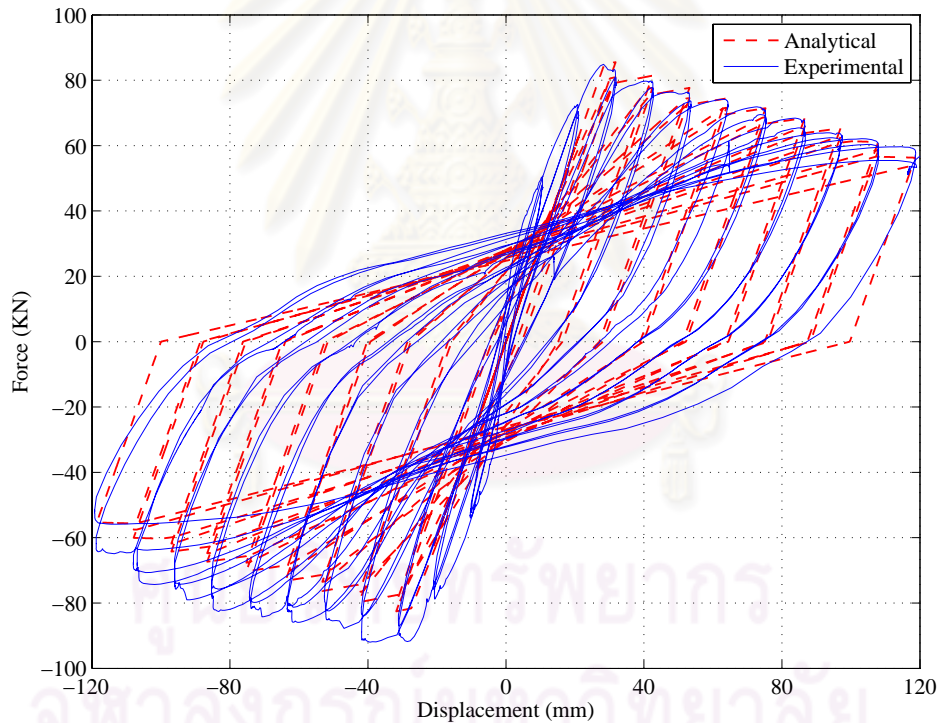
Figure 5.22 Comparison of force-displacement relation from laboratory test of a ductile RC column and numerical model for plastic hinge.

The degrading parameters of plastic hinge model calibrated against the experimental result of the mild degrading column and severe degrading column (Sezen, 2000) are shown in Table 5.1.

Table 5.1 Degrading parameters of plastic hinge model calibrated from experimental
results of mild and severe degrading RC column

Degrading Parameters for a plastic hinge		Severe degradation	Mild degradation
Unloading Stiffness Degradation	$\gamma K1$	0.00	1.00
	$\gamma K2$	1.00	0.10
	$\gamma K3$	0.00	1.00
	$\gamma K4$	1.00	1.00
Reloading Stiffness Degradation	$\gamma D1$	0.50	0.03
	$\gamma D2$	0.00	0.00
	$\gamma D3$	1.00	5.00
	$\gamma D4$	0.00	0.00
Strength Degradation	$\gamma F1$	0.00	1.00
	$\gamma F2$	1.00	0.37
	$\gamma F3$	0.00	1.00
	$\gamma F4$	1.10	0.43
Energy Dissipation	γE	4.50	54

Following the step by step of the proposed procedure to estimate the seismic
demand of degrading structure in section 2.4.1 (stage 2), the degrading parameters of
the equivalent degrading SDF system for mild and severe degradation systems are
shown in Table 5.2.

In Table 5.2, the degradation level of degrading structures can be identified by
the dissipated energy paremeter (γE). The small value of γE indicate the severe
degrading structure whereas the mild degrading structure is display by the large value
of γE.

Table 5.2 Degrading parameters of plastic hinge model calibrated against from the experimental results of mild and severe degrading RC column.

Degrading Parameters for a plastic hinge		Severe degradation	Mild degradation
Unloading Stiffness Degradation	$\gamma K1$	0.00	1.00
	$\gamma K2$	1.00	0.10
	$\gamma K3$	0.00	1.00
	$\gamma K4$	1.00	1.00
Reloading Stiffness Degradation	$\gamma D1$	0.50	0.03
	$\gamma D2$	0.00	0.00
	$\gamma D3$	1.00	5.00
	$\gamma D4$	0.00	0.00
Strength Degradation	$\gamma F1$	0.00	1.00
	$\gamma F2$	1.00	0.37
	$\gamma F3$	0.00	1.00
	$\gamma F4$	1.10	0.43
Energy Dissipation	γE	4.50	54

Figure 5.23 Median floor displacement of a real RC. 8 story building determined by NLRHA and the proposed procedure. The degrading parameters of plastic hinge-rotation relation are calibrated from mild degrading RC. Column.

Figure 5.23 shows the median floor displacement of 8-story building determined by the proposed procedure. These results demonstrate that the proposed procedure provides overestimation of median floor displacement of the real RC building though the building are excited in high intensity level (0.7g). Consider Figure 5.24, the overestimation of floor displacement tends to increase when the intensity level is increased by about 10% in $A(T_1)=0.5g$ and 40% in $A(T_1)=0.70g$. In contrast, the bias of the severe degrading structure tends to underestimate when the intensity level is increased.
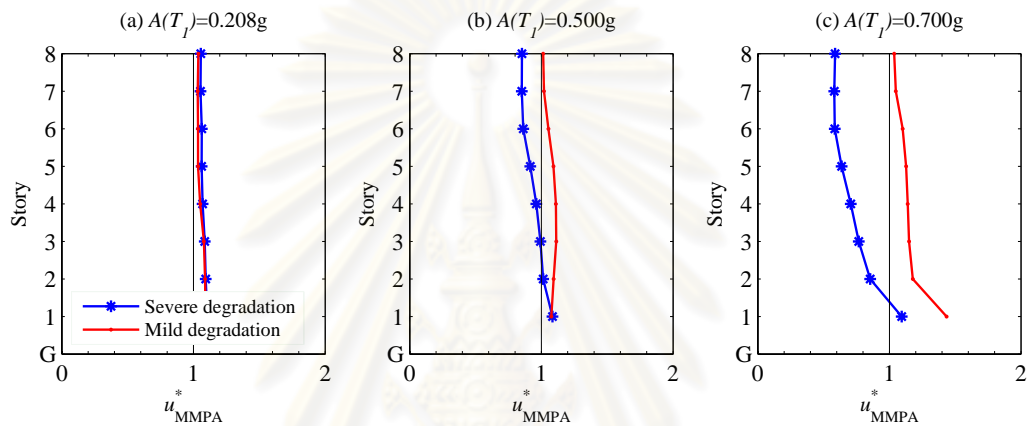
Figure 5.24 Comparison of median floor displacement ratio of the real RC. 8 story building when the moment-rotation relationship of plastic hinge are modeled as mild and severe degrading systems.
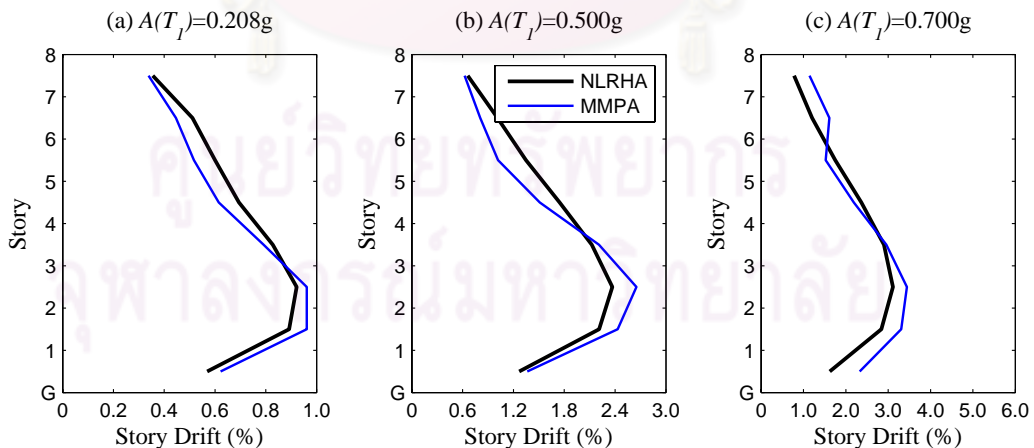
Figure 5.25 Median story drift demand of the real RC. 8 story building determined by NLRHA and the proposed procedure when the plastic hinge-rotation relation are modeled as the mild degrading system.

Next, the bias of median story drift demand are shown in Figure 5.27. In each intensity level, the proposed procedure provides overstimation of story drift demand in lower half whereas underestimates in upper half of building. Consider in Figure 5.28, the bias of the severe degrading structure tends to increase when the intensity level is increase. In contrast, the bias of mild degrading structure in terms of underestimation tends to decrease when the intensity level is increased.
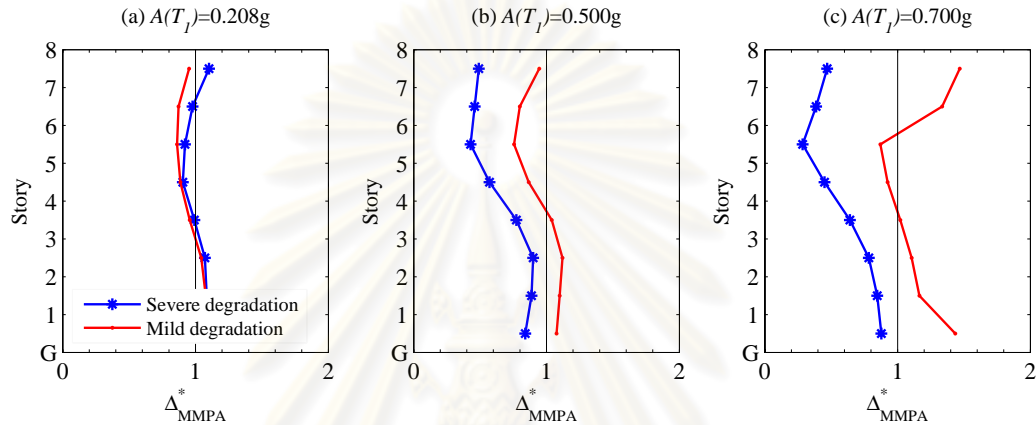
Figure 5.26 Comparison of median story drift ratio of the real RC. 8 story building when the moment-rotation relationship of plastic hinge is modeled as mild and severe degradation systems.

According to comparative response of mild and severe degrading structure estimated by the proposed procedure. When the degrading structures are excited in high intensity level, the bias of mild degrading structure in terms of underestimation tends to decrease. In contrast, the bias of severe degrading structure in terms of underestimate tends to increse when the intensity level is increased.

5.6 Comparative Evaluation of Bias in the Real RC 8-Story Building vs Generic Frames.

Figure 5.27 shows the bias of median story drift demands of generic frames and a real RC 8-story building. the results show that the shape of bias of 9-story generic frame designed with low strength level (R=4 and 6) is quite similar to those of a real RC frame subjected to severe ground motion ($A(T_1)$=0.5g and 0.7g). In the

lower half of both buildings, The bias of a real RC buildng is larger than those of generic frame in the lower half of building because the inelastic behavior in a real building becomes significant.
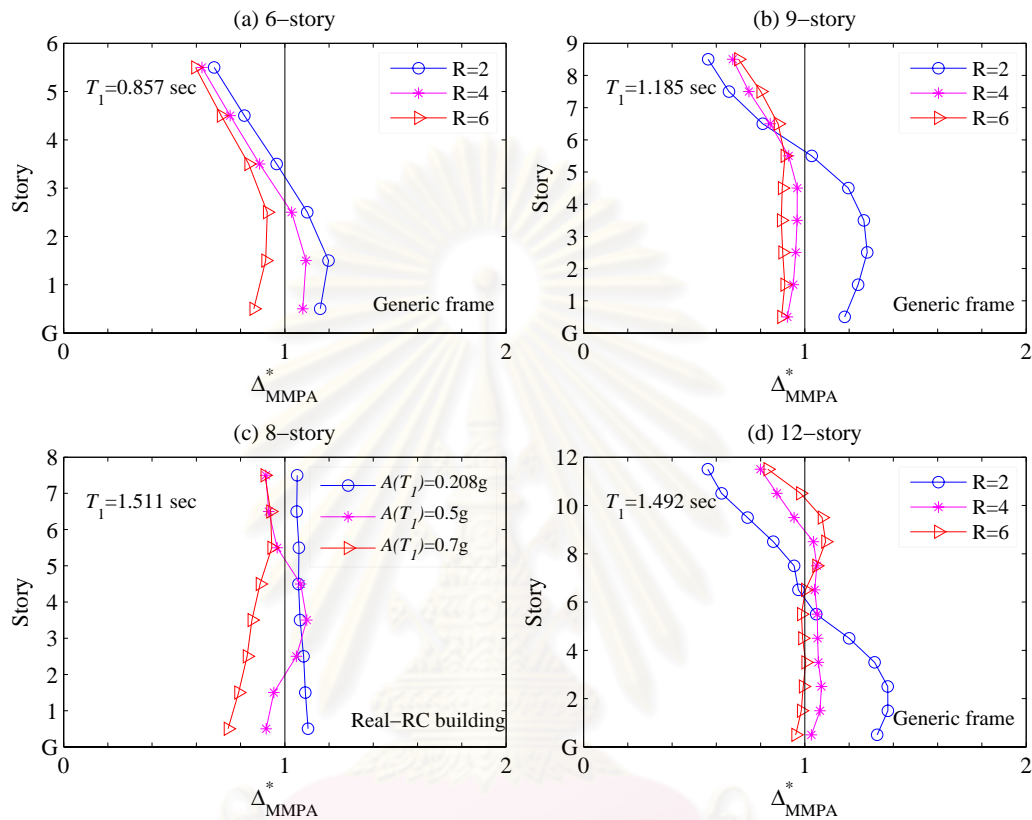
Figure 5.27 Comparison of median story drift ratios of 6-, 9-, 12-story generic frames and a real RC 8-story building subjected to a set of LMSR ensemble.

CHAPTER VI

CONCLUSIONS

The objectives of the research are to develop and to evaluate the modal pushover analysis (MPA) procedure in estimating seismic demands of degrading structures for practical implementation.

The procedure to estimate the peak (target) roof displacement of a degrading RC frame building by using deformation of a degrading equivalent SDF system has been presented. The force-deformation relation of the degrading equivalent SDF system can be determined by monotonic and cyclic pushover analysis, and its parameters are not sensitive to the displacement history used in the cyclic pushover analysis. Investigation of the accuracy of the proposed procedure led to the following conclusions:

1. Using degrading equivalent SDF systems in estimation of peak (target) roof displacement of degrading RC buildings provides more accurate estimatations than using non-degrading SDF systems.

2. The accuracy of the proposed procedure for estimating target roof displacement deteriorates when the strength of the structure is weaker, and the structure experiences significant inelastic deformation.

3. The accuracy of the proposed procedure deteriorates when the structure becomes taller, and the effect of higher modes increases.

4. Among all generic frames considered, the largest bias in term of median of peak roof displacement ratios is no more than 15% occurred in the case of 9-story frame with R =6. However, for the real 8-story building when the spectral acceleration at the fundamental period equals to 0.7g, the bias is as high as 25% due to severe degradation and collapses indicated by numerical instability.

5. The degrading parameters of the equivalent degrading SDF system are not sensitive to the load history protocol.

6. Using the proposed method can estimate the seismic demand more accurate than the conventional MPA procedure, especially for the building excited by ground motion with high intensity level.

7. The bias of the non-ductile structure tends to increase when the intensity level increases. In contrast, the bias of ductile structure in terms of underestimation tends to decrease when the intensity level increases.

8. For ductile structure, the proposed procedure provides good estimate seismic demand. The bias does not exceed 20%, and 40% for the floor displacement and the story drift demand respectively.

9. The proposed procedure cannot indicate the actual inelastic limit state of structure when the building is excited to a large displacement because of the collapse mechanism in …….WHAT?

REFERENCES

American Society of Civil Engineers (2000). Prestandard and commentary for the seismic rehabilitation of buildings. Washington, DC: Federal Emergency Management Agency, FEMA-356.

Applied Technology Council (ATC) (1997). NEHRP Guidelines for the seismic rehabilitation of buildings (FEMA-273). Washington, D.C: Building Seismic Safety Council, Federal Emergency Management Agency.

Aschheim, M. and Black, E. (1999). Effects of prior earthquake damage on response of simple stiffness-degrading structures. Earthquake Spectra, 15(1): 1-24.

Bobadilla, H. and Chopra, A.K. (2007). Modal pushover analysis for seismic evaluation of reinforced concrete special moment resisting frame buildings. Earthquake Engineering Research Center (EERC) Report No. UCB/EERC-2007-01. University of California. Berkeley, California.

Chenouda, M. and Ayoub, A. (2008). Inelastic displacement ratios of degrading systems. Journal of Structural Engineering, 134(6): 1030-1045.

Chintanapakdee, C. and Chopra, A.K. (2003a). Evaluation of modal pushover analysis using generic frames. Earthquake Engineering and Structural Dynamics, 32(3): 417-442.

Chintanapakdee, C. and Chopra, A.K. (2003b). Evaluation of the modal pushover analysis procedure using vertically "regular" and irregular generic frames. Earthquake Engineering Research Center (EERC) Report No. UCB/EERC-2003/03. University of California Berkeley, California.

Chopra, A.K. and Kan, C. (1973). Effects of stiffness degradation on ductility requirements for multistory buildings, Earthquake Engineering and Structural Dynamics, 2(1): 35-45.

Chopra, A.K. and Goel, R.K. (2002). A modal pushover analysis procedure to estimate seismic demands for buildings. Earthquake Engineering and Structural Dynamics, 31(3): 561-582.

Chopra, A.K. Goel, R.K., and Chintanapakdee, C. (2003). Statistics of single-degree-of-freedom estimate of displacement for pushover analysis of buildings. Journal of Structural Engineering, 129(4): 459-469.

Chopra, A.K., Goel, R.K., and Chintanapakdee, C. (2004). Evaluation of a modified MPA procedure assuming higher modes as elastic to estimate seismic demands. Earthquake spectra, 20(3): 757-778.

Goel, R.K., and Chopra, A.K. (2004). Evaluation of modal and FEMA pushover analyses: SAC buildings. Earthquake spectra, 20(1): 225-254.

Gupta, B. and Krawinkler, H. (1998). Effect of stiffness degradation on deformation demands of SDOF and MDOF structures, 6th U.S. National Conference on Earthquake Engineering.

Haselton, C.B. and Deierlein, G.G. (2007). Assessing seismic collapse safety of modern reinforced concrete moment-frame buildings. John A. Blume Earthquake Engineering Center Report No. 152. Standford University, California.

Intarakamheng, N. and Ruangrassamee, A. (2004). Seismic response analysis of a reinforced concrete building by cyclic pushover method. Master dissertation. Chulalongkorn University, Bangkok.

Jia, M.M., Lu, D.G., Zhang, S.M. and Jiang, S.L. (2008). Modal and cyclic pushover analysis for seismic performance evaluation of buckling-restrained braced steel frame, 14th World Conference on Earthquake Engineering, 12-17 October Beijing, China.

Kalkan, E. and Kunnath, S.K. (2006). Assessment of current nonlinear static procedures for seismic evaluation of buildings, Engineering Structures, 29(2007): 305-316.

Kim, S. and D'Amore, E. (1999). Push-over analysis procedure in earthquake engineering, Earthquake Spectra, 15(3).

Krawinkler, H. (2009). Loading histories for cyclic tests in support of performance assessment of structural components. [Online] Available from: http://peer.berkeley.edu/events/2009/icaese3/cd/files/pdf/KRAWINKLER_24. pdf. [2009, July 17]

Lowes, L.N., Mitra, N. and Altoontash, A. (2003). A Beam Column Joint Model for Simulating the Earthquake Response of Reinforced Concrete Frame. Pacific Engineering Research Center (PEER) Report 2003/10. University of California Berkeley, California.

Miranda, E. and Garcia, J.R. (2002). Influence of stiffness degradation on strength demands of structures built on soft soil sites, <u>Engineering Structures,</u> 24(10): 1271-1281.

Opensees (2008). <u>Open System for Earthquake Engineering Simulation, Pacific Earthquake Engineering Research Center (EERC),</u> [Online] University of California Berkeley. Available from: http://opensees.berkeley.edu/ [2008, July 01]

Otani, S. (1981). Hysteresis models of reinforced concrete for earthquake response analysis, <u>Journal of Faculty of Engineering, University of Tokyo,</u> XXXVI(2): 407-441.

Park, Y. and Ang, A. (1985). Mechanistic seismic damage model for reinforced concrete. <u>Journal of Structural Engineering,</u> 111(4): 722-739.

Panagiotakos, T.B. and Fardis, M.N. (2001). Deformations of reinforced concrete members at yielding and ultimate. <u>ACI Structural Journal,</u> 98(2): 135-147.

Pekoz, H.A. and Pincheira, J.A. (2004). Seismic response of stiffness and strength degrading single-degree-of-freedom systems, <u>13th World Conference on Earthquake Engineering,</u> 1-6 August Vancouver, Canada.

Pujol, S. (2002). <u>Drift Capacity of Reinforced Concrete Columns Subjected to Displacement Reversals.</u> Doctoral dissertation. Purdue University.

Qi, X. and Moehle, J.P. (1991). Displacement design approach for reinforced concrete structures subjected to earthquakes. <u>Earthquake Engineering Research Center (EERC) Report No. UCB/EERC-91/02.</u> University of California Berkeley, California.

Rahnama, M. and Krawinkler, H. (1993). Effect of soft soils and hysteresis models on seismic design spectra. <u>John A. Blume Earthquake Engineering Research Center Report No. 108.</u> Stanford University, California.

Wang, M.L. and Shah, S.P. (1987). Reinforced concrete hysteresis model based on the damage concept. <u>Earthquake engineering and structural dynamics,</u> 15: 993-1003.

Sezen, H. (2000). <u>Seismic Behavior and Modeling of Reinforced Concrete Building Columns.</u> Doctoral dissertation. University of California Berkeley, California.

Singhasut, W. and Ruangrassamee, A. (2008). <u>Seismic Performance of Reinforced-Concrete Bridge Columns in Thailand Under Cyclic Loading.</u> Master dissertation. Chulalongkorn University, Bangkok.

Shimazaki, K. and Sozen, M.A. (1985). Seismic drift of reinforced concrete structures Special Research Paper (Draft). Department of Civil Engineering, University of Illinois at Urbana-Champaign.

Song, J.K. and Pincheira, J.A. (2000). Spectral displacement demands of stiffness- and strength-degrading systems, Earthquake Spectra, 16(4): 817-851.

Yu, Q.-S, Pugliesi, R., Allen, M., and Bischoff, C. (2004). Assessment of modal pushover analysis procedure and its application to seismic evaluation of existing buildings, 13th World Conference on Earthquake Engineering, 1-6 August Vancouver, Canada.

APPENDIX A

CYCLIC PUSHOVER CURVE AND FORCE-DISPLACEMENT

RELATIONSHIP OF EQUIVALENT-SDOF SYSTEM FOR

GENERIC FRAMES

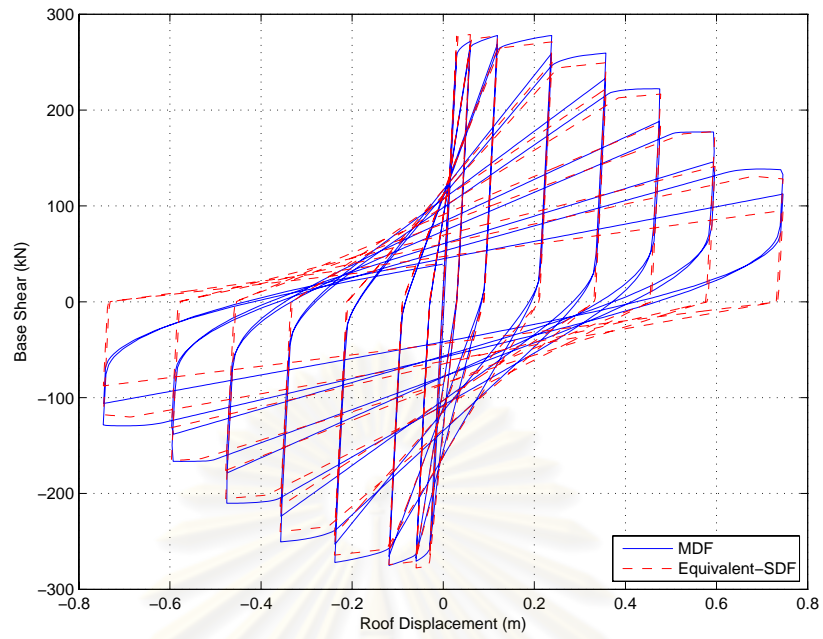**GENERIC FRAME**

1. 3-Story Building
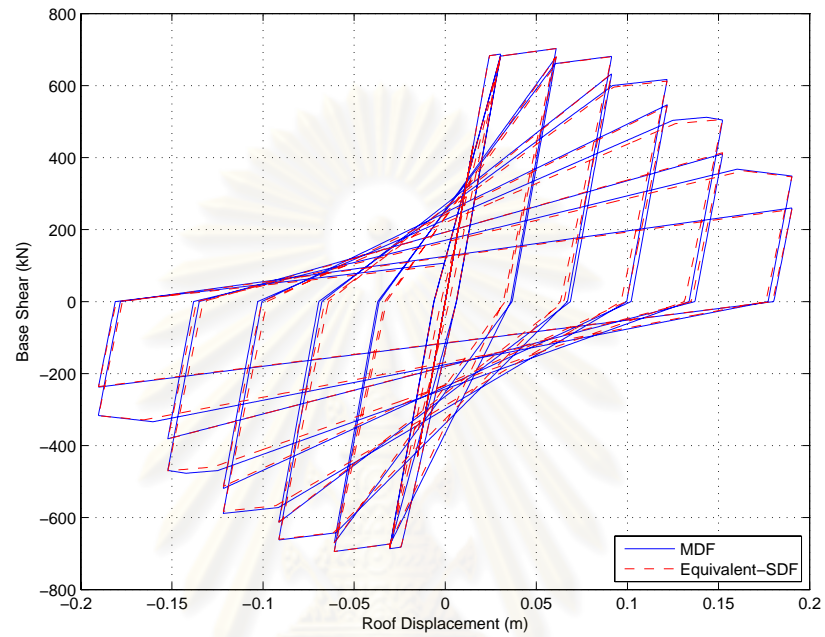
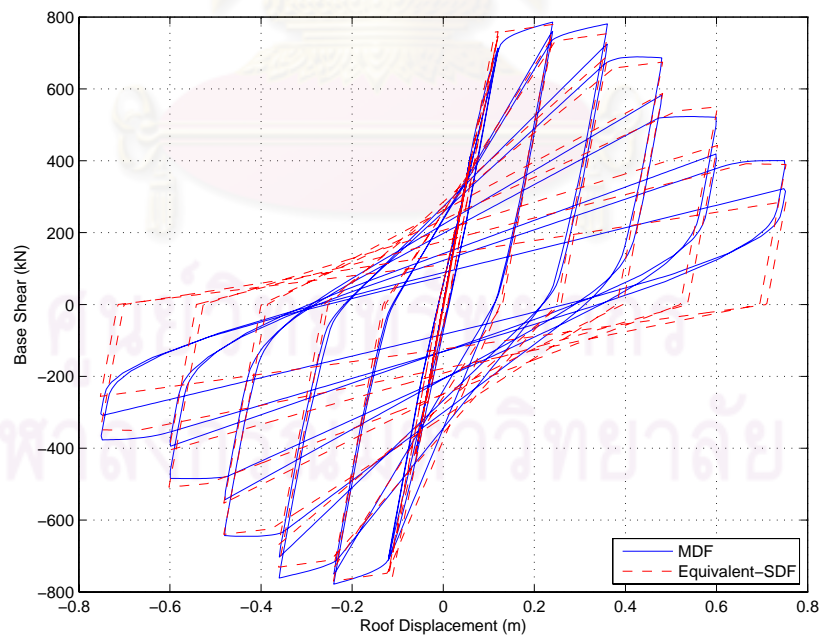**Mode 1:** Cyclic pushover curve of the 3-story building with R=2 due to $s_1^* = \mathbf{m}\phi_1$
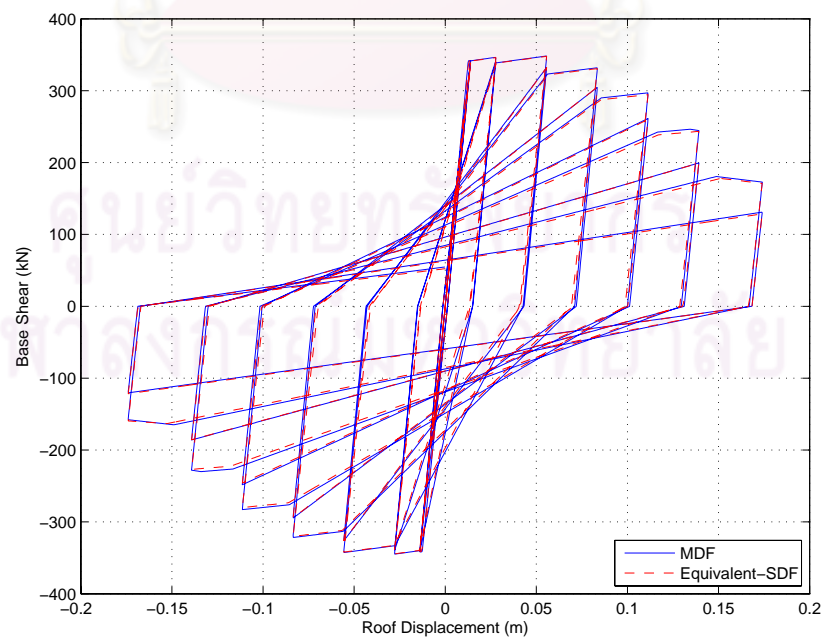
Mode 1: Cyclic pushover curve of the 3-story building with R=4 due to $s_1^* = \mathbf{m}\phi_1$
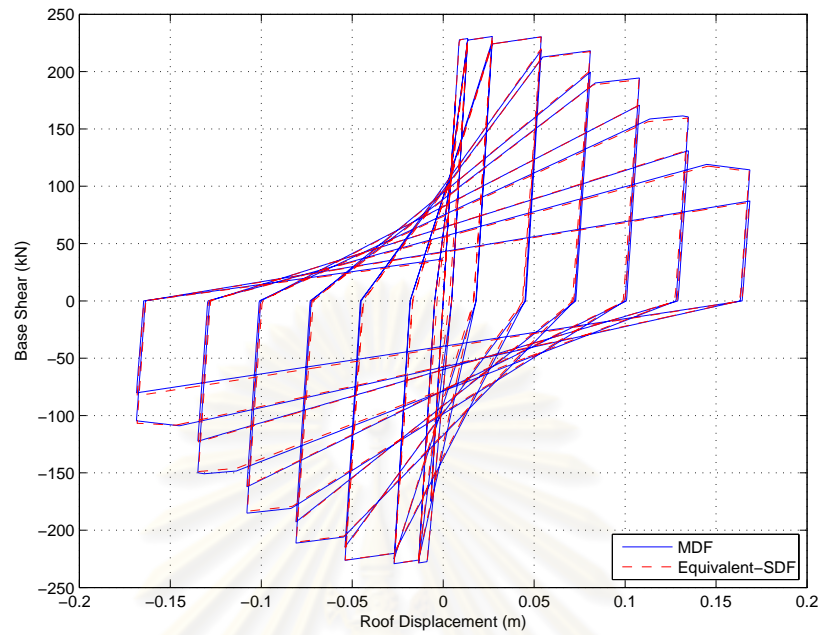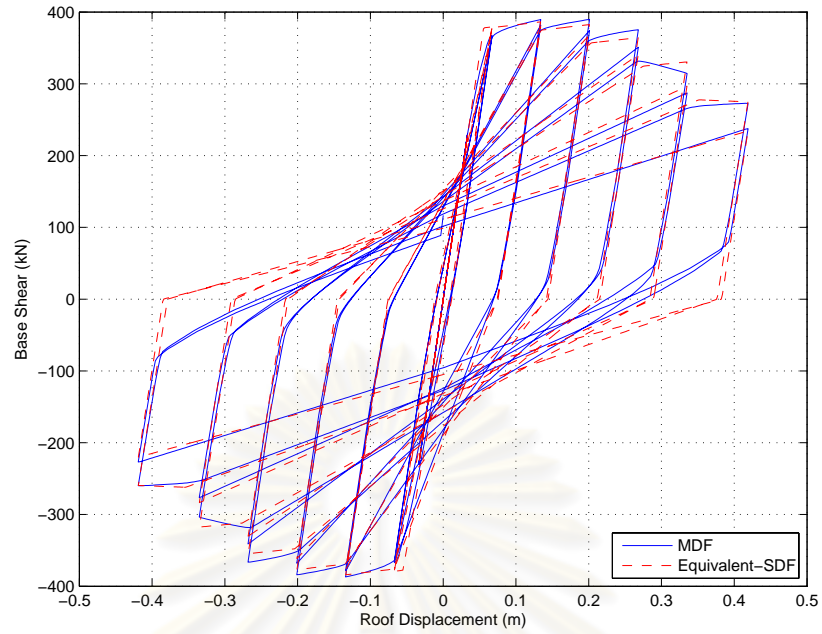

Mode 1: Cyclic pushover curve of the 3-story building with R=6 due to $s_1^* = \mathbf{m}\phi_1$
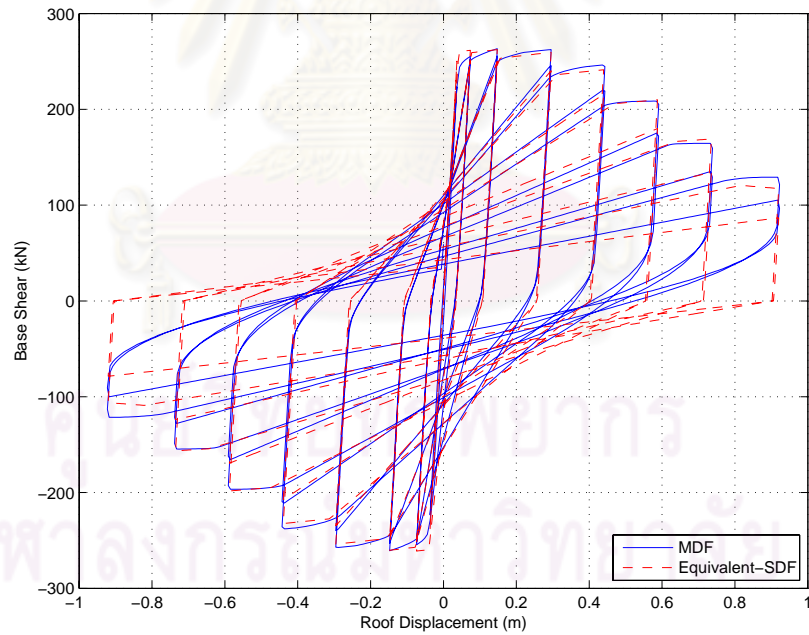
2. 6-Story Building
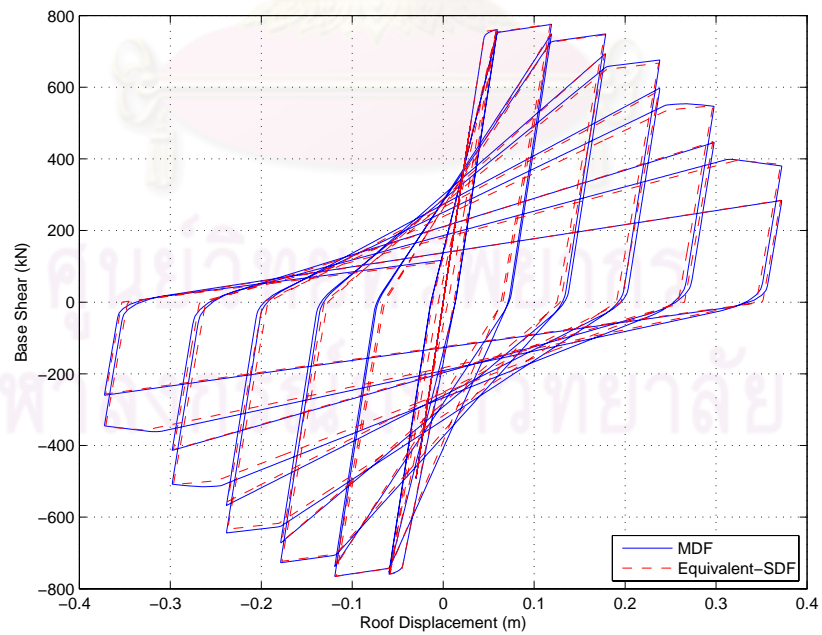
Mode 1: Cyclic pushover curve of the 6-story building with R=2 due to $s_1^* = \mathbf{m}\phi_1$
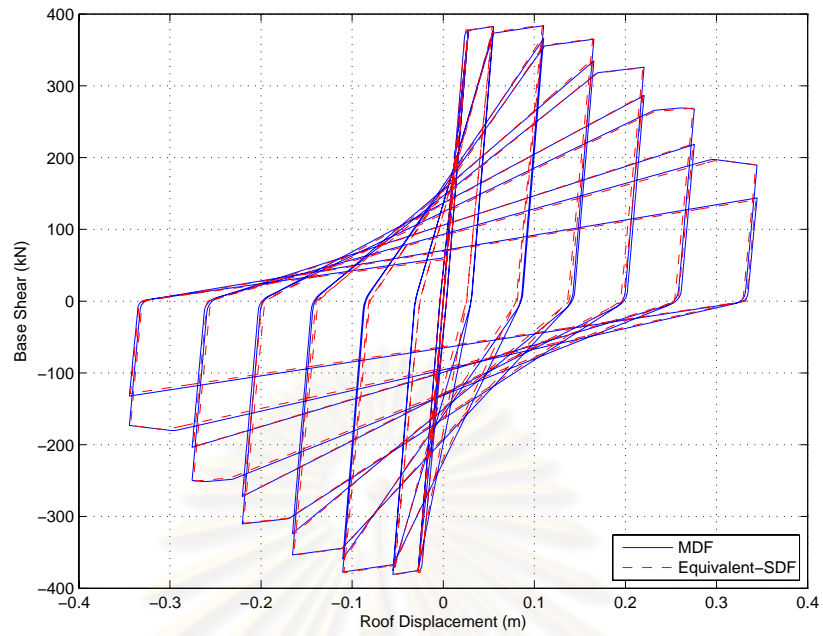
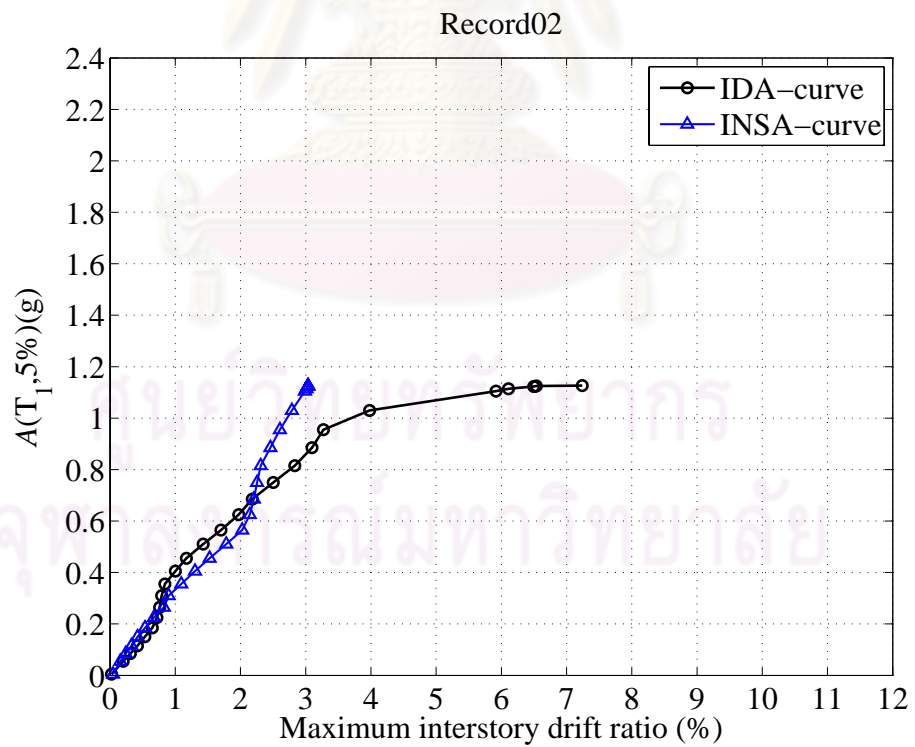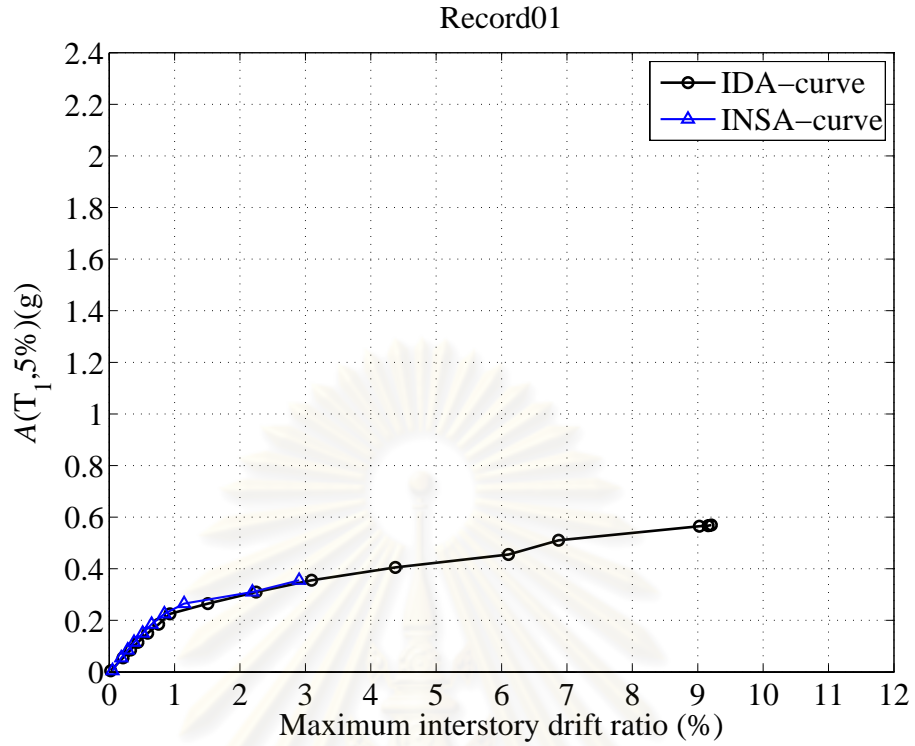**Mode 1:** Cyclic pushover curve of the 6-story building with R=4 due to $s_1^* = \mathbf{m}\phi_1$
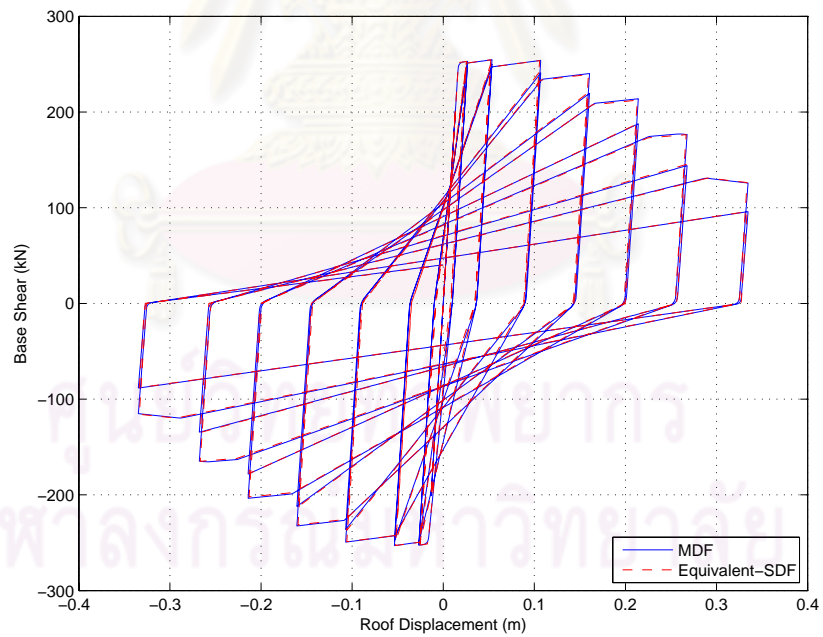
Mode 1: Cyclic pushover curve of the 6-story building with R=6 due to $s_1^* = \mathbf{m}\phi_1$

3. 9-Story Building
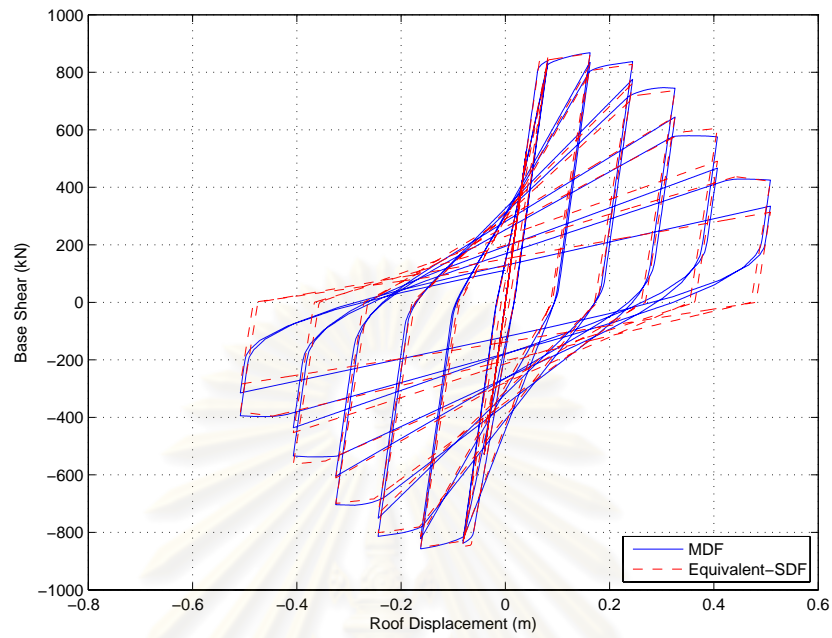
Mode 1: Cyclic pushover curve of the 9-story building with R=2 due to $s_1^* = \mathbf{m}\phi_1$
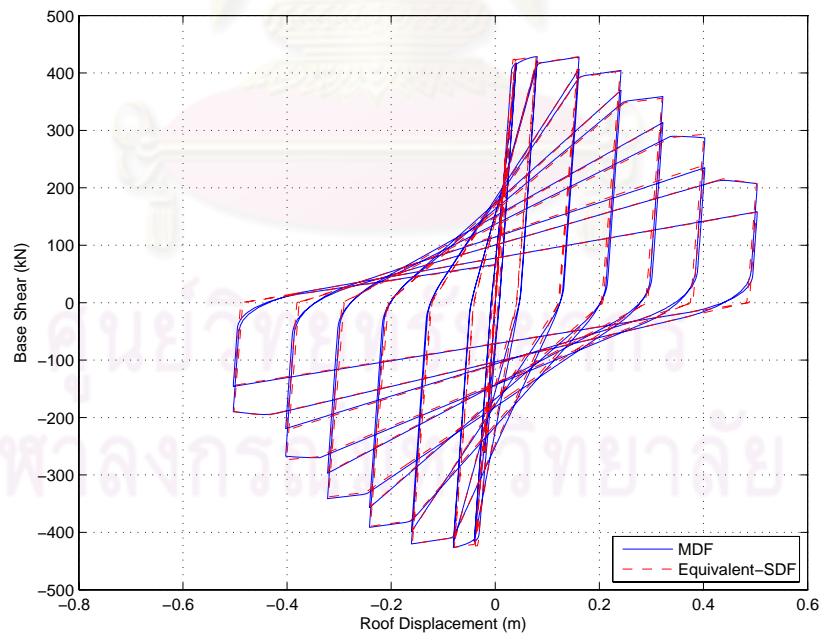
Mode 1: Cyclic pushover curve of the 9-story building with R=4 due to $s_1^* = \mathbf{m}\phi_1$
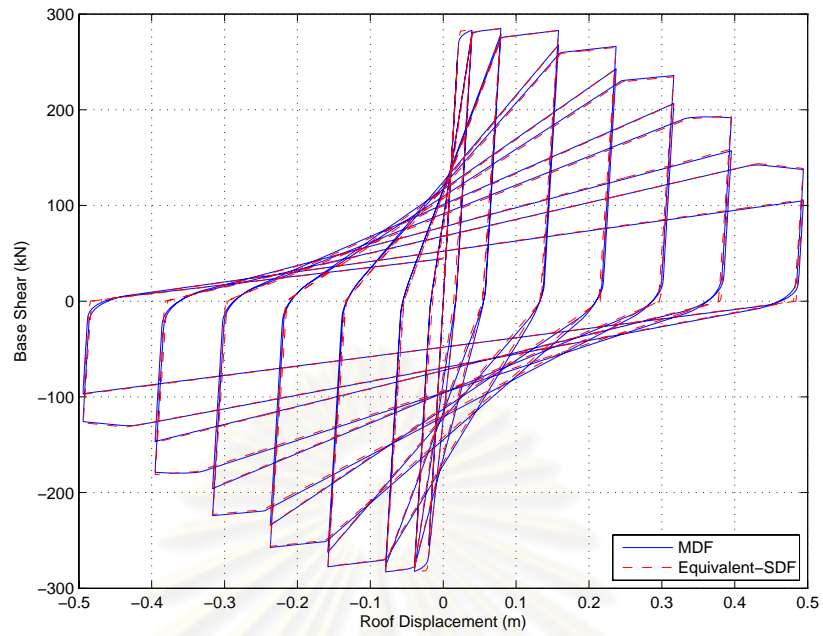
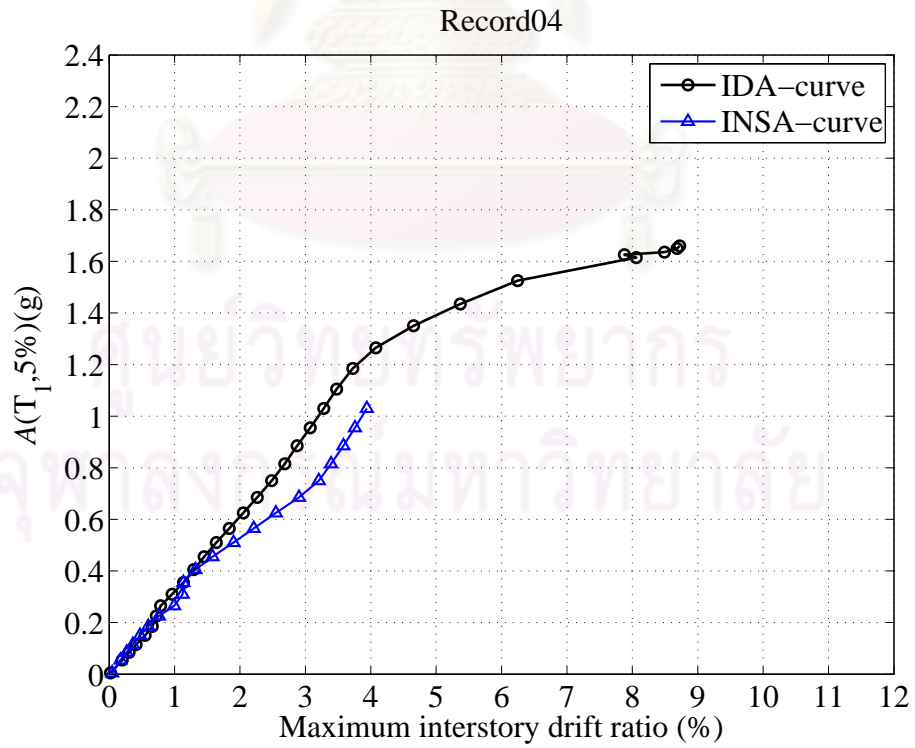**Mode 1:** Cyclic pushover curve of the 9-story building with R=6 due to $s_1^* = \mathbf{m}\phi_1$

4. 12-Story Building
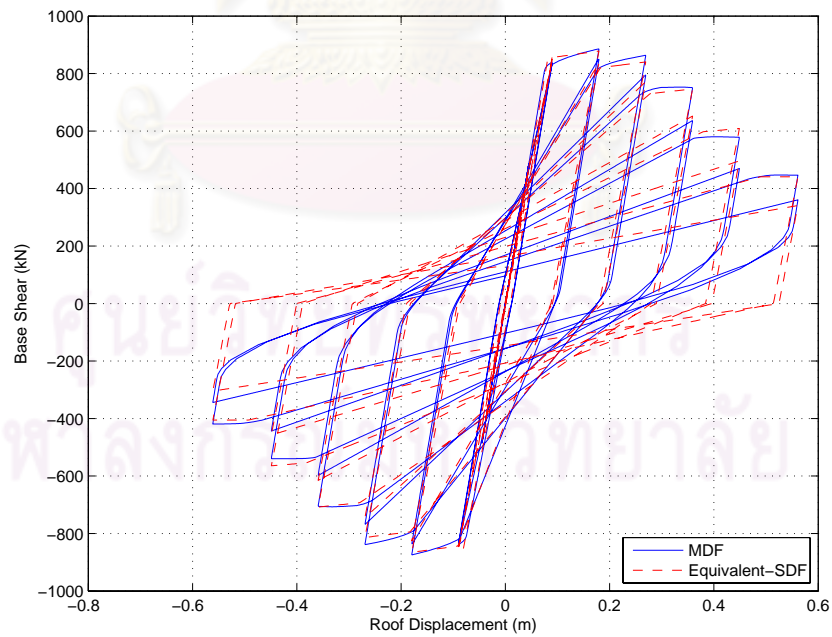
Mode 1: Cyclic pushover curve of the 12-story building with R=2 due to $s_1^* = \mathbf{m}\phi_1$
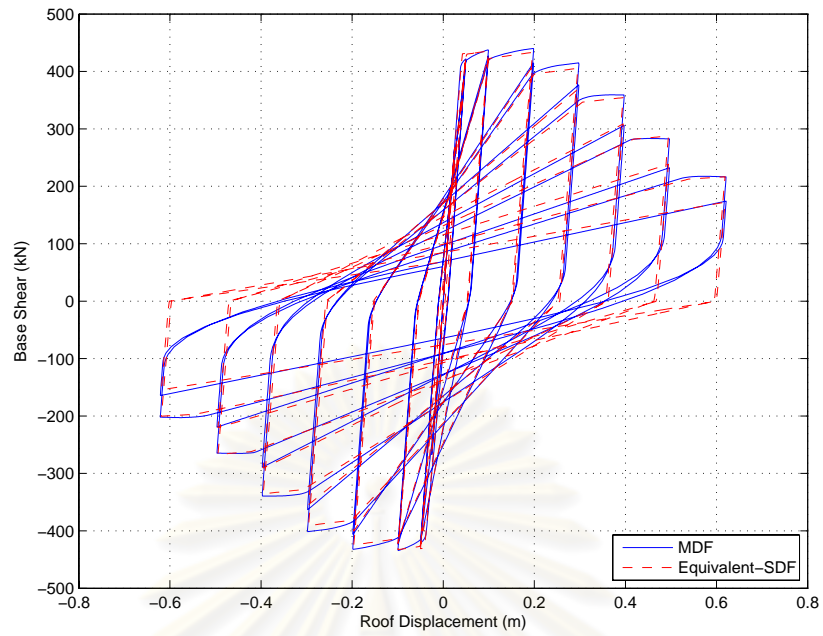
Mode 1: Cyclic pushover curve of the 12-story building with R=4 due to $s_1^* = \mathbf{m}\phi_1$
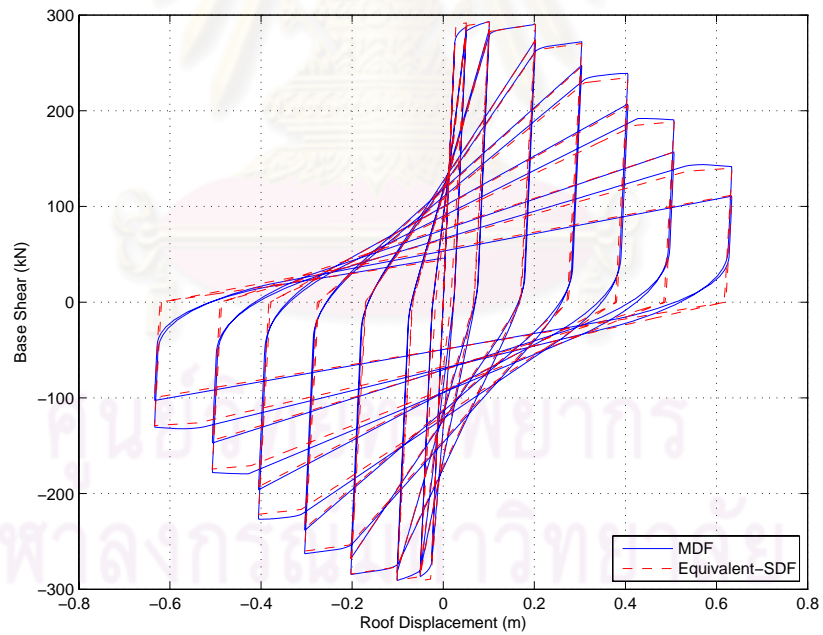
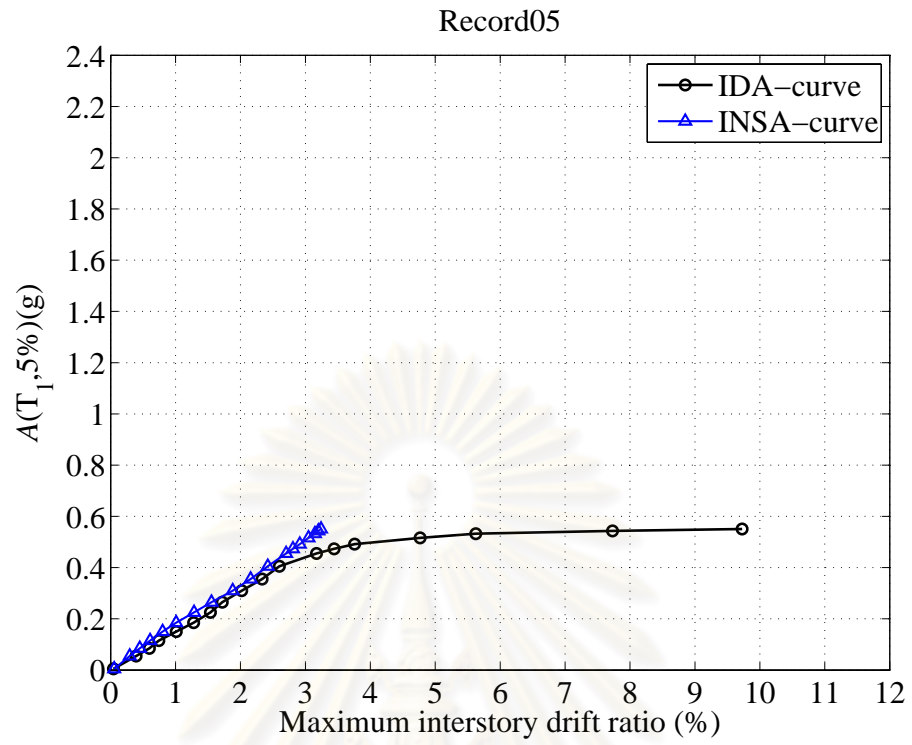**Mode 1:** Cyclic pushover curve of the 12-story building with R=6 due to $s_1^* = \mathbf{m}\phi_1$

5. 15-Story Building
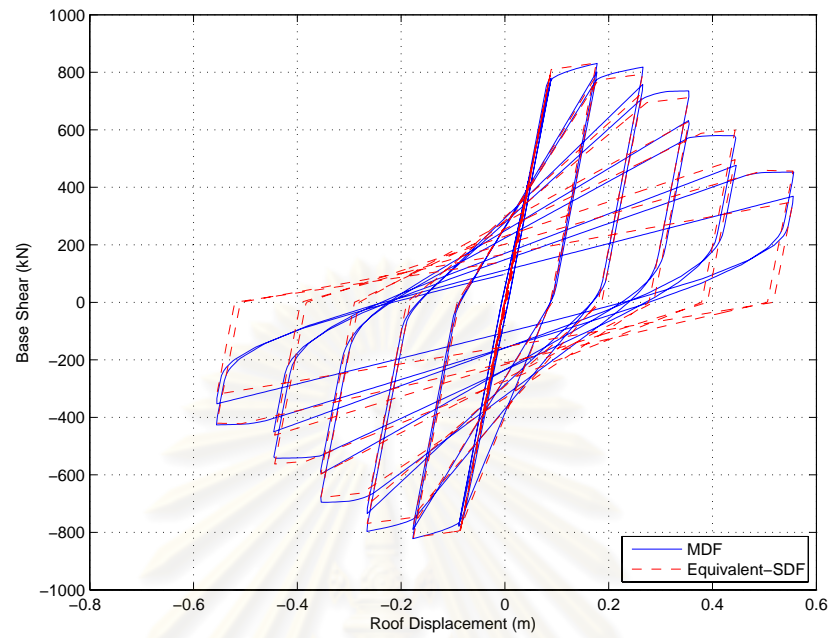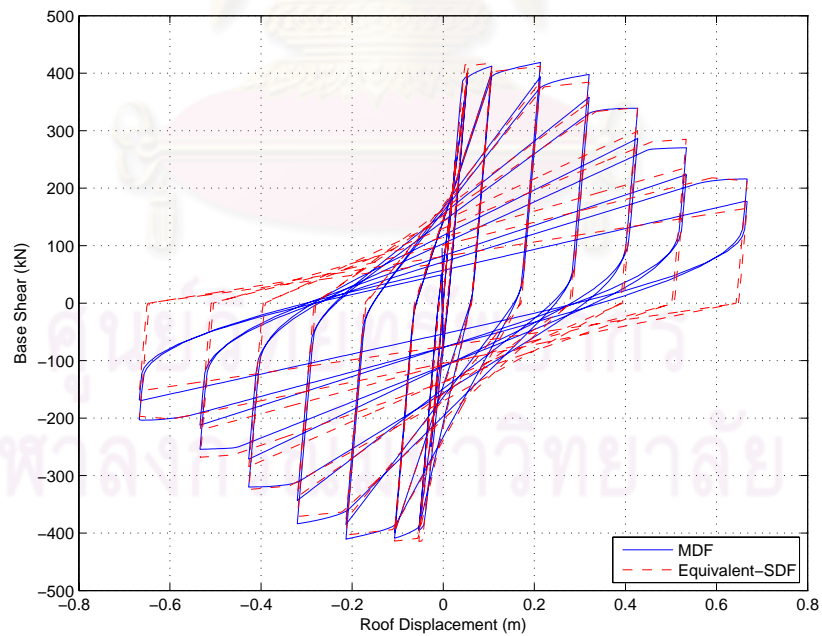
Mode 1: Cyclic pushover curve of the 15-story building with $R=2$ due to $s_1^* = \mathbf{m}\phi_1$

Mode 1: Cyclic pushover curve of the 15-story building with $R=4$ due to $s_1^* = \mathbf{m}\phi_1$

Mode 1: Cyclic pushover curve of the 15-story building with R=6 due to $s_1^* = \mathbf{m}\phi_1$

6. 15-Story Building

Mode 1: Cyclic pushover curve of the 18-story building with R=2 due to $s_1^* = \mathbf{m}\phi_1$

Mode 1: Cyclic pushover curve of the 18-story building with R=4 due to $s_1^* = \mathbf{m}\phi_1$

Mode 1: Cyclic pushover curve of the 18-story building with R=6 due to $s_1^* = \mathbf{m}\phi_1$

APPENDIX B

**COMPARATIVE OF THE INCREMENTAL DYNAMIC
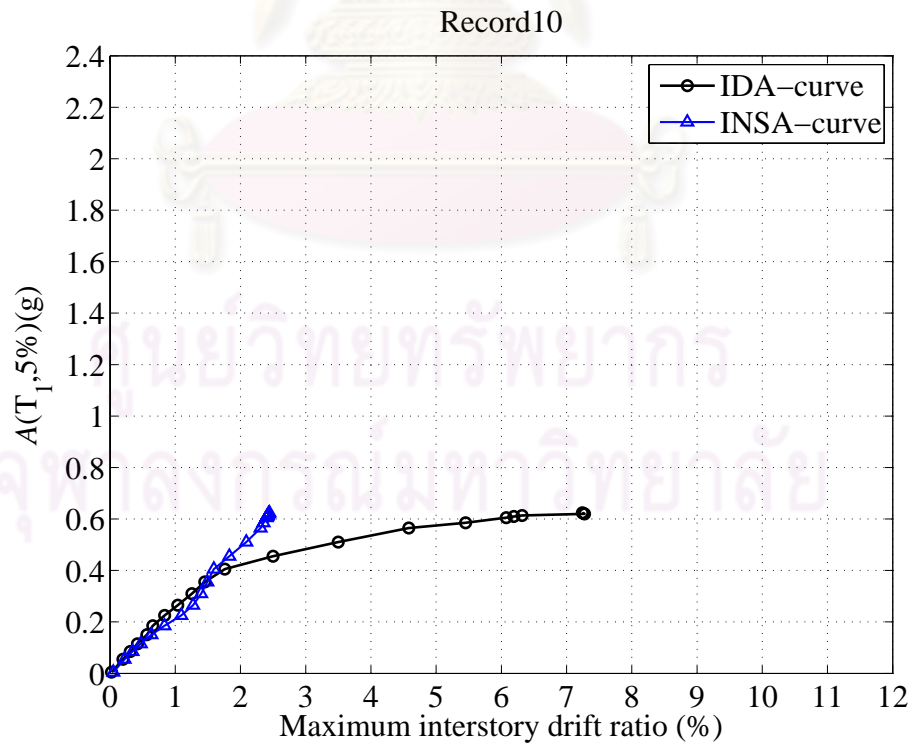ANALYSIS AND THE INCREMENTAL NONLINEAR STATIC
ANALYSIS**

Record01

Record02

Record03

Record04

Record05

Record06

Record07

Record08

Record09

Record10

Record11

Record12

Record13

Record14

Record15

Record16

Record17

Record18

Record19

Record20
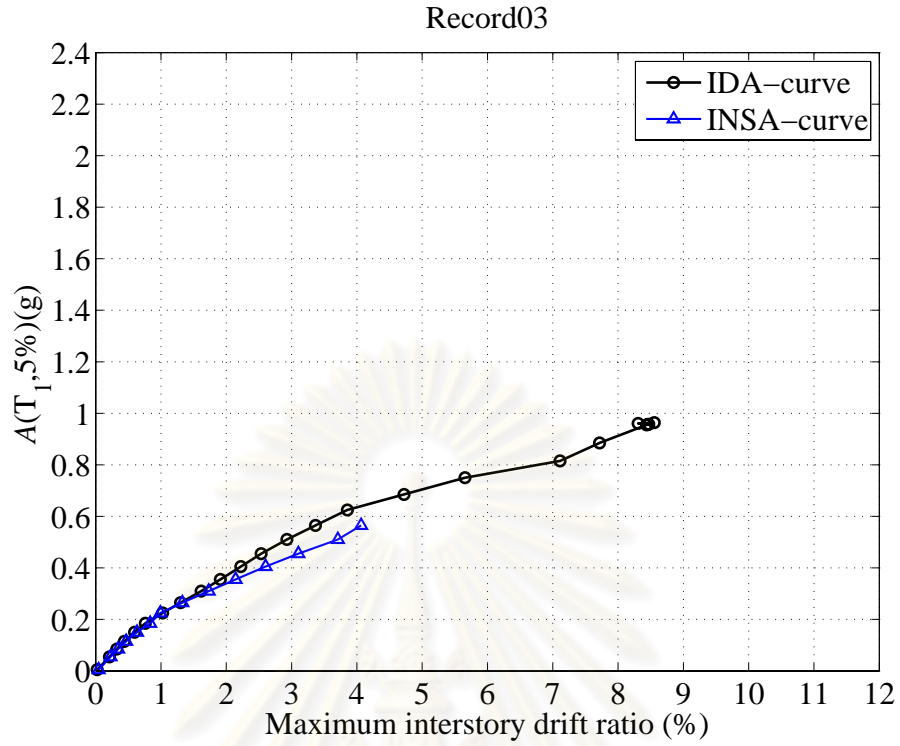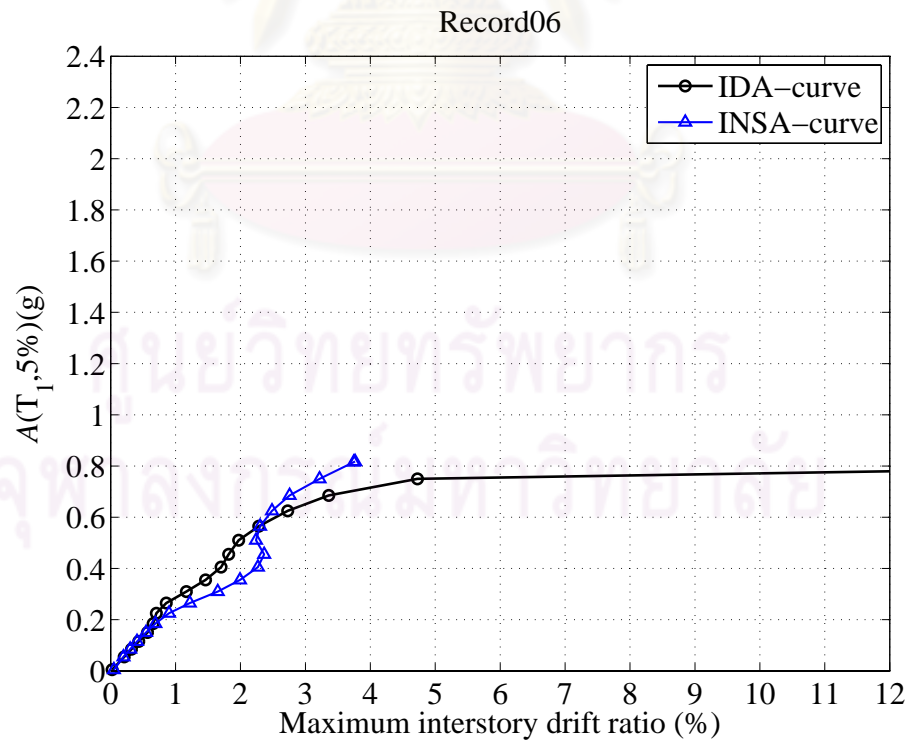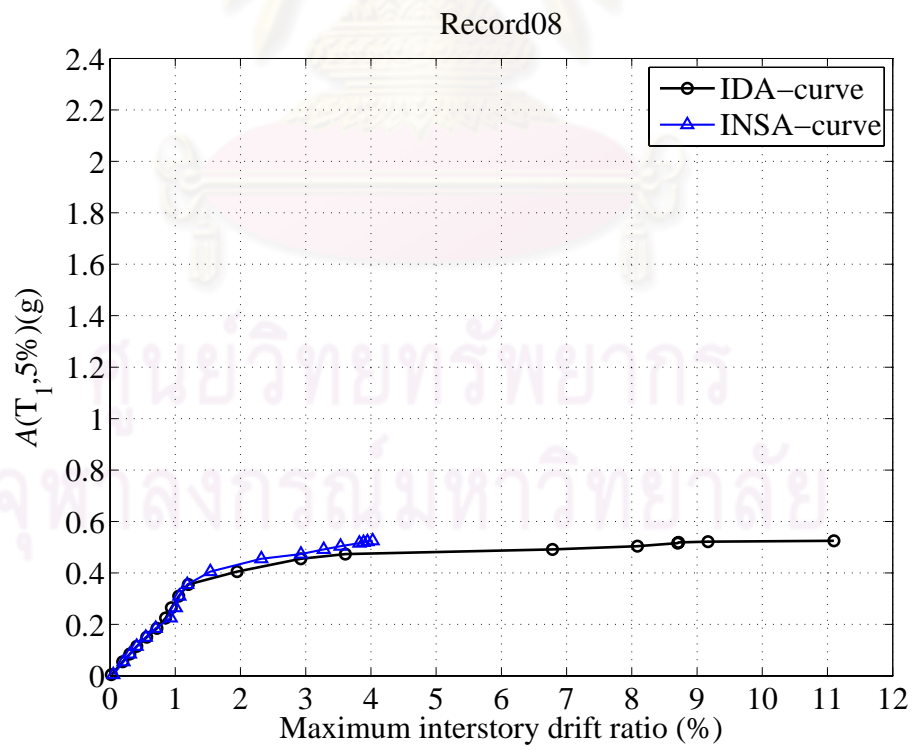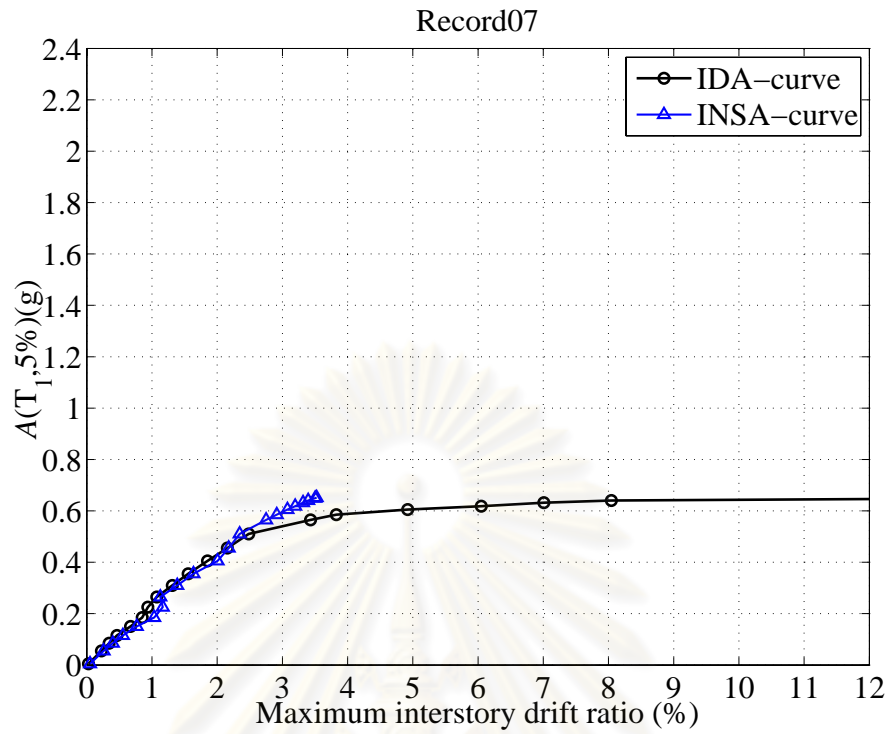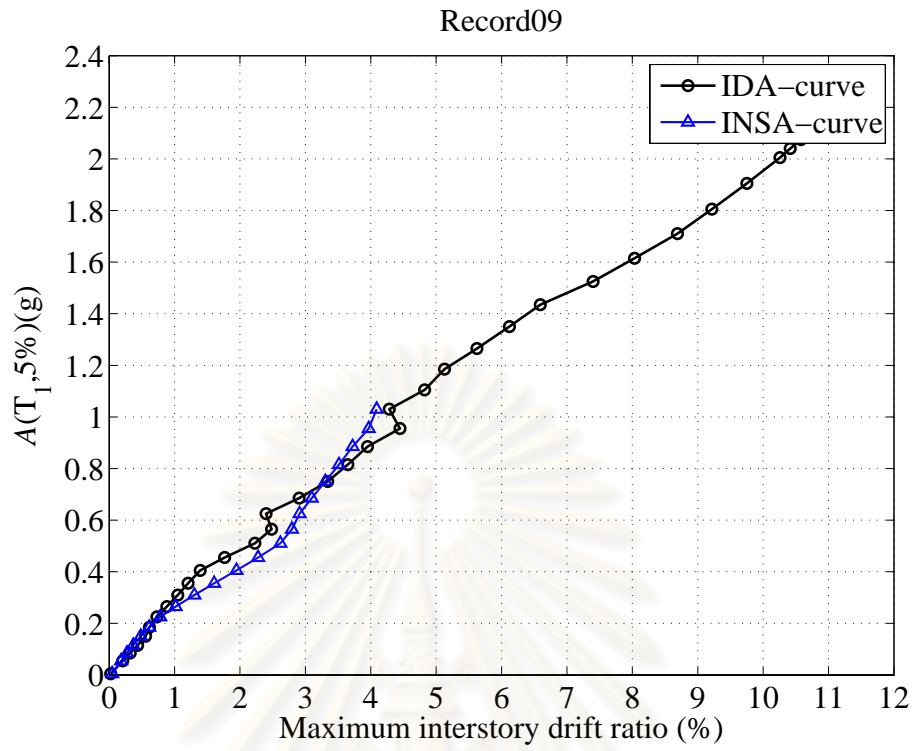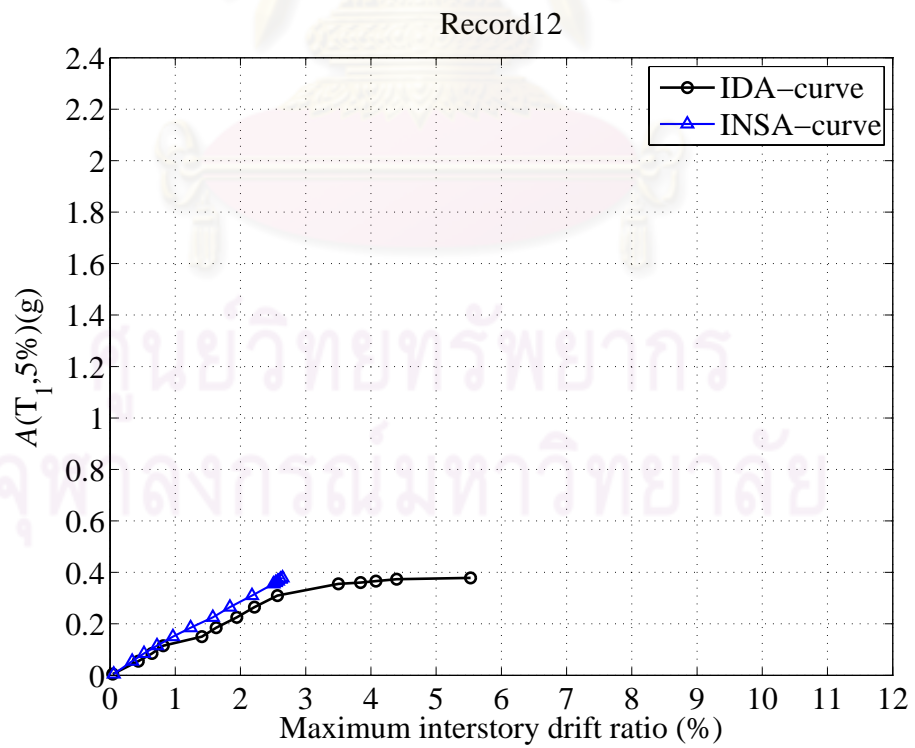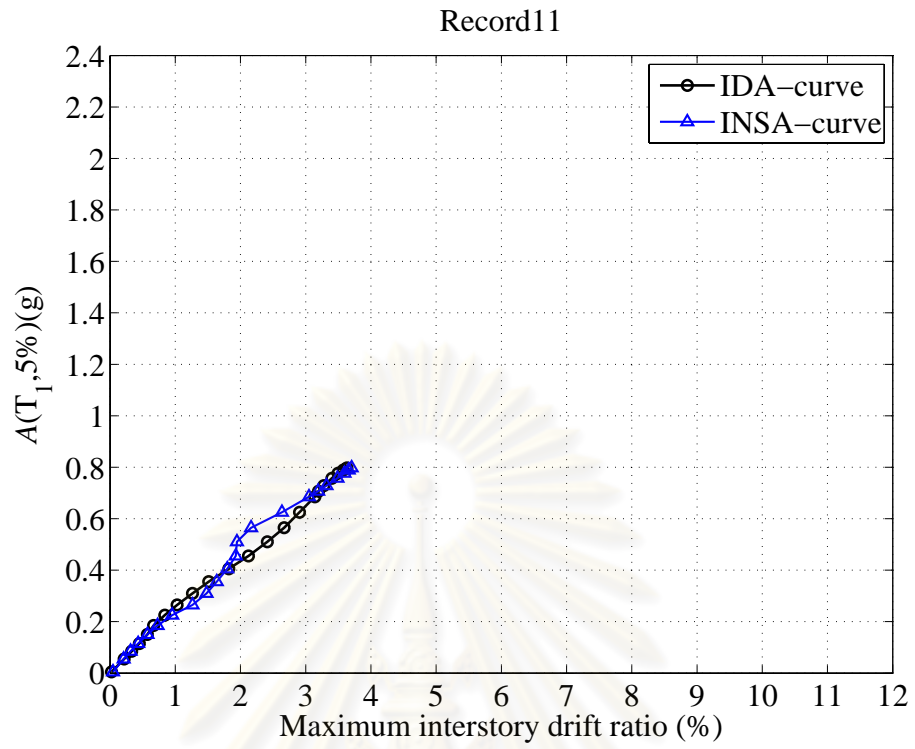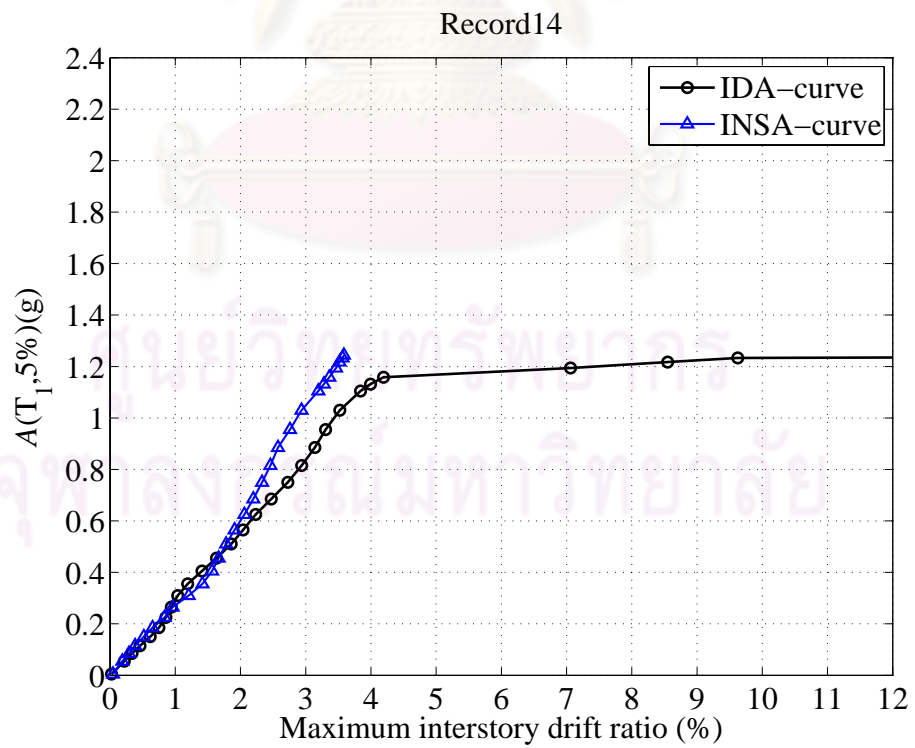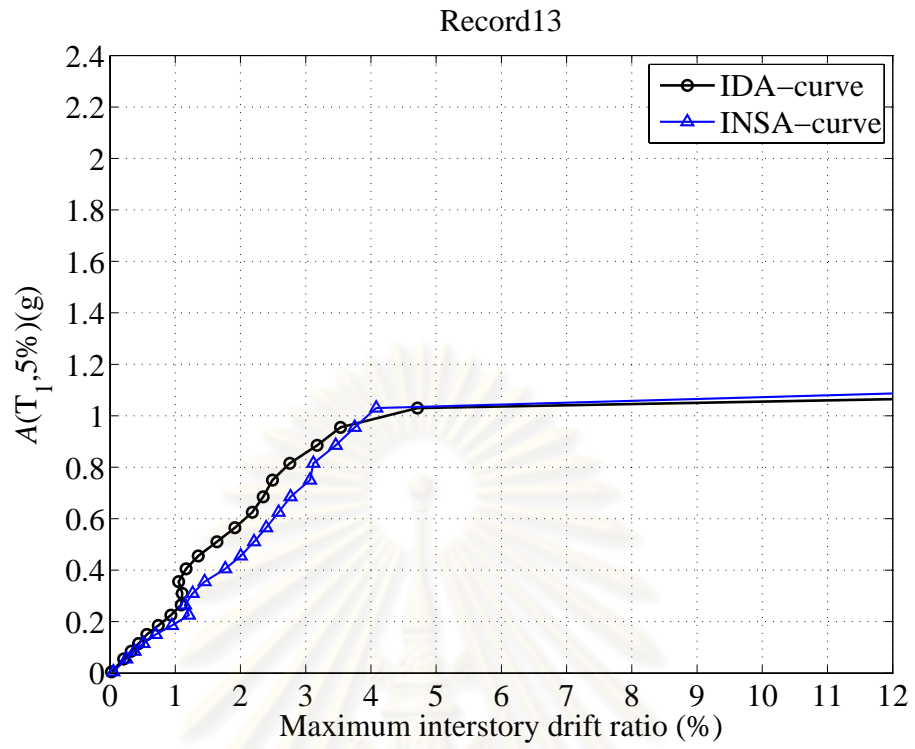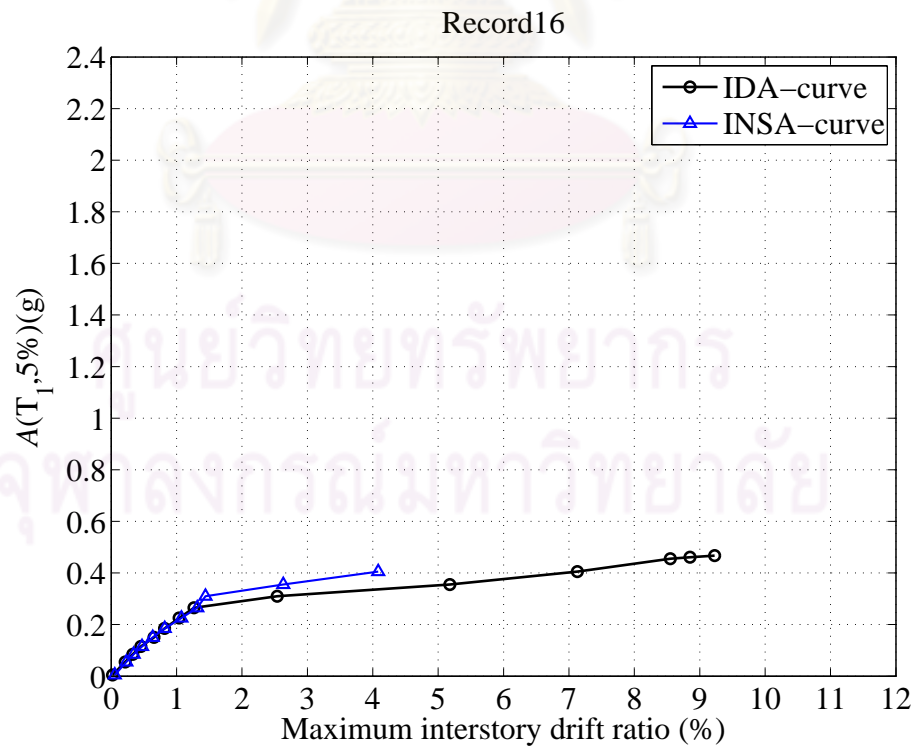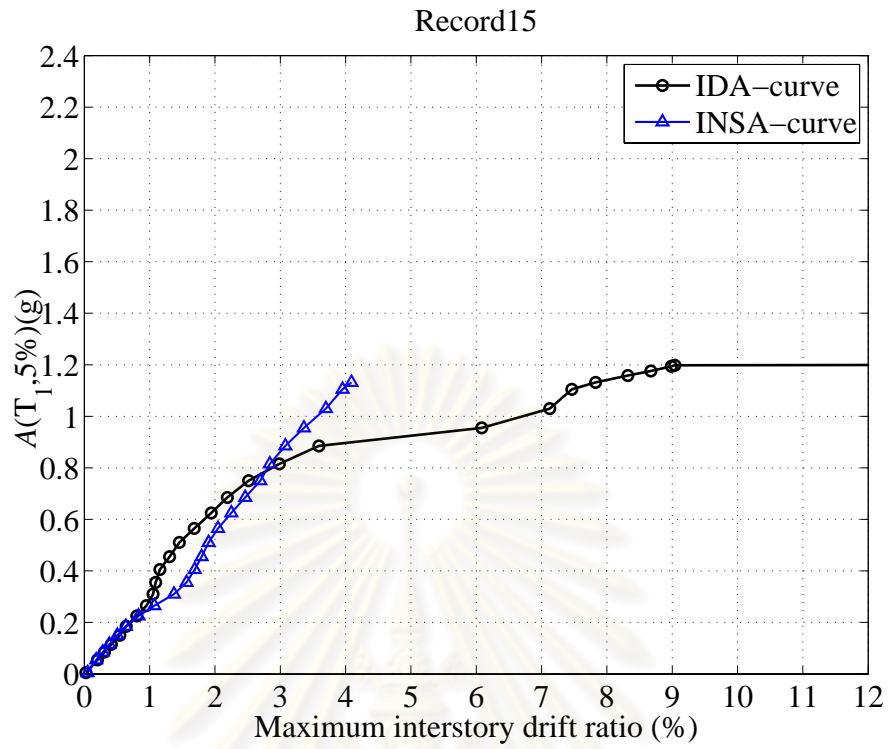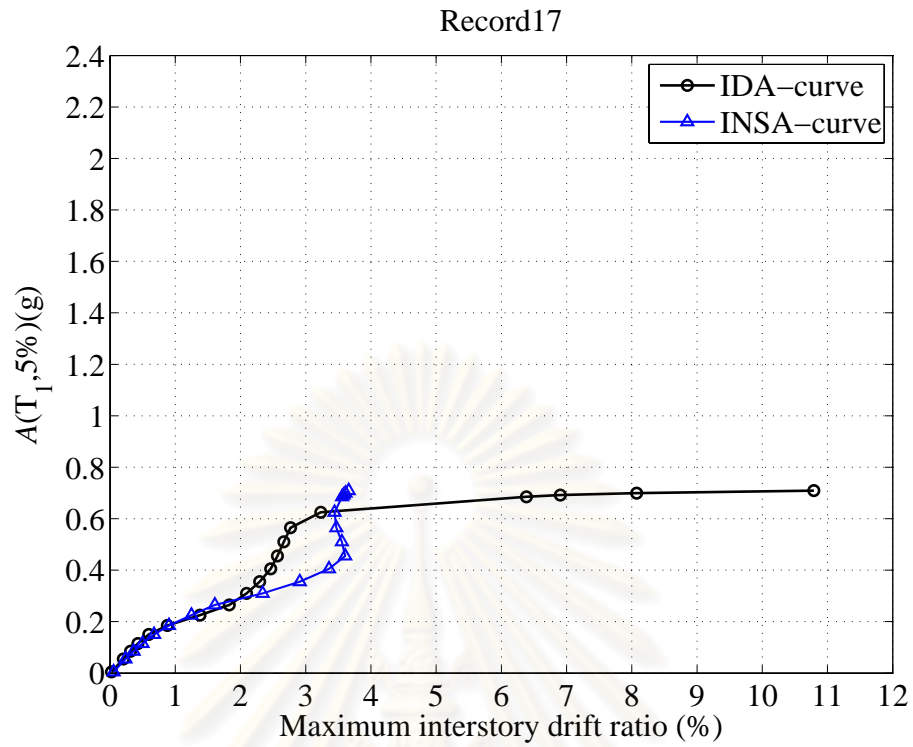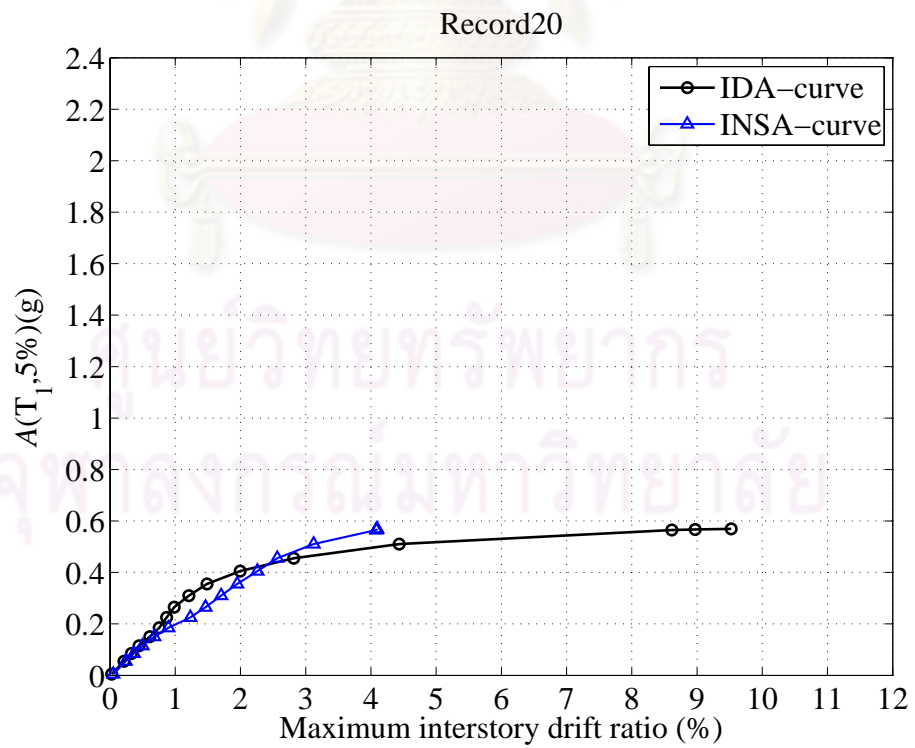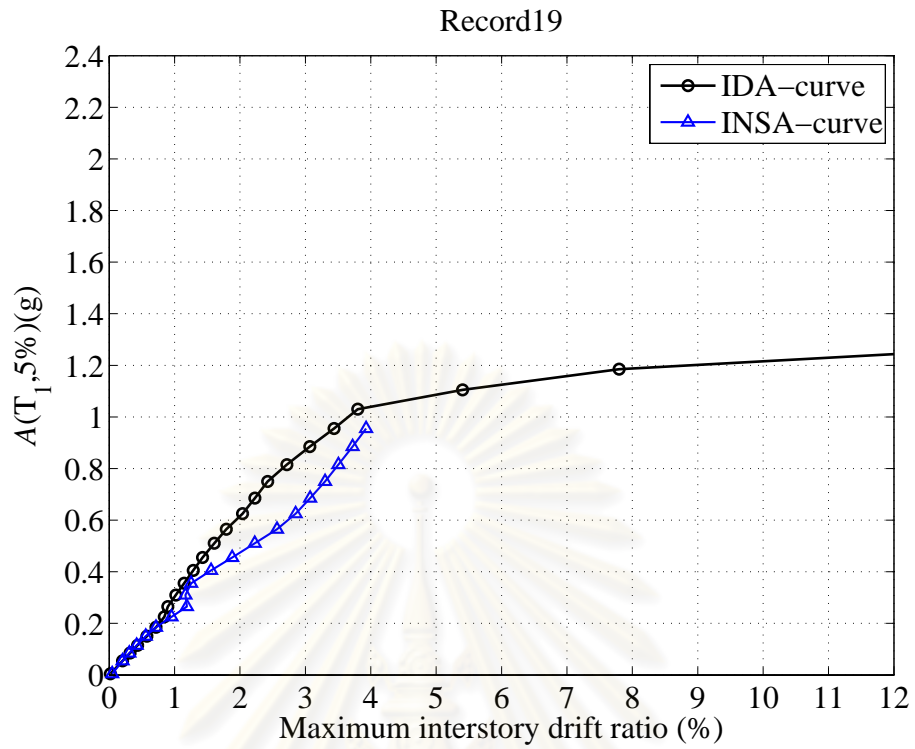
APPENDIX C

VERIFICATION OF FUILURE MODE OF COLUMNS FOR THE
REAL RC 8-STORY BUILDING

1. Column C1

1.1 Determine P-M Interaction

Figure 1 P-M interaction diagram of column C1 of a real RC 8-story building

1.2 Moment Capacity (ϕM_n)

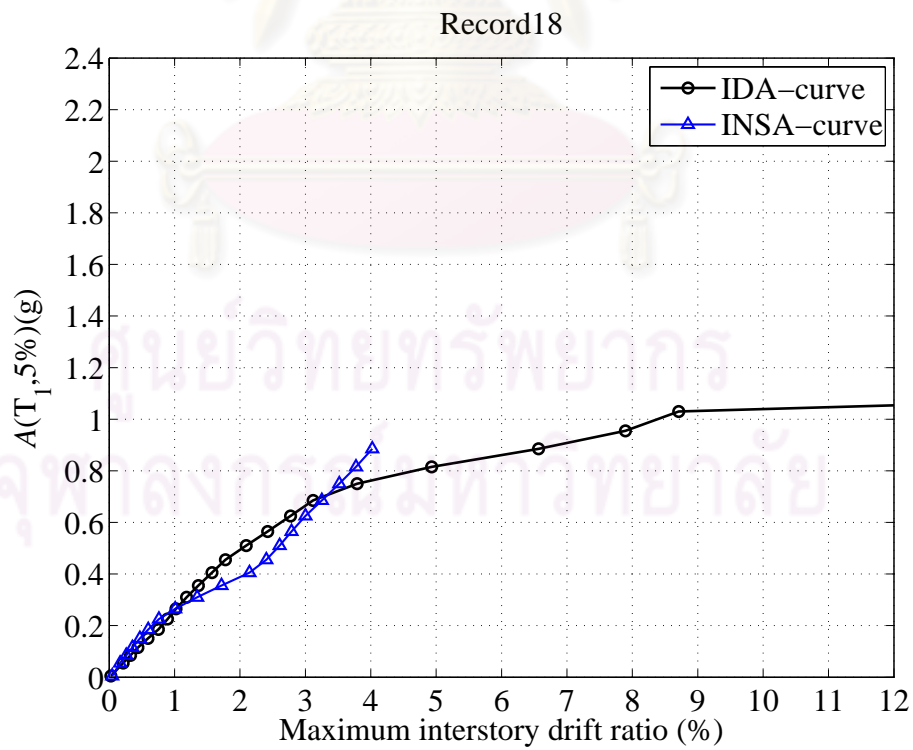Axial compression on column (N_u); N_u = 1030 kN (Factor load). From interaction diagram in Figure 1, nominal bending mement of column C1, ϕM_n, equal to 210 kN-m when the axial load in column, $P_{\max}$, equal to 1030 kN.

1.3 Shear Force During Develop Plastic Hinge

$\phi M_n = 210$ kN-m.

V_{PH}

H = 3.1 m.

V_{PH}

$\phi M_n = 210$ kN-m.

<u>Equilibrium;</u>

$\sum M = 0$; $V_{PH} \times 3.1 = 210 \times 2$

$V_{PH} = 135.48$ kN

1.4 Shear Capacity of Section

Nominal shear strength of column subjected to axial compression provided by concrete (V_c) can be determined as Eq. (11-4) in ACI 318-08

$$V_c = 2\left(1 + \frac{N_u}{2000A_g}\right)\sqrt{f_c'}b_w d$$

where $N_u = 1030$ kN (231,471 lb), $A_g = 248$ in^2, $f_c' = 3413.6$ psi, $b_w = 15.75$ in, $d = 14.06$ in.

$$V_c = 37,952 \text{ lb. (168.88 kN)}$$

Nominal shear strength due to shear reinforcement (V_s) can be determined as Eq. (11-15)

$$V_s = \frac{A_v f_{yt} d}{s}$$

Where $A_v = 0.487$ in^2, $f_{yt} = 56,893$ psi, $d = 14.06$ in., $s = 7.874$ in

$$V_s = 49,474 \text{ lb. (220.15 kN)}$$

$$\phi V_n = \phi V_c + \phi V_s$$

$$\phi V_n = (0.85 \times 37,952) + (0.85 \times 49,474)$$

$$= 74,312 \text{ lb (330.67 kN)}$$

Therefore, $\phi V_n > V_{PH}$ collapse mechanism of column C1 controlled by flexure mode.

2. Column C3

2.1 Determine P-M Interaction
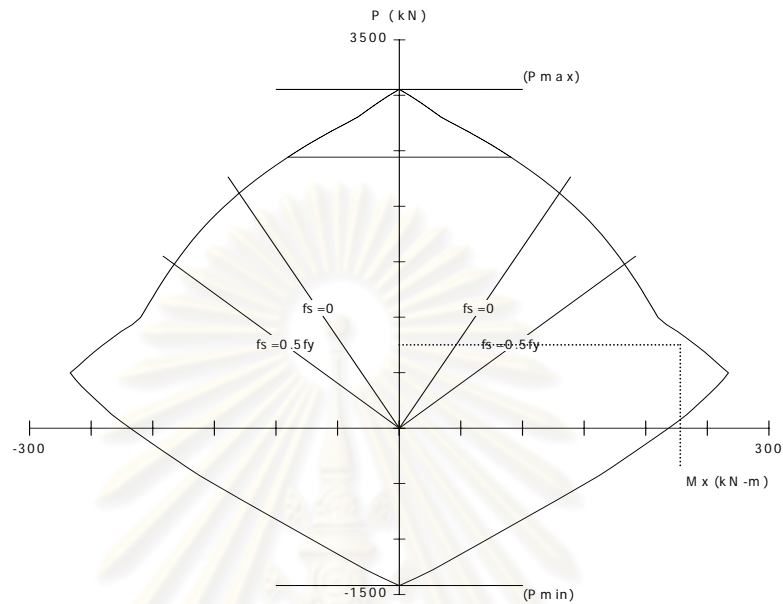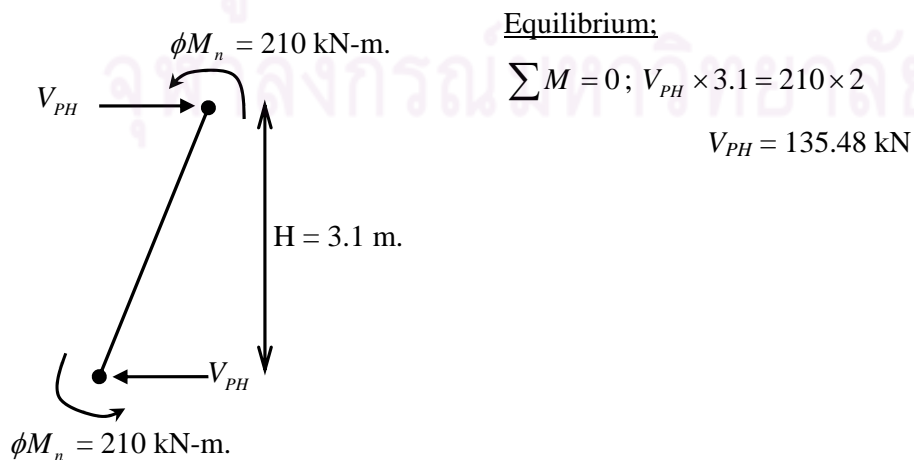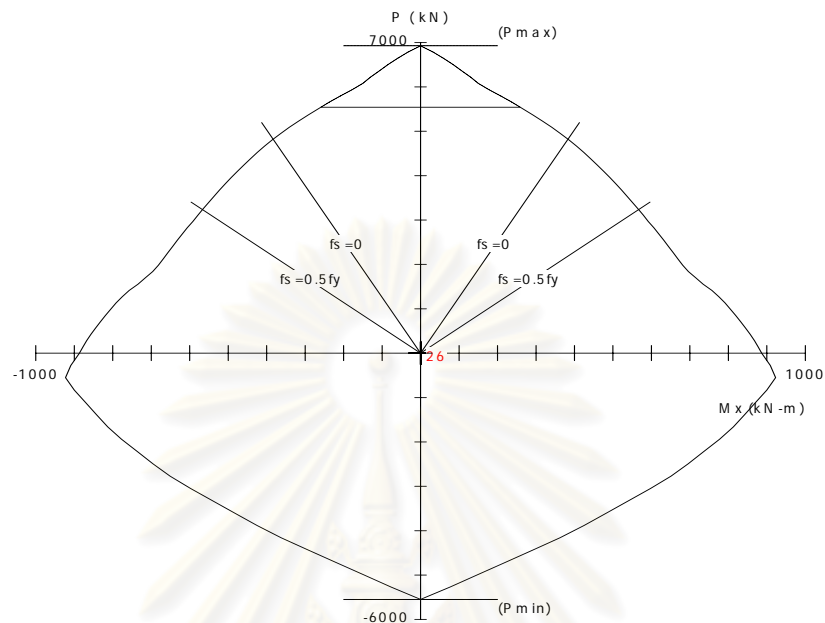

Figure 2 P-M interaction diagram of column C1 of a real RC 8-story building

2.2 Moment Capacity (ϕM_n)

Axial compression on column (N_u); N_u = 1776.42 kN (Factor load). From interaction diagram in Figure 2, Nominal bending moment of column C3, ϕM_n, equal to 482 kN-m when the axial load in column, $P_{\max}$, equal to 1776.42 kN.

2.3 Shear Force During Develop Plastic Hinge

$\phi M_n = 482$ kN-m.

V_{PH}

$H = 3.1$ m.

V_{PH}

$\phi M_n = 482$ kN-m.

Equilibrium;

$\sum M = 0$; $V_{PH} \times 3.1 = 482 \times 2$

$V_{PH} = 311$ kN
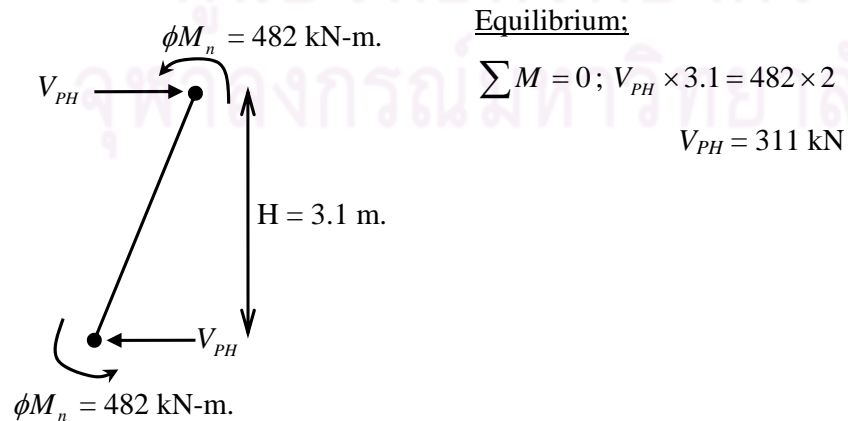
2.4 Shear Capacity of Section

Nominal shear strength of column subjected to axial compression provided by concrete (V_c) can be determined as Eq. (11-4) in ACI 318-08

$$V_c = 2\left(1 + \frac{N_u}{2000A_g}\right)\sqrt{f_c'}\,b_w d$$

where $N_u = $ 1776.42 kN (399,214 lb), $A_g = 372$ in^2, $f_c' = 3413.6$ psi, $b_w = 15.75$ in, $d = 21.91$ in.

$$V_c = 61,960 \text{ lb. (275.71 kN)}$$

Nominal shear strength due to shear reinforcement (V_s) can be determined as Eq. (11-15)

$$V_s = \frac{A_v f_{yt} d}{s}$$

Where $A_v = 0.263$ in^2, $f_{yt} = 34,135$ psi, $d = 21.91$ in., $s = 9.843$ in

$$V_s = 19,983 \text{ lb. (88.92 kN)}$$

$$\phi V_n = \phi V_c + \phi V_s$$

$$\phi V_n = (0.85 \times 61,960) + (0.85 \times 19,983)$$

$$= 69,651 \text{ lb (310 kN)}$$
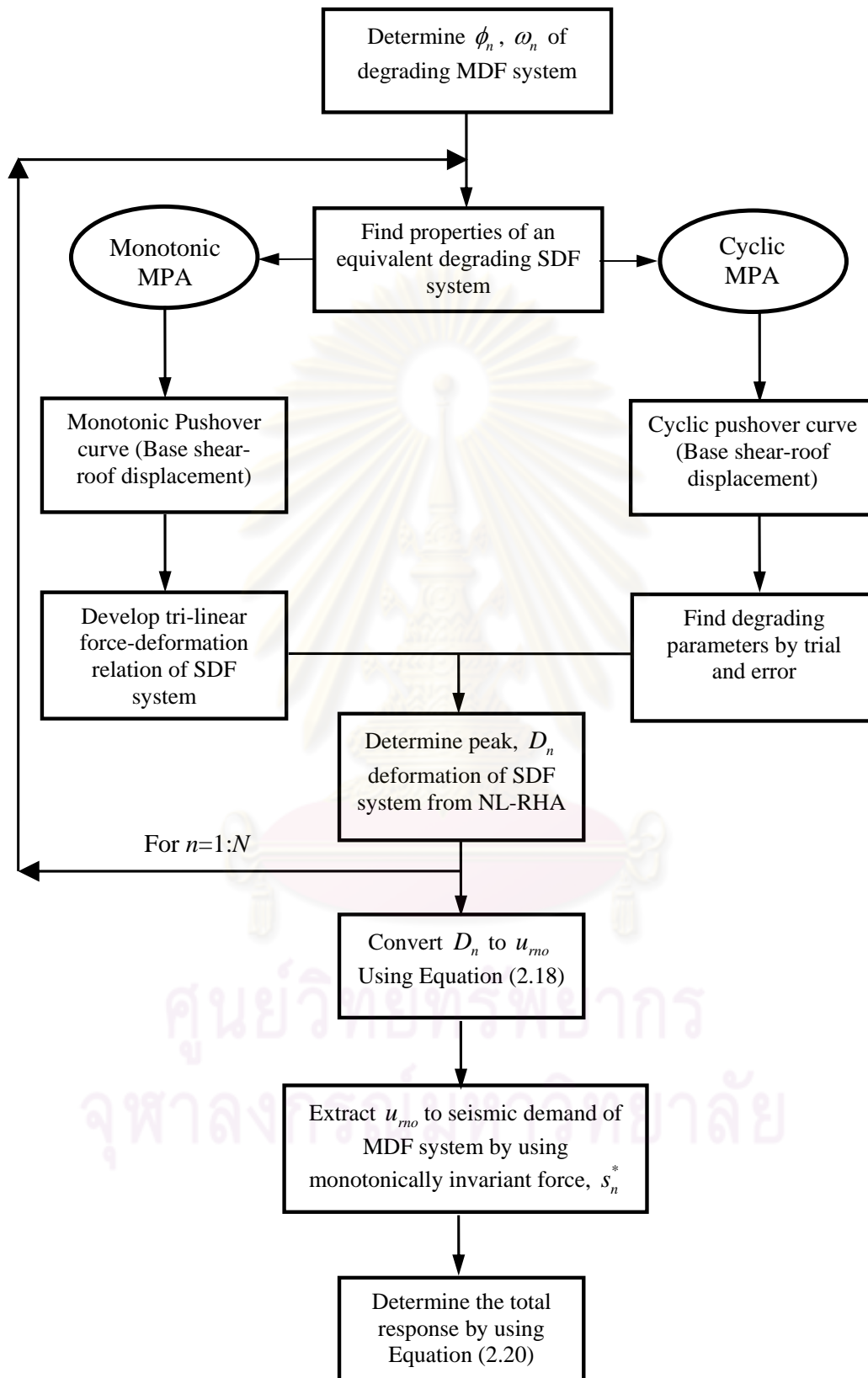
$\therefore$ The shear strength of column C3 (ϕV_n) is very close to horizontal shear force (V_{PH}) which develop the plastic hinges. Therefore, the failure mode of column C1 is controlled by flexure failure mode.

APPENDIX D

STEPS INVOLVED IN MODAL PUSHOVER ANALYSIS FOR DEGRADING STRUCTURES

```
┌─────────────────────────┐
│ Determine φ_n, ω_n of   │
│ degrading MDF system    │
└─────────────────────────┘
```

$$\text{Determine } \phi_n, \omega_n \text{ of degrading MDF system}$$

Find properties of an equivalent degrading SDF system

Monotonic MPA

Cyclic MPA

Monotonic Pushover curve (Base shear-roof displacement)

Cyclic pushover curve (Base shear-roof displacement)

Develop tri-linear force-deformation relation of SDF system

Find degrading parameters by trial and error

Determine peak, D_n deformation of SDF system from NL-RHA

For $n=1:N$

Convert D_n to u_{rno} Using Equation (2.18)

Extract u_{rno} to seismic demand of MDF system by using monotonically invariant force, s_n^*

Determine the total response by using Equation (2.20)

BIOGRAPHY

Mr. Amornchai Jaiyong was born in Bangkok, Thailand on June 11th, 1977. He graduated high school from Phra Pathom Witthayalai located in Nakhon Pathom provice. He then entered Mahidol University, Thailand and obtained Bachelor Degree in Civil Engineering in 2000. After received a bachelor's degree, He worked as a civil engineer in construction companies.

In 2005, Mr. Amornchai Jaiyong received a M.Eng. degree in Civil Engineering from Chulalongkorn University.

In 2007, He received scholarship from the Commission on Higher Education, Ministry of Education, Thailand to continued in Ph.D. program in his major of Civil Engineering. His research interests include various areas of earthquake engineering and vibration.